A Simplified Pavement Condition Assessment and its Integration to a Pavement Management System

by

Jose Roberto Medina Campillo

A Dissertation Presented in Partial Fulfillment
of the Requirements for the Degree
Doctor of Philosophy

Approved March 2018 by the
Graduate Supervisory Committee:

Kamil Kaloush, Co-Chair
Shane Underwood, Co-Chair
Michael Mamlouk
Jeffrey Stempihar

ARIZONA STATE UNIVERSITY

May 2018

ABSTRACT

Road networks are valuable assets that deteriorate over time and need to be preserved to an acceptable service level. Pavement management systems and pavement condition assessment have been implemented widely to routinely evaluate the condition of the road network, and to make recommendations for maintenance and rehabilitation in due time and manner. The problem with current practices is that pavement evaluation requires qualified raters to carry out manual pavement condition surveys, which can be labor intensive and time consuming. Advances in computing capabilities, image processing and sensing technologies has permitted the development of vehicles equipped with such technologies to assess pavement condition. The problem with this is that the equipment is costly, and not all agencies can afford to purchase it. Recent researchers have developed smartphone applications to address this data collection problem, but only works in a restricted set up, or calibration is recommended. This dissertation developed a simple method to continually and accurately quantify pavement condition of an entire road network by using technologies already embedded in new cars, smart phones, and by randomly collecting data from a population of road users. The method includes the development of a Ride Quality Index (RQI), and a methodology for analyzing the data from multi-factor uncertainty. It also derived a methodology to use the collected data through smartphone sensing into a pavement management system. The proposed methodology was validated with field studies, and the use of Monte Carlo method to estimate RQI from different longitudinal profiles. The study suggested RQI thresholds for different road settings, and a minimum samples required for the analysis. The

implementation of this approach could help agencies to continually monitor the road network condition at a minimal cost, thus saving millions of dollars compared to traditional condition surveys. This approach also has the potential to reliably assess pavement ride quality for very large networks in matter of days.

DEDICATION

To my wife Ana Maria, and my kids Roberto, Manuel Alfonso, and Daniel. I love you!

ACKNOWLEDGMENTS

I would like to express my gratitude to both of my advisors Dr. Kamil Kaloush and Dr. Shane Underwood for trusting in me, and for giving me the opportunity to work with them. The support that I have received from them has given me the confidence to continue with my career in the field of transportation engineering.

My committee members Dr. Jeffrey Stempihar, and Dr. Michael Mamlouk for collaborating with me in my research and throughout my long term at ASU.

A special thanks to City of Phoenix engineers, Ryan Stevens, Todd Nunn, and James Williams, and Rob Dolson from the City of Maricopa, for their willingness to help and for taking their time to provide the necessary information for my research.

I want to thank my friends and colleagues in our pavement group Akshay Gundla, Ramadan Salim, Hossein Noorvand, Padmini Gudipudi, Sravani Vadlamani, Aashay Arora, Dirk BeGell, Gonzalo Arredondo, Ashraf Alrajhi.

Many thanks to all the people who volunteered their time and vehicles to carry out the ride quality experiments and the windshield condition surveys.

Thanks are also due to laboratory coordinator Jeff Long, and laboratory manager Peter Goguen for being there whenever I needed them.

I would also like to acknowledge Consejo Nacional de Ciencia y Tecnologia (CONACYT) for sponsoring my PhD work at ASU. I will always appreciate the opportunity that the Mexican government has given me to pursue my PhD degree.

TABLE OF CONTENTS

Page

CHAPTER Page

CHAPTER Page

LIST OF TABLES

Table Page

Table Page

Table Page

LIST OF FIGURES

Figure Page

Figure Page

Figure Page

Figure Page

Chapter 1 Introduction

According to the Bureau of Transportation Statistics until 2015 there were 2.7 million miles of paved roads in The United States (1). Due to traffic loading, environmental effects and other factors, pavements deteriorate gradually over time and must be maintained, rehabilitated, or reconstructed from time-to-time. The direct economic expense of these activities is estimated at more $51 billion a year in 2015 (2). These activities can also lead to increased societal and environmental costs and can become a hazard to road users. Some estimates of the user-cost of these issues have suggested that the total impact from these activities is as high as $76.8 billion dollars of user cost annually. Most of this cost occurs due to increased wear and tear on the vehicles (estimated from $178 to $832 dollars a year) (2-4), but also in lost time due to construction related delays. With these impacts, there is a strong need to effectively maintain and manage the network infrastructure in a good serviceable condition. Since the 1960's, agencies and researches have been aware of the idea of preserving and operating the road infrastructure in a systematic and cost-effective way in order to guarantee its serviceability through the life span of the network (5, 6). The use of computers and the development of new informatics technologies, put the concept of asset management system into practice during the 1970's (7, 8). In today's world with the surge of mobile technologies and increase in connectivity and data processing, asset management, data collection and processing can be expanded even further. It is this possibility that leads to this Ph.D. on integrating distributed, crowd sourced smart phone based sensing into pavement management decisions.

1.1 Background

The pavement infrastructure network is a valuable asset that needs to be preserved using limited resources in the best cost-effective way. Pavement management systems and pavement distress assessment have been implemented in developed countries for decades to evaluate the condition of a pavement at a network and project levels. Based on historical data, pavement condition models are also used to predict pavement deterioration, used them as a tool to schedule pavement maintenance, and develop multi-year rehabilitation plans. One issue with current practices is that it requires qualified raters to carry out manual pavement distress surveys. Despite the availability of manuals to rate the condition of pavements for given distresses, there is always some kind of subjectivity involved. Another tool used for assessing pavement condition is the use of automated distress vehicles or equipment. The problem with this type of equipment is that it is costly and not all agencies can afford to purchase one. Pavement condition surveys are usually carried once a year or every two years to continually keep on calibrating the pavement condition models. Some researches has suggested to increase the frequency of pavement condition surveys for early detection of pavement abnormalities, and that the lack of frequent surveys usually tend to underestimate the maintenance cost at a network level (9). In reality, these models can benefit from more frequent pavement condition data collection to improve upon the accuracy of the developed pavement management programs. This study is intended to address these limitations by developing a simple and feasible method to continually and systematically quantify pavement condition of the entire road network by using technologies already embedded in new cars, smart phones, and other devices that may be developed for this

purpose. With the surge of big data and crowdsourcing techniques, this study presents a methodology to implement this data collection into a Pavement Management System (PMS) with the goal of achieving 100% automation.

1.2 Research Objective

The objective of this study is to develop a framework for measuring pavement ride quality from real time data collection and crowdsourcing techniques, and to integrate roughness measurements in a pavement management system.

The approach to achieving this study objective is shown in Figure 1-1. As seen from the flowchart in this figure, the study first involves two separate, but related, studies. The first (data collection) involves understanding smartphone sensing, the potential for using this sensing to measure pavement ride quality, the challenges in collecting the data, and to develop effective processing algorithms to process the data. Other more specific aspects of this part of the study are:

a. Developing a model to estimate pavement roughness that can later be implemented in a smartphone or mobile device application.
b. Develop a stochastic approach for crowdsourcing data collection based on multifactor uncertainty. Some of the factors to evaluate in the case of roughness measurements are: speed, vehicle type and distribution, cellphone device, cellphone mount, etc. Use of Monte Carlo simulation to estimate sample size.

The second step in this research is to integrate the smartphone roughness measure into a PMS. For this aspect two steps are needed;

a. Establish a Ride Quality and/or International Roughness Index (IRI) based deterioration function.
b. Assessment using ride quality index as a unique pavement condition indicator compared to a multi indices used typically in PMS.

The final step in the proposed research is verification of the smartphone based PMS using a case study from an actual road network; the City of Maricopa, Arizona was selected for this effort.

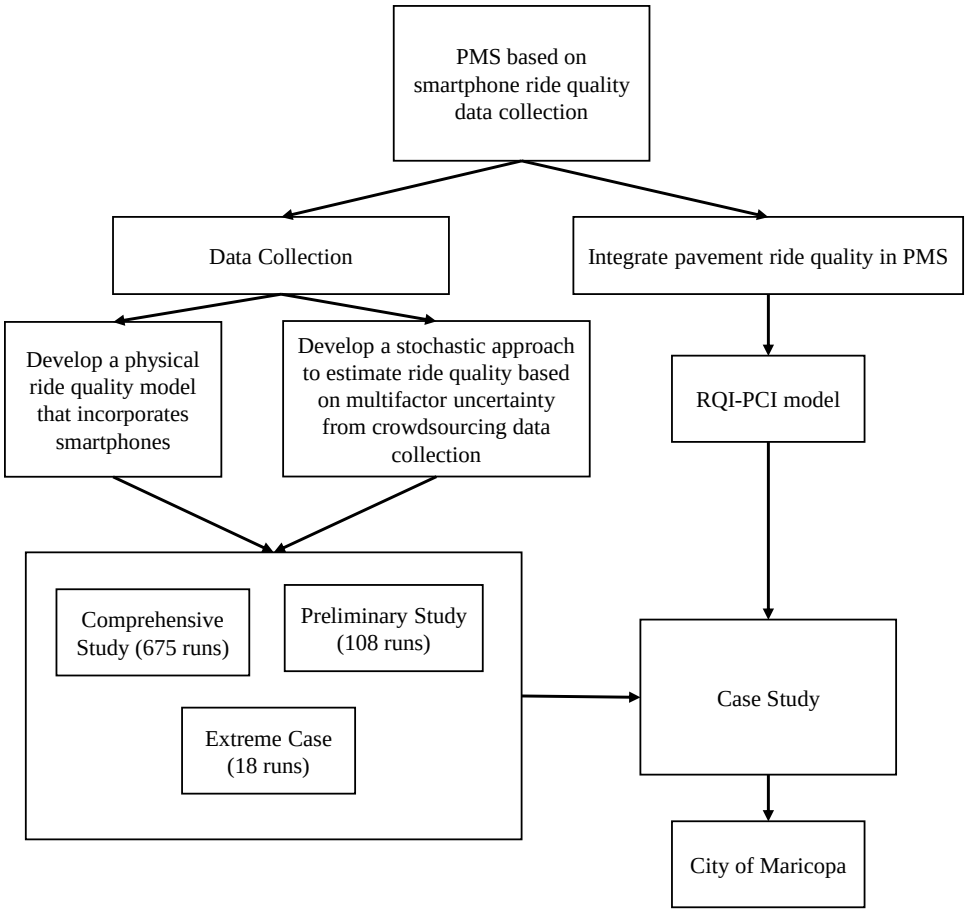

Figure 1-1. Research Schematics

1.3 Dissertation Outline

This dissertation consists of six chapters.

Chapter 1: Introduction

This section provides an overall introduction and background of this study, the needs for this research as well as the research objectives.

Chapter 2: Literature Review

This chapter covers some of the literature review regarding pavement management systems, pavement performance indices, roughness measurements, and some of the work already done by others regarding mobile device roughness studies and smartphone use in detecting abnormalities in the pavement. Then, finalized this chapter with some review on crowd sourcing data collection, the central limit theorem and the Monte Carlo Simulations.

Chapter 3: Smartphone Data Collection and Field Studies

This chapter provides the results from the three experimental studies to evaluate ride quality using smartphones. The first experiment named Preliminary Study, was carried out with the objective of identifying the variability in roughness measurements given 1 vehicle and different factors and try to validate the approach in a more controlled system. The second study named Comprehensive Study was to calibrate the model to a broader and more real life scenario. This Comprehensive Study presents the statistical analysis from all the RQI runs and showing the significance of each factor considered. The third study, referred to as Extreme Case, was to identify the impact of using heavy duty trucks to RQI values in comparison to a passenger vehicle.

Chapter 4: Parametric Assessment of the Factors Affecting Ride Quality Index Estimation and Sample Size Determination

This chapter explains the methodology for the backcalculation of the cellphone mount response and the statistical distribution from the experimental data. It also includes an analysis on the effect of the mount and vehicle suspension to the Ride Quality Index by performing Monte Carlo simulations on different LTPP InfoPave database profiles. The chapter ends by setting up the criteria for convergence and sample size needed to estimate the Ride Quality Index.

Chapter 5: Integration of RQI into PMS

This chapter presents a method to integrate Ride Quality Index into a Pavement Management System by identifying the relationship between pavement condition index (PCI) to RQI, and based on these results propose maintenance threshold limits or triggers.

Chapter 5 also includes a case study from the City of Maricopa road network. It provides general information about the city, and show the results from PCI windshield distress surveys and RQI data. This study was limited to only one RQI sample for each road section.

Chapter 6: Summary, Conclusions and Future Work

Provides summary of the findings and conclusions from this research and the needs for future work.

Chapter 2 Literature Review

2.1 Pavement Management Systems

2.1.1 General Overview

In general terms, pavement management or asset management can be defined as: *"A systematic process of maintaining, upgrading, and operating physical assets cost-effectively." (8)*

Pavement management systems represent a combination of engineering, economics, and informatics to provide enough information to make effective decisions. The typical components of a typical PMS are:

- A database with all the network inventory
- A methodology to assess pavement condition and pavement performance
- Data analysis platform able to prioritize needs and optimization of best cost-effective alternatives.
- Reports in the form of tables and Graphical Information System linked maps.

PMS emerged largely in the 1980's, but the needs and ground work were largely laid in the preceding decades. By the late 60s and early 70s most of the highway system was already built and the need for a network maintenance and rehabilitation management plan was growing due to pavement deterioration, and decrease in available resources (7, 8, 10). Typically pavements were maintained when there was a critically distressed pavement that represented a safety issue for road users, so early pavement management addressed what was referred as "crises management" (8). The U.S. Army that was in charge of 560 million square yards of pavements found that filling potholes and making

emergency repairs was a costly short term solution and the need for a systematic, objective, and long term planning approach was needed (11, 12).

In 1980, the city of Phoenix, Arizona and Charlotte, North Carolina, hosted the first workshop on pavement management with the goal of defining some set of criteria and priorities for the short and long term activities for a better pavement management (6). The states of Arizona, Utah, Washington, California, and Idaho were the pioneer states who started developing procedures for a systematic maintenance program. By 1982, Arizona developed a program to optimize pavement maintenance on its 7,400 mile network with savings of 14 million dollars in the first year and an estimated saving of $101 million dollars over the next 4 years (5). Today all states in the U.S. have a pavement management system (13).

Since agencies have restricted budgets, the use of a pavement management systems are helpful in assisting the decision-making process and justifying maintenance and rehabilitation strategies. It is of great importance the quality of the data that feeds the system and the accuracy of the models use to predict pavement deterioration.

2.1.2 Pavement Condition Models

The key analytical elements that permit effective usage of a pavement management system are pavement condition models. These models depend on the type of performance measure adopted by agencies. Some pavement condition models are based on subjective visual inspection, they can be objective measurements for specific distresses, or a combination of both. According to each agency's polices, some with less resources may want to use models which predicts performance based on traffic or time,

some agencies that would like to collect more detailed information about the pavement deterioration may use complex indices as a function of material properties, climate or traffic (8). Regardless of the performance model adopted, the main goal is to predict the future pavement condition for a multi-year analysis on pavement performance, maintenance and rehabilitation planning, budget allocations, and estimating life-cycle cost (14). Different approaches have been adopted by different agencies across the country and many studies have proposed different methodologies for pavement management optimization. Carnahan, et al. (1987) proposed an optimization approach in the decision making using a Markov process to model the cumulative damage of pavement condition (15). Bianchini (2012) proposed to Alabama Department of transportation the use of fuzzy mathematical theories to define a pavement condition index or rating (16). Sotil and Kaloush suggested the use of a time-deterioration superposition model for pavement condition index (17). Gowda, et al (2015) suggested a PMS model based on just engineering criteria for budget prioritization (14).

As it is known, having a timely maintenance and rehabilitation pavement program helps maintain the pavement network in an overall good condition with limited budget (8, 14, 16, 18). In order to achieve this goal, it is important that the pavement condition models accurate predict the pavement deterioration so timely maintenance can be triggered.

In practice, there are two basic pavement deterioration models used in pavement management systems: probabilistic and deterministic models. Deterministic models are models used to predict the functional or structural performance of a pavement. In most of the cases, these deterministic models uses regression to determine a specific performance

metric value such as condition, structural capacity, and ride quality index from either traffic or time. Probabilistic models are models that predict a range of values of the pavement condition. The future condition of the pavement uses probability functions to estimate the transition from the current pavement condition to a range of future conditions. Markov and semi-markov chain transition models are typically used as probabilistic models when not enough historical data exists (8). Markov models are based on the actual pavement condition and the probability that after some time (usually 1 year) will transition to a different condition.

Whether to use a probabilistic or deterministic performance model will be based on the specific objectives of individual agencies. Project level and network level require different types of performance models. Usually at a project level, a more detailed model will be preferable than network level models. The different uses for these models are summarized in Table 2-1 (19).

Table 2-1. Types of Models at Different Levels Used by Agencies (19).

Level	Deterministic				Probabilistic	
	Primary Response	Structural	Functional	Damage	Survivor Curves	Transition Process Models
National Network				✓	✓	✓
State or District Network		✓	✓	✓	✓	✓
Individual Project Level	✓	✓	✓	✓		

The advantage of probabilistic models is that they can be used when agencies does not have enough historical data from pavement condition. Therefore, based on the agency experience, they can create probabilistic transition matrices that can effectively

predicts the future condition (8, 20-24). Probabilistic models are more commonly used at the network level since there are good to estimate the overall performance of a network. The problem with these models is that just gives the probabilities of changing from one pavement condition to another without giving any insight and details on the causes (8, 19). Deterministic models are good for either network level or project level, especially when a combination of indices are used. This way deterministic models can provide a better insight and be more specific details on the causes of pavement deterioration (8, 19). Because a more detailed inspection on the pavement condition is needed to create deterministic models, this approach is time consuming and expensive (8, 25, 26).

The limitation for most of the models used is that are based on limited available data, usually agencies collect distress measurements every year, or two, depending on road class or traffic, and it can be time consuming, labor intensive for manual surveys and costly if specialized automated survey equipment is used (8, 27-29). With respect to these needs, this research strives to develop a methodology to continually measure pavement condition to accurately predict pavement condition.

2.2 Pavement Performance Measures

Pavement performance measures are scores or ratings for a pavement segment that reflect the condition of the pavement and are used to help manage a pavement network. Since management is context sensitive, multiple rating systems exist, and agencies usually adopt their rating system that fits their needs based on experience. Usually, the condition rating adopted has a numerical scale that can be related to a good or poor pavement performance. In pavement management systems, a pavement condition index

can help to trigger pavement rehabilitation alternatives, provide an overall network condition, estimate maintenance and rehabilitation cost, and also track the performance of different pavement types (8). There are many types of rating systems, but the most popular ones and will be describe in more detail are the Present Serviceability Index (PSI), Pavement Condition Index (PCI), Structural Number (SN), and the International Roughness Index.

2.2.1 Pavement Serviceability Index

Introduced by the American Association of State Highway and Transportation Officials, the Present Serviceability Index (PSI), is an index with a scale from 0 to 5 that was developed from the experiences of a panel of "expert" subjective ratings on the condition of a pavement. For this index, a typical terminal serviceability range is 2 to 3 (depending on pavement functional class), meaning a pavement with a PSI below 2 to 3 may require attention (reconstruction, rehabilitation, etc.) The subjective ratings that formed the basis of PSI were termed the present serviceability rating (PSR), while PSI is the name given to the quantity that was correlated to the PSR using objective pavement performance measures, see Equation (2-1) (30). Where PSI is the present serviceability index, SV is the mean of the slope variance in the two wheel-paths, C+P are a measure related to cracking and patching, and RD is the rutting in the wheel-paths.

$$PSI = 5.03 - 1.91\log(1+SV) - 0.01\sqrt{C+P} - 1.38RD^2 \qquad (2\text{-}1)$$

The significance of PSI is that is utilized in the 1993 AASHTO Pavement Design Guide methodology (both new design and overlay) since the design equations ultimately describe the relationship between PSI and traffic load (Equivalent Single Axle Load) or time.

2.2.2 Pavement Condition Index

In the late 70s the U. S. Army Corps of Engineers developed a way to rate pavement condition for their decaying airfields. The pavement condition rating consisted in the following criteria:

1. Separate pavement section in manageable sizes.
2. Identify pavement distress, severity and extend for which they developed guidelines on how to carry out pavement distress evaluation.
3. Deduct values were assigned for each distress type, severity and extent level.
4. The total number of deduct values are added.
5. A corrected deduct value is determined based on the number of observed distresses.
6. The pavement condition rating is determined in a scale from 0-100.

This rating system is referred to as Pavement Condition Index (PCI). This method tries to eliminate the subjectivity rating by giving a more detailed evaluation of a pavement segment. The findings of this research were used as the base to develop ASTM standard D6433. Figure 2-1 shows the standard PCI rating scale (31, 32). Similar to the ASTM standard, the Long-Term Pavement Performance Program (LTPP) developed a

distress identification manual to provide a standardize methodology to collect distress information. This method is convenient because main distresses are quantified and can trigger different rehabilitation strategies depending on the severity and distress type.

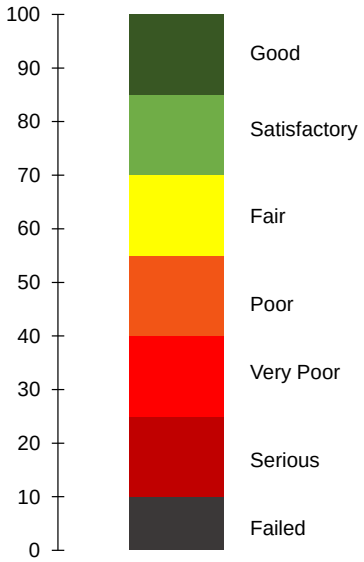

Figure 2-1. ASTM D6433 Standard PCI Rating Scale (31).

2.2.3 Pavement Structural Number

Structural capacity is typically measured using the falling weight deflectometer (FWD) or the rolling weight deflectometer (RWD), and frequently expressed as structural number (SN). The SN is a value that indicates the pavement structural requirements to sustain the designed traffic load (33-36). The 1993 AASHTO Guide for Design Pavement Structures provides a methodology on how to calculate the remaining service life of a pavement from the effective modulus of a pavement structure based on the deflection and load measurements collected by a FWD. Given the effective modulus of a pavement, the structural number is computed and the remaining structural service life can be estimated.

Besides the FWD, SN can be empirically calculated based on the structural layer distresses, thickness and drainage characteristics. Typically, SN is used at a project level to calculate the layer thickness of a pavement overlay required to sustain traffic loads. More agencies are starting to implement some kind of structural number index for a network level PMS (37).

2.2.4 Ride Quality

There are many ways and indices to measure ride quality that have evolved over the years. Ride quality is considered a direct measurement of the cumulative effects on user comfort and satisfaction with the pavement condition. A more detailed review on ride quality measures is given in the following section.

2.3 Measures of Ride Quality

Road smoothness has shown to be one of the main factors to rate the highway network according to surveys carried out at a national and local level. Typically road users care more about ride comfort that other road characteristics (38).

The present serviceability rating (PSR) developed in the 1950's by the Highway Research Board, in which they used the AASHO Road Test facility to define PSR as a subjective judgement from a panel of observers to the ability of a road to serve the intended traffic. Observers drove on the AASHO test track many times to rate their ride quality in a scale from 0 to 5 shown in Figure 2-2. The relative error in PSR measurements was about 19% which represented a limitation of its use.

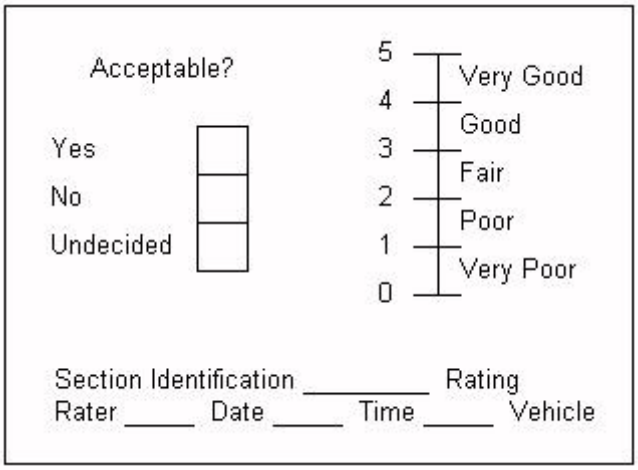

Figure 2-2. Example for PSR (38).

Panel ratings are subjective measures that depend on the instructions given to the rater and implicit biases by the rater (38, 39). In addition, these human based ratings are difficult to correlate to objective ratings and is one reason why panel based rating systems were not a viable solution for widespread evaluation.

Between the late 60s and the 80s agencies worked in establishing a measure for pavement smoothness such a ride quality index or a standardized profile index to provide a specific value that can be related to the road profile (40). In the National Cooperative Highway Research Program (NCHRP) Report 275 the profile index (PI) is defined as the root mean square (RMS) profile height of a section of a highway after applying a band-pass filter (10-50 Hz) (39). According to Sayers there are 4 basic steps to estimate any roughness index: 1) The number of profiles needed, 2) the filtering process of the data, 3) the calculation methods to determine the single number index (i.e. cumulative absolute values of the numbers), and 4) the scale or units that are used for the index (38).

In early 80s the NCHRP funded a project with the objective to investigate the effect of road surface profile on ride quality and provide an index that can be used to estimate road

roughness. In summary, researchers developed the Ride Number (RN) based on mathematical transform of a road profile. The mathematical expressing to calculate RN is given in two forms a linear and a nonlinear equation.

$$RN = -1.47 - 2.85\log(PI) \quad (2\text{-}2)$$

$$RN = 5e^{-11.72\,PI^{0.89}} \quad (2\text{-}3)$$

Researches went further and attempted to correlate the RN to the mean ratings from a panel of 30 raters. What it is interesting to note is that most of the time the individual ratings varied considerably but the mean rating from a group was very consistent. It was determined that an approximate size of 30 raters was enough to get a consistent result (41).

2.3.1 Vehicle Response Models and Indices

Many vehicle response models have been utilized to characterize pavement roughness, and most of them are based on the International Roughness Index (IRI). Many of these models assume constant speed and the suspension parameters referred as the golden car parameters, even though the suspension of actual vehicles differ from those golden parameters, plus the road users in urban areas do not drive at a constant speed. The roughness indices currently used in the United States for pavement management systems are mainly the IRI, and Profile Index (PI), but other exists such as the Mean

Roughness Index (MRI), Half Car roughness Index (HRI), and Ride Quality Index among others.

2.3.1.1 Profilograph Index

The Profilograph Index (PrI) is not the same as the Profile Index used to calculate RN. The PrI index is being used for long time in Portland cement concrete pavements to measure initial smoothness and give payment incentives to contractors (39, 41, 42). A description on how to estimate the PrI is described in California Test Method 526 in brief PrI is defined as "inches per 0.1 mile in excess of a zero (null) blanking band" (43). The blanking band is a reference line which is usually traced at the average profile height. Then the height from the peaks to the reference line is measured, and the summation of all these count over the 0.1 mile segment are computed with units of in/mi or mm/km (44). This index is one of the most popular indices in pavement management systems and has been adopted by many states in the U. S., Table 2-2 (45-48).

Table 2-2. Number of States that Uses PrI as Smoothness Indicator (46).

Source	Hot Mix Asphalt	Portland Cement Concrete
Perera and Kohn (2002)	16	25
The Transtec Group, Inc.	14	28
Merritt, et al. (2015)	9	20

2.3.1.2 Full-Car Roughness Index

The Full Car Roughness index was proposed by Capuruço, et al (2005) as an alternative measure to characterize pavement roughness. The model combines the full car suspension, the pitch, roll and yaw to estimate road roughness, Figure 2-3. This model

represents a more accurate representation of an actual vehicle than the quarter car model used in IRI, and therefore is more effective in estimating ride quality (45, 46). However, a limitation is the computational effort needed to estimate the index and the complexity of a model with high degree of freedom (42, 46). The equation of motions of this the Full-Car response model are shown in APPENDIX A.

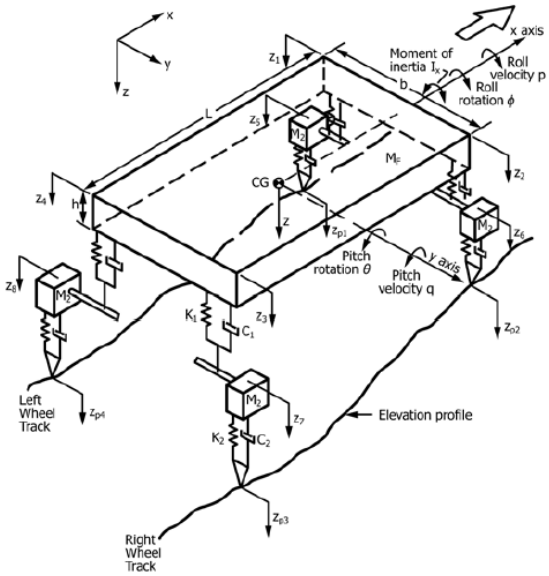

Figure 2-3. Full-Car Response Model (Source: ASTM E1170).

2.3.1.3 Half-Car Roughness Index

The Half-Car Index (HRI) is another roughness measure calculated by accounting for the wheel track from both wheels. The elevation profile from both wheels are averaged, and then the index is calculated by estimating the vertical displacement of the body of the vehicle relative to the mass below the suspension traversing along a longitudinal profile. The mechanical model is shown in Figure 2-4. One of the disadvantages of this model is that the measuring device from both sides has to be aligned before they are averaged. In order to calculate HRI is necessary to have the

measuring device in both sides, otherwise would be very difficult doing two passes and then aligning the profiles. Furthermore, it was found that it provides no more valuable information and is highly correlated to IRI (38, 50). Merritt, et al. (2015) reported that in the U. S. three states uses HRI as specification for asphalt concrete pavements and only one state for PCC pavements (49). The equation of motions of this the Half-Car response model are shown in APPENDIX B.

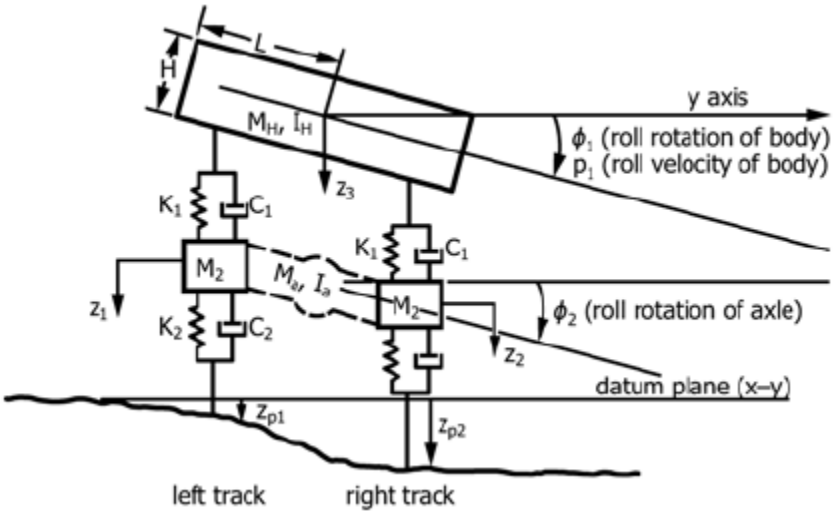

Figure 2-4. Half-Car Response Model (Source: ASTM E1170).

2.3.2 The International Roughness Index Model

By definition, the IRI is a "scale for roughness based on the simulated response of a generic motor vehicle to the roughness in a single wheel path of the road surface" (51). To calculate IRI, the road elevation profile is first filtered using the 250 mm moving average filter before and then the Golden Quarter Car model is use to simulate the vehicle suspension response to the pavement surface at a reference vehicle speed of 80 km/h.

Figure 2-5 shows the schematics of the Golden Quarter Car Model. By applying Newton's 2nd law of motion, the damped mass-spring model can be written as shown in Equation (2-4) and Equation (2-5).

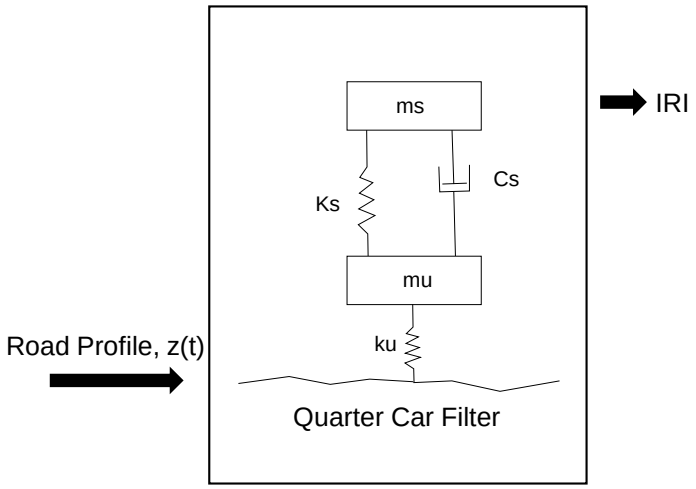

Figure 2-5. Vehicle Response Model.

$$m_s\ddot{z}_s + c_s\left(\dot{z}_s - \dot{z}_u\right) + k_s\left(z_s - z_u\right) = 0 \tag{2-4}$$

$$m_u\ddot{z}_u + c_s\left(\dot{z}_u - \dot{z}_s\right) + k_s\left(z_u - z_s\right) + k_t\left(z_u - Y\right) = 0 \tag{2-5}$$

Where $m_s\ddot{z}_s$ is the force acting on the sprung mass m_s, $\ddot{z}_s$ is the vertical acceleration of the sprung mass, c_s is the damping coefficient, $\dot{z}_s$ is the vertical motion of the sprung mass, $\dot{z}_u$ is the vertical motion of the un-sprung mass, k_s is the stiffness constant, z_s is the vertical displacement of the sprung mass, z_u is the vertical displacement of the un-sprung mass, k_t is the stiffness of the tire and Y is the profile input

The parameters used to calculate IRI are known as the golden car parameters, these parameters are summarized in Table 2-3. These parameters are the suspension system

constants that represents a typical passenger car from the 80's when the IRI model was developed. Usually, the parameters are presented in IRI literature normalized to the sprung mass for applicability purposes to a wider range of vehicles (42).

Table 2-3. Golden Car Parameters (42).

Parameter	Value
k_s/m_s (s^{-2})	63.3
k_u/m_s (s^{-2})	653
c_s/m_s (s^{-1})	6
m_u/m_s (-)	0.15

From the vehicle suspension response system and using the golden car, IRI is calculated by taking the accumulated suspension travel over a distance traveled by a vehicle at a speed of 80 km/h, Equation (2-6).

$$IRI = \frac{1}{L}\int_{t_0}^{t_f} \left| \dot{z}_s(t) - \dot{z}_u(t) \right| dt \tag{2-6}$$

Where L is the longitudinal distance along the profile, t_0 and t_f are the initial and final time traveled at a constant speed of 80 km/h, and $\dot{z}_s$ and $\dot{z}_u$ are the sprung and unsprung vertical motion respectively. IRI is calculated by first simulating the response impulse due to the road profile, then uses the quarter car response model to estimate the sprung and un-sprung mass motion, and finally estimate IRI.

The Mean Roughness Index is calculated by averaging the individual IRI measurements from the left and right wheel tracks.

2.3.3 Linking Ride Quality and Pavement Performance

Due to the inability of roughness measuring devices to produce repeatable results, NCHRP funded research that developed a roughness index based on a quarter car mechanical filter to the road profile. This work established so-called "Golden Car" parameters for this mechanical filter that would represent average vehicle conditions at the time. In 1980s, the World Bank expanded this research to create the International Roughness Index with the purpose of standardizing a roughness index in which ride comfort could be measured (38, 52). With the basic research complete, engineers began to apply the IRI to existing road networks and making observations with respect to the IRI value, functional classification, and overall pavement condition. Sayers (1986) proposed a range of IRI values as a general guide for different types of road, and recommended that this measure was mainly to estimate overall vehicle cost due vehicle wear due to pavement roughness, it could serve as measure to estimate ride quality, and get an overall insight in surface condition, Figure 2-6 (53).

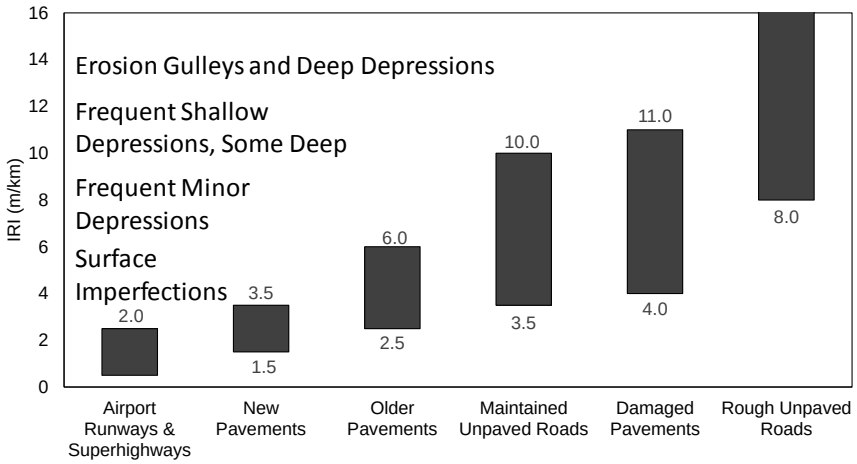

Figure 2-6. IRI Ranges for Different Types of Roads (53).

A second major research area in ride quality measures has been the correlation of IRI to other pavement performance measures and then integration of IRI into pavement management systems. When IRI was developed, the state-of-the-practice pavement management systems were based on PSR, and in order to adapt IRI to PSR, further correlations were developed. Research done by Paterson and Al-Omari, both carried out independent studies and found a correlation between PSR and IRI using an exponential model expressed in Equation (2-7). The parameter *a* was determined by regression analysis based on sections from different types of pavements and from different states (54, 55).

$$PSR = 5e^{-a(IRI)} \tag{2-7}$$

The World Bank later developed a PMS software named Highway Development and Management Model (HDM-IV) that uses IRI as one of the main pavement condition indicators to develop maintenance programs (56, 57). The IRI prediction equation developed by the Word Bank and used in the HDM-IV software is shown in Equation (2-8).

$$\Delta RI = 134e^{mt} MSNK^{-5.0} \Delta NE4 + 0.114\Delta RDS = 0.0066\Delta CRX + 0.003h\Delta PAT + 0.16\Delta POT + mRI_t\Delta t \tag{2-8}$$

Where ΔRI is the increase in roughness over time period Δt, *MSNK* is a factor related to pavement thickness, structural number and cracking, $\Delta NE4$ is the incremental

number of equivalent standard-axle loads in ESALs, ΔRDS is the mean rut depth in mm, ΔCRX is the percent change in cracking area, ΔPAT is the percent change in surface cracking, ΔPOT is the increase in total volume of potholes measured in m^3/lane km, m is an environmental factor, RI_t is the roughness at time t in years, and h is the average deviation of a patch from the original pavement profile in mm.

It should be noted that there are many other roughness indices similar to IRI but they are not as widely available (38). The importance of using IRI is that it is the roughness measurement that has been adopted worldwide. The United States adopted IRI as the standard reference roughness index for the Highway Performance Monitoring System (HPMS) since the 1990's. Synthesis 501 from the National Cooperative Highway Research Program (NCHRP) reported that 40 states out of 42 that responded the survey, collect roughness data at network level and 28 at a project level (13). In Europe IRI is one of the smoothness parameters used to measure road unevenness characterization (46, 58, 59). Múčka (2017) presented an overview of IRI application and specifications for different countries. A summary of the countries that has adopted IRI for roughness measure is shown in Table 2-4. A more detailed information on specifications ranges by countries can be found elsewhere (60).

Table 2-4. Use of IRI by Different Countries (60).

Country	Road Type	Country	Road Type
Australia	AC/PCC	Kazakhstan	AC/PCC
Belarus	AC/PCC	Lithuania	AC/PCC
Bosnia and Herzegovina	AC/PCC	New Zealand	Highway
Canada-British Columbia	AC	Norway	AC
Canada	AC	Philippines	AC/PCC
Chile	AC/PCC	Poland	AC
Costa Rica	AC/PCC	Portugal	AC
Czech Republic	AC/PCC	Russia	AC/PCC
El Salvador	AC/PCC	Slovakia	AC/PCC
Estonia	AC	Slovenia	AC/PCC
Honduras	AC	Spain	AC
Hungary	AC	Sweden	AC
Ireland	AC	Ukraine	AC/PCC
Italy	AC/PCC	Uruguay	AC/PCC

2.3.4 Traditional IRI Measurement Systems

There are many tools available to measure pavement profile or pavement roughness. One of the popular devices in the 1920s where the response-type road roughness measuring systems (RTRRMS). RTRRMS, also called road meters, are transducers that record suspension motion of a vehicle, typically a passenger car, truck or a trailer. Some of the most popular RTRRMS devices were the Cox meter, the PCA, and the Mays Ride Meter (38). Figure 2-7, shows a typical schematics of a Mays meter.

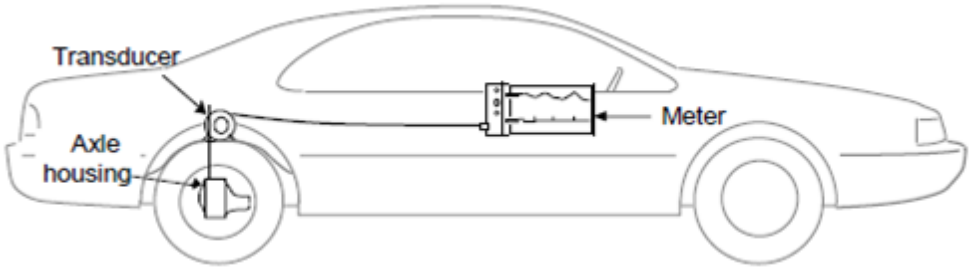

Figure 2-7. Schematic of a Car with a RTRRMS or Mays Meter (14).

Some of the conclusions made by NCHRP Report 275 (39) from the measurements taken from RTRRMS devices were as follow.

1. High correlation with subjective rating (mean panel ratings (MPR)) on asphalt pavements, and poor correlation to PCC pavements. The report proposed to use a transform between response type meters and MPR given in Equation (2-9) for asphalt concrete pavements. Where *MPR* is the mean panel rating, *RN* is the ride number and *MRM* is the roughness statistic calculated with response-type system.

$$RN = MPR = 8.66 - 2.70\log\left(MRM\right) \tag{2-9}$$

2. They found a good correlation with the quarter car statistic for all surfaces (asphalt, PCC and composites). This relationship is given in Equation (2-10), where *QC* is the quarter car statistic.

$$MRM = -47.47 + 1.44(QC) \tag{2-10}$$

However, some of the problems encountered with road meters is the lack of reproducibility by another meter since the response was dependent on the vehicle used to collect the roughness (38, 52).

Profiles are measured by a tool known generically as a profiler, and the most common form used for calculating the IRI is the inertial profiler. The components of an inertial profiler are an accelerometer, a laser height sensor and a longitudinal distance measuring instrument. The device is typically around 15 x 10 cm and can be mounted to

a vehicle at a fixed location (see Figure 2-8). The accelerometer measures the instant height of the vehicle and the laser transducer measures the relative distance from the ground to the accelerometer.

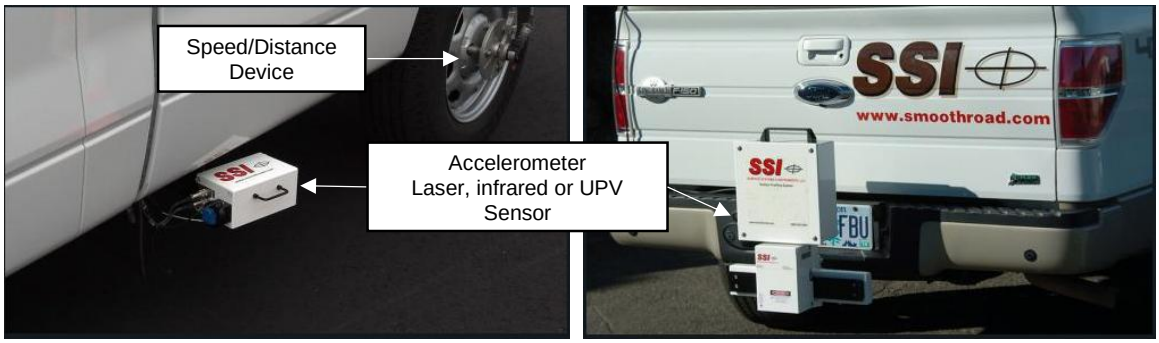

Figure 2-8. Simple Inertial Profilers (Source: SSI)

Today, agencies and private contractors record pavement roughness using high sensitivity inertial profilers. AASHTO R 57 describes the operating and calibration procedures for inertial profiling systems. By this standard the longitudinal calibration has to be on a straight and level section of roadway at least 161 meters long within a 0.05 percent of the true length. The vertical calibrations is performed by measuring the thickness of flat plates or blocks within an accuracy of 0.00254 cm. For a network level data collection is recommended to perform these calibration on a monthly basis.
The main problem with this methodology is that the equipment is relatively expensive to collect pavement roughness measurements. Some studies have reported that the collection and analysis of pavement roughness without including the equipment cost can range from $1.40 to $6.25 with an average cost per kilometer of $3.83 (61, 62). This means that for the state of Arizona with a network of approximate 14,880 centerline kilometers (63) the cost to collect roughness measurements would be about $57,000. For

a network like the City of Phoenix which consist of 1,440 centerline kilometers of arterials and collectors and another 6,240 centerlines kilometers of local streets, the cost would be around $30,000 (64). This would be the approximate cost for one time roughness measurement for the entire network. If the agency would like to monitor the entire network in a monthly basis the approximate yearly cost for the Arizona State and the City of Phoenix networks would be around $680,000 and $350,000 respectively.

2.3.5 Mobile Device Roughness Studies

Some researchers have proposed inexpensive alternatives involving the use of smartphones or sensors already embedded in new vehicles to collect this information. Some of these studies are summarized in the following subsections.

2.3.5.1 Road Impact Factor

Bridgelall proposed a new index called the road impact factors (RIF) that it is vehicle speed independent and the wavelength is less biased than the IRI which magnifies wavelengths 2.1 and 17.6 m/cycle (18, 65). The RIF is the average g-force experienced by the sprung mass per meter of longitudinal distance shown in Equation (2-11). Where $R_{\bar{v}}^{L}$ is the road impact factor, L is the distance traveled in the longitudinal direction, $g_z(t)$ is the vertical g-force, $v(t)$ is the velocity and t is the time traveled over a longitudinal profile.

$$R_{\bar{v}}^{L} = \sqrt{\frac{1}{L}\int_{0}^{L/\bar{v}} \left| g_z(t)v(t) \right|^2 dt} \qquad (2\text{-}11)$$

It proposed the use of this RIF in connected vehicles and studied the precision of measurements using inertial profilers mounted in a modified van from the North Dakota Department of Transportation (NDDOT) survey crew. A 2007 Subaru Legacy sedan and an Apple iTouch placed flat on the dashboard was also used in this study. This research focuses more in inertial profilers rather than mobile devices. The variability from the results when using the single mobile device were much larger than the ones using the inertial profiler. Also, the analysis does not account for the differences in mobile device measurement. It is mentions in the conclusions that present methods to produce roughness indices cannot be scale up to practical uses because it requires calibration from individual vehicle response.

In order to get a better insight in the reliability of the RIF, Bridgelall recently carried out a study to capture the effects on variable speed and different vehicles. This study used a total of 18 different buses while driving in their normal operation schedules. It was found that within 30 measurements the RIF indices distributed normally with a margin of error less than 6%. It was also shown that by increasing the number of samples from the same vehicle classification at typical driving speeds the precision of the measurements increases (66). However, the fact that the average RIF-indices converges to a single value is not a unique property of this roughness index. The fact that after a reasonable number of samples the results converge to a single value is due to the Central Limit Theorem explained later in this chapter. The study carried out and presented in this document shows a framework to collect a ride quality index based on random sampling of a vehicle spectra that typically uses the roads and to determine a sample size needed to obtain a precise ride quality value.

2.3.5.2 Roughness Capture

Islam developed a smartphone application called Roughness Capture to estimate *IRI* which actually measures the acceleration from the smartphone sensor, then using a Matlab code to recover the pavement profile by double integration of the sensor data and also he used the linear state space representation of the Quarter Car. Either by direct double integration of the sensor data or the use of the state space model, the acceleration is first filtered to cutoff wavelength less than 1.2 m and higher than 30.5 m. This study included five different smartphones and four sedan type vehicles. The data was collected at a sampling rate of 140 points/second at a speed of 80 km/h. The roughness measurement showed good agreement with IRI measurements from the inertial profiler on sections where the road was considered smooth (IRI<0.50 m/km). As the IRI increased, the measurements from the cellphone underestimated the reference data up to a coefficient of variation of 22%. At the end the authors suggested that a higher sampling from smartphones will improve the accuracy of the measurements and also that crowd sourced IRI measurements will be helpful in the IRI predictions. This research also included the statistical analysis to see the impact of smartphones measurements and the impact on different vehicles (61, 67). As expected, the measurements vary from smartphones and from vehicles. The author suggest that with crowd sourcing the difference will be less, but they do not provide any analytical or experimental analysis to prove it.

2.3.5.3 Visco-Elastic Approach

Chen et. al. developed a viscoelastic model to estimate IRI using smartphones. The model is similar to the Quarter Car vehicle response model, but only considers the sprung mass. In this case the model becomes a relatively simple Voigt model with the suspension components of the vehicle k_s and c_s, with a force F represented by the sprung mass m_s, a is the measured acceleration from the smartphone, and X is the simulated motion between the sprung and un-sprung mass, Figure 2-9. Measurements from 39 different road sections were taken using an inertial profiler and the cellphone measurements. After the calibration for the single vehicle, the results were close to those measured by the inertial profiler with an R^2 of 0.91 (68). The use of a small fleet of vehicles where some test runs can be performed to calibrate the model parameters was recommended by the authors.

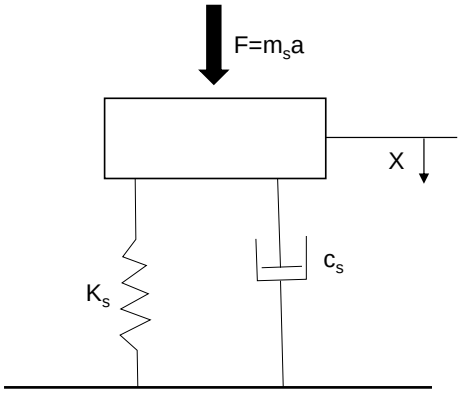

Figure 2-9. Model Schematics.

2.3.5.4 RoadLab™

Wang and Guo (2016) worked on a project funded by the World Bank and with the collaboration of the Belarus national road management agency to develop a

smartphone app to estimate IRI/pavement condition and to use crowdsourcing for the data collection. The pilot test consisted in finding sections greater than 400 meter long with homogenous roughness. Then each section was divided into 100 meter segments. It is not mentioned in the study the number of test locations used. The factors to develop their model were: 1) Pavement condition, 2) Four vehicle speeds, 3) two fixed locations for the cellphone (dashboard and windshield mount), and one non fixed location directly on the car seat, and 4) vehicle suspension variation (hard, medium and soft). For the suspension variation, the authors did not provide detail information on the suspension parameters. The model was developed by using calibration by regression, field experiment was carried out to collect acceleration data from smartphones and then related the vertical acceleration to pavement roughness. The regression model used is shown in Equation (2-12). Where Y_i is the predicted pavement condition, $X^{VS}{}_i$ is the future standard deviation derived from the vertical acceleration on a given segment, $speed_i$ is the driving speed at a given location. $\beta_{0,}\beta_1$ and β_2 are calibration coefficients based on the experimental data.

$$Y_i = \beta_0 + \beta_1 X_i^{VA} + \beta_2 X_i^{VA} * speed_i \qquad (2\text{-}12)$$

The results from this model showed a linear relationship between the standard deviation and the estimation of IRI when the cellphone was fixed and no relationship when the phone was not fixed on the seat. In order to address the variability with car suspension, four vehicles where used; a BMW, Ford, Gorkovsky Avtomobilny Zavod (GAZ), and a Volkswagen (the specific model for each vehicle was not mentioned). In

general, all four vehicles showed similar results. When, comparing the data collected from the smartphones to the values collected with high precision inertial profilers the coefficient of determination between the smartphone and the reference was 0.57.
To integrate the data collected from many vehicles using crowd sourcing, the authors proposed an empirical Bayesian approach. This approach is a statistical tool to make better estimates after each sample is collected, it keeps updating the IRI measurements after each sample. The form presented for this approach is given in Equation (2-13).

$$IRI_{updated} = w_1 * IRI_{current} + (1 - w_1) * IRI_{smpartphone} \quad (2\text{-}13)$$

Where $IRI_{current}$ is the first IRI sample, either from an inertial profiler or a smartphone, $IRI_{smartphone}$ is the IRI calculated from the smartphone, and w_1 is a weighing factor set at 0.9 with the assumption that the current IRI is more reliable that the single IRI sample from the smartphone (69). Even though the author presented the empirical Bayesian approach to estimate the current IRI based on crowdsourcing data collection, the authors did not account for the randomness of data collection. In other words, this study does not show the effect of randomly selecting vehicles from different vehicle classification to estimate IRI. Furthermore, in the case of not historical data on IRI, the authors do not estimate the minimum of samples require for data convergence.

2.3.5.5 Roadroid™

Roadroid™ is a commercially available smartphone app to estimate pavement roughness. In one of their first studies, the authors used three different vehicles and drove the same section at six different speeds with five replicates for each case using 2 smartphone devices. The experiment results showed differences between vehicles at different speeds, and the smartphone. Based on this, the authors developed their algorithm and calibrated accordingly. Similar to other models, the smartphone picks up the vertical acceleration from the vehicle and with the developed algorithm an IRI estimate is calculated (70, 71). The Roadroid™ app has been used in projects in Sweden, Burma, Afghanistan, Turkey, and other places (72, 73). This application, can be used with any smartphone, however, some recommendations on mobile devices are given, to provide a better estimate. This app is not intended to use it as a crowdsourcing device but instead to use it by agencies with a small vehicle fleet to carry out the data collection, always at a recommended speed of 50 km/h since changing speeds has shown repeatability issues (74).

2.3.5.6 BumpRecorder™

The BumpRecorder™ is another commercially available smartphone/mobile device application developed in Japan by Yagi (2010). To estimate IRI the BumpRecorder™ model first makes an estimates of the suspension parameters, then using the spring parameters the equation of motion of one mass model is used. The model schematics is shown in Figure 2-10, and the response model is shown in Equation (2-14). Where L_z is the sprung mass vertical movement, u is the un-sprung mass vertical

movement, ω is the angular frequency, h is the estimated damping ratio and f is the estimated resonant frequency.

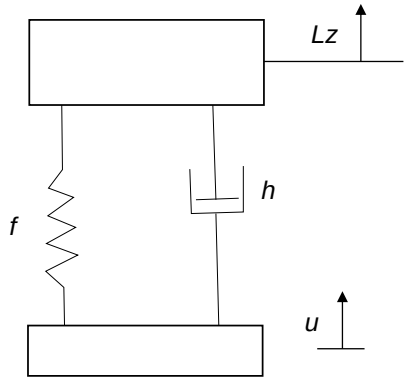

Figure 2-10. Model Schematics BumpRecorder.

$$\ddot{L}_z + 2h\omega\left(\dot{L}_z - \dot{u}\right) + \omega^2(L_z - u) = 0 \qquad (2\text{-}14)$$

The developer of the BumpRecorder™ app states that with this model, the longitudinal profile is calculated, and then the quarter car simulation is applied, this way the result will be independent of the device used (75).

2.3.5.7 Smartphone Sensor Abnormality Detection Studies

In a study made by Eriksson et. al. (2008) they develop an algorithm to identify potholes using 3-axis acceleration sensors with a GPS devise. The device was installed in 7 taxis, and it was placed in the same location to reduce variability in the analysis. The taxis acquired data for 9730 km in total, 174 km of road was covered with ten or more repeated passes, and 2492 km of non-repeated roads were covered. Eriksson describes the method they used for filtering data and their algorithm was trained so that it can make pothole detection more accurate (76).

Another research carried out by Mednis et al (2011) used android smart cell phones for their pothole detection. They used a different approach than Eriksson by using different cell phones and developed their own algorithm for pothole identification which includes a self-calibration (77).

A study made by Koch, et. al. (2013) had a different approach in detecting potholes. This approach is video based assessment and they assure that this methodology can have a better assessment on the severity and extent of potholes. The video analysis consists in texture analysis of the pavement. The algorithm can detect a change in texture and relate it to potholes (78).

2.4 Big Data Collection and Applications

There are many definitions of big data, but in general it is mostly agreed that big data consists of a large and complex data set that is generated from different sources that provides a better insight, improves decision-making, and enables process automation in a fact-based management system (79-81). Big data analytics requires extensive use data, and advanced statistical and quantitative analytic techniques to analyze the data volume, the velocity, the reliability and the variability of this big data sets to make decisions (82). The analytic methods are categorized basically in three: Descriptive, Prescriptive, and Predictive. Descriptive methods provides a description of the system and gives an idea of what is happening. Predictive methods uses the information to create projection models of the system and help look into future possible outcomes. Prescriptive methods are intended to analyze the big data based on a performance measure to identify what are the best practices in a system (83, 84). This research study is based on prescriptive analytics

in which the performance measure is a ride quality index with the sole purpose of optimize the road network condition given a limited budget.

2.4.1 Crowd Sourcing

Databases are typically generated by companies to analyze specific performance indicators in their business. These databases can become very large and in modern practice big data analytics are used to identify trends and optimize processes (85). In recent years, crowd-sourcing has gain importance, especially in the informatics industry, but it can be applied in many fields. Practically, crowd-sourcing refers to the practice where in companies do not perform data collection, and instead open services to the public in exchange for data. It can be considered as a participatory approach from a group large enough to solve a problem that would otherwise be expensive, labor intensive, and/or inefficient (85). Goodchild calls citizen science when describing crowdsourcing using the public. With increasing connectivity and availability of smartphones, portable devices and sensors for data collection there are many project involving citizen science to provide useful insight for specific topics. Crowdsourcing in the sense of using the public has been helpful in monitoring air and environmental quality, geo-mapping, travel time estimators, and others (86). The popularity of this approach has increase since is a cost-effective way to collect information, especially in projects where continuous monitoring and planning is needed (85). Current practices in pavement condition assessment limits the continuous monitoring of a road network because it would be time consuming and expensive.

2.4.2 Central Limit Theorem

The Central Limit Theorem states that when independent identical random variables are added regardless of the distribution and properly normalized, will have the distribution converge into normality as the number of sample size increases. Assume x_1, $x_2,\ldots, x_n$ are random independent variables with the same distribution, the average value is given by Equation (2-15) and as the number of samples goes to infinity, the mean will always converge to a normal distribution, regardless of the distribution of x with variance σ^2. Also, the variance is inversely proportional to the sample size N (87, 88). This implies that larger the sample size, smaller the standard error.

$$\bar{X}_N = \frac{1}{N}\sum_{i=1}^{N} x_i \qquad N \to \infty \tag{2-15}$$

2.4.3 Monte Carlo Simulations

The methodology to estimate ride quality in this study is based on a big data collection through a crowdsourcing sensor solution that uses real time measurements. Since the measurements are taken from random vehicles and not the entire population, the values for the suspension parameters, smartphone mount and other factors are unknown, the proposed solution to this is to assume a probabilistic likelihood of the parameters and interpret those measurements through the lenses of these probabilistic distributions. The method adopted to deal with this effect is the Monte Carlo method.

The Monte Carlo method is a multivariate statistical method that uses stochastic distributions of variables in some physical process to predict o simulate the outcome and variability of a given system (89). The output variable from a model is calculated based on the random input variable for which the statistical distribution of the random variable is known (90). The key of a Monte Carlo simulation is to know the probability distribution of the input variable. The probability distribution of the input variable can be known by using any statistical software. Based on the probability distribution of the input variable, one can generate random numbers and perform as many simulations needed to calculate the average, standard deviation, the standard error and confidence interval. The usefulness of the Monte Carlo simulation is that given the input statistics of the roughness measurement model parameters, thousands of simulations can be run until the computed value converges into a single value within an acceptable margin of error.

A key element in this study is to estimate the minimum number of random samples necessary to yield a reliable estimate of the mean ride quality for a given pavement, i.e., to identify the conditions necessary for convergence. Since the data contains multiple factors that can induce variability in the results, the hypothesis is that, by collecting a sample big enough, the results will converge to a specific value based on the central limit theorem. As the sample size increases, the de standard error decreases. Since this study takes random sampling of ride quality measurements, there is not an exactly deterministic result. For this study, an acceptable error has to be set to determine the sample size for a given road section. This study used the Monte Carlo method to estimate sample size.

2.5 Summary

A pavement management system is required to systematically schedule maintenance in a timely manner to improve the overall pavement network condition. There are many different performance indices available that can be used to evaluate pavement condition. The success of a pavement management system will be dependent on how good these performance indices are calculated. In current practices, agencies uses sophisticated equipment to monitor pavement condition. This equipment is usually expensive and not all agencies can afford to purchase it. Another method is to carry out manual condition surveys, but this approach is time consuming and requires some level of expertise to rate the condition of a pavement. With today's computational capabilities and vehicle connectivity it is possible to develop a framework to continuously monitor road condition not by making high precision and costly equipment, but rather by embracing the variability in the data collection and a large number of samples.

As stated before, there are many performance indices used in pavement management system. One that is of importance for this research is the IRI as a measure of pavement roughness. IRI is a widely accepted performance index, and has been used as a base by many researchers that have tried to characterize pavement roughness using inertial sensors embedded in smartphones. When researchers, propose a solution to roughness measurements using smartphone, usually they try to build a model with very limited information or a very controlled set up, and focus only in calibrating their model to a specific setting. Then, it is assumed that by using crowdsourcing, the accuracy of their data will improve. What they fail to account in their studies are two things; 1) the variability from many factors such as different vehicles, driver, speed, cellphone and

other factors, and 2) they do not provide a number of how large the dataset needs to be in order to reach convergence in their roughness measurements.

While the idea of using inertial sensors in smartphone is novel, the proposed use of this technology does not establish a framework where ride quality measurement can be randomly collected from a vehicle spectra and how this measurement can be integrated into a pavement management system. This research study presents a framework for ride quality data collection and how it can be integrated into a pavement management system.

Chapter 3 Smartphone Data Collection Field Studies

3.1 Introduction

This chapter describes the methodologies used for data collection and analysis. It also includes the description of a study divided in three different sub-experiments;

- Sub-experiment one, Preliminary Study, was carried out with the objective of adjusting the ride quality model, and to identify possible factors that can affect the data collection from a single vehicle.
- Sub-experiment two, the Comprehensive Study, was to calibrate the ride quality model to a broader and more real life scenarios that includes different vehicle classifications on a larger scale.
- Sub-experiment three, Heavy Vehicle Study, was carried out to evaluate an extreme scenario by comparing ride quality measurements to heavy duty commercial trucks.

3.2 Data Collection and Analysis

3.2.1 Automatic Road Analyzer

It is a common practice to collect road profiles using highly sophisticated equipment to later estimate ride quality or pavement roughness indices. Since 2009 the City of Phoenix has been using an Automatic Road Analyzer (ARAN), to monitor pavement condition, Figure 3-1. By practice, the city collects distress information on arterials and collectors every two years. The ARAN is mainly equipped with high definition cameras and inertial profilers. The distresses are quantified by processing the

high definition videos and the IRI is calculated from the profiler measurements. Results, as reported by the City of Phoenix are used in this study.

Figure 3-1. City of Phoenix ARAN (Source: AZcentral.com).

3.2.2 Smartphone Sensing

The methodology used for this study involves the use of smartphones which are equipped with 3-axis accelerometers, gyroscope, GPS, and other sensors. The smartphone is placed on the windshield with a cellphone mount (Figure 3-2), and then, a generic smartphone application is used to collect the information from these sensors. The methodology to process and analyze the output from the accelerometer measurements are explained in more detail in the following sections as are the specific make and model of phones used.

Figure 3-2. Smartphone Set Up in a Windshield.

Most smartphones are equipped with 3-axis accelerometer and other sensors. There are many android and iOS applications that can be used to record this acceleration. The two applications used for this study were AndroSensor and SensorLog for android and iOS devices respectively. These applications begin recording when the user selects record and continue until the user pauses or cancels the collection. The programs then create a comma delimited file that can be exported to Excel. These applications record a timestamp, the geographical position, the 3-axis acceleration, and the pitch, roll and yaw. Depending on the capabilities of the device, the applications can record vibrations at very high speed, between 10-100 samples per second or even more. In this research, a sampling rate of 10 data points per second was adopted based on the moderate speeds that were used.

A primary input for the modeling here is the vertical velocity and displacement, which are related to measured acceleration through integration. From the linear equations of motion the vertical velocity and displacement of the cellphone, sprung mass and unsprung mass can be calculated by Equations (3-1) and (3-2).

$$\dot{z}(t) = \int \ddot{z} d(t) \tag{3-1}$$

$$z(t) = \int \dot{z} d(t) \tag{3-2}$$

In this research, the integrals were solved numerically using the trapezoidal rule, Equation (3-3) and (3-4).

$$\dot{z} = \int_{t_i}^{t_{i+1}} \ddot{z}(t)dt \approx \left[\frac{\ddot{z}(t_i) + \ddot{z}(t_{i+1})}{2}\right] \times (t_{i+1} - t_i) \tag{3-3}$$

$$z = \int_{t_i}^{t_{i+1}} \dot{z}(t)dt \approx \left[\frac{\dot{z}(t_i) + \dot{z}(t_{i+1})}{2}\right] \times (t_{i+1} - t_i) \tag{3-4}$$

As an example, Figure 3-4 shows the input acceleration, and the calculated vertical velocity and displacement of the smartphone.

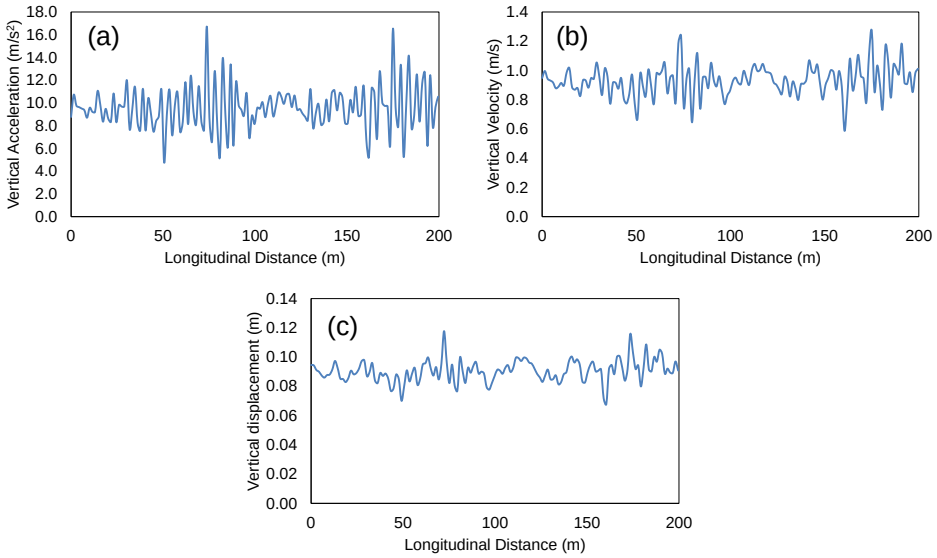

Figure 3-3. Sample Calculation of Cellphone Motion. (a) Input Acceleration; (b) Velocity; (c) Displacement.

A smartphone data collection introduces a physical component not related to the overall ride quality of the vehicle. In short, by using a smartphone to record motion, the smartphone is recording the motion of the smartphone itself and not the motion of the sprung and un-sprung mass. Another important consideration is the position or orientation of the smartphone, and that the mobile device must be fixed either in the windshield or on the dashboard. Smartphones are equipped with 3-axis accelerometer as well with gyroscope sensors that can record the acceleration in the vertical, longitudinal and transverse axis as well as the pitch, roll and yaw. Knowing this information, the resultant vertical acceleration can be computed from the vertical component of each acceleration.

To calculate the response of the sprung mass, a quarter car based approximation (essentially an assumption that the vehicle is completely symmetric) is first adopted and then the mount is modeled using a spring and dashpot suspension assumption. In this case, similar to the quarter car model, the smartphone roughness measurement model is composed of the un-sprung mass and the sprung mass system plus the contribution from the cellphone movement. The schematic of this model is shown in Figure 3-4.

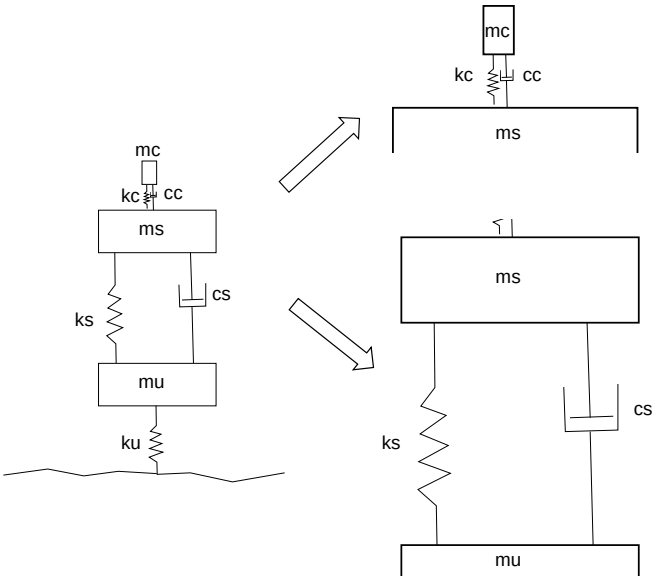

Figure 3-4. Physical Smartphone Measurement Model.

By decoupling the response model which include the smartphone mounting set up, the force acting on the smartphone can be describe by Equation (3-5).

$$F_c(t) = m_c\ddot{z}_c = -m_c g - c_c\dot{z}_c(t) + k_c\left[h - z_c(t)\right] + F_s(t) \tag{3-5}$$

Where F_c is the resultant force acting on the cellphone, $\ddot{z}_c$ is the resultant vertical acceleration of the smartphone, c_c and k_c are the cellphone mounting system damping and stiffness coefficients, and F_s is the force due to the sprung mass. When in equilibrium, similar to the sprung mass response model, and re-arranging the expression in terms of the sprung mass vertical acceleration, $\ddot{z}_s$, the model can be written as shown in Equation (3-6).

$$\ddot{z}_s(t) = \frac{m_c}{m_s}\ddot{z}_c(t) + \frac{c_c}{m_s}\dot{z}_c(t) + \frac{k_c}{m_s}z_c(t) \tag{3-6}$$

Since the ratio of the cellphone mass to the sprung mass is very small (m_c/m_s), Equation (3-6) can be reduced to Equation (3-7).

$$\ddot{z}_s(t) = \frac{c_c}{m_s}\dot{z}_c(t) + \frac{k_c}{m_s}z_c(t) \tag{3-7}$$

Where the vertical acceleration of the sprung mass can be calculated from the stiffness coefficient of the smartphone mounting, k_c, and the vertical displacement of the smartphone z_c. the acceleration of the unsprung mas is given by Equation (3-8). Where $\ddot{z}_u$ is the vertical acceleration of the unsprung mass m_u.

$$\ddot{z}_u(t) = \left[\ddot{z}_s(t) + \frac{c_s}{m_s}\dot{z}_s(t) + \frac{k_s}{m_s}z_s(t)\right]\frac{m_s}{m_u} \tag{3-8}$$

Assuming the golden car parameters, the only unknowns in the system are k_c and c_c. The stiffness and damping parameter in the model is backcalculated using the solver function from Excel. Taking a reference IRI measurement from high precision equipment, it is assumed that the roughness calculated using the data collected by the smartphone must be equal to the reference IRI, therefore, the k_c and c_c parameters can be backcalculated to get the same result as the reference. Once this value is known, the typical vehicle response model can be applied to estimate the vertical motion of the sprung and un-sprung mass and then calculate the ride quality index (RQI) the same way IRI is calculated. With input acceleration $\ddot{z}_c$, using trapezoidal rule for numerical

integration to compute the vertical velocity and displacement, and assuming an arbitrary coefficient for the smartphone mount stiffness, Equations (3-7) and (3-8) can be used to calculate $\ddot{z}_s$ and $\ddot{z}_u$. Figure 3-5 shows the plot for the motion response of the smartphone, sprung and un-sprung mass.

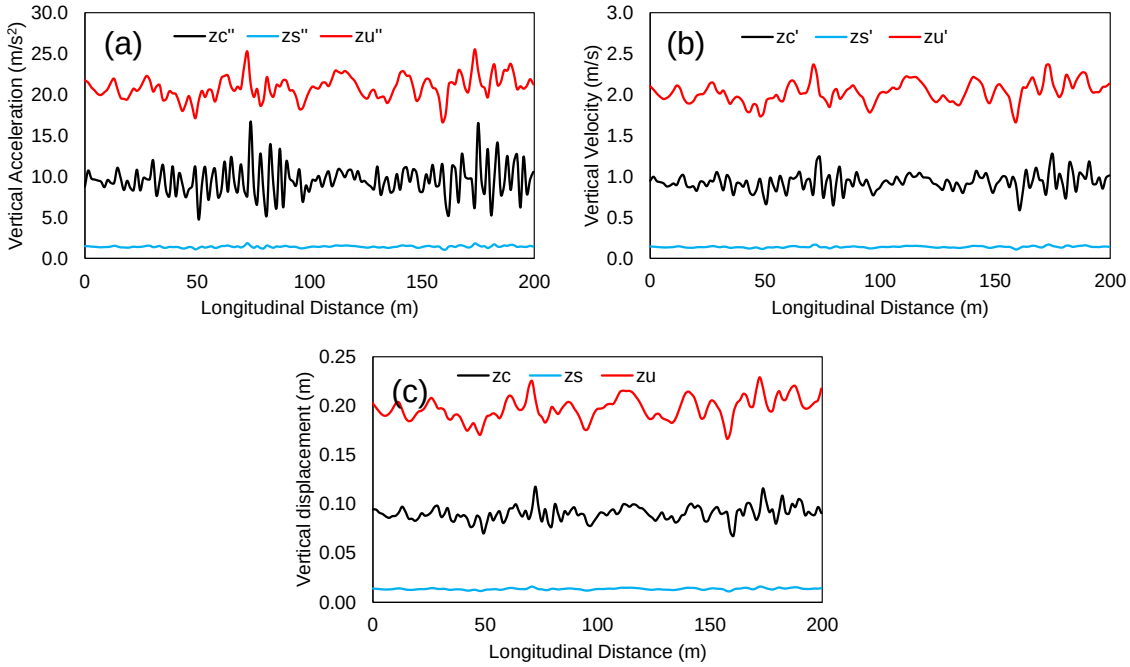

Figure 3-5. Vehicle Response Measurements for Some Arbitrary Coefficient.

3.3 Preliminary Study

The main objective of the preliminary study was to carry out a small study to refine the smartphone ride quality measurement model and to get a better insight from multi-factor variability. A preliminary study on ride quality was carried out in three pavement locations in the city of Phoenix. A total of 36 runs from a full factorial design of experiment (DOE) with three replicates were performed on each section. To be consistent with the City of Phoenix surveying practices, the data was collected on the

right lane for a two-lane road and on the middle lane for a three-lane road section. For illustrative purposes only, results were compared to those collected from the city of Phoenix's Pavement Management Group. Table 3-1 summarizes the factors used for this design, and the full DOE is shown in Table 3-2. The study locations and individual factors are described in more detail later.

Table 3-1. Factors Used for DOE.

Factors	Quantity
Location	3
Vehicle	1
Smartphones	2
Speed	2
Mounts	3

Table 3-2. Full Factorial DOE

Run	Speed	Cellphone	Mount	Run	Speed	Cellphone	Mount
1	S1	C1	M1	19	S1	C2	M1
2	S1	C2	M1	20	S2	C1	M1
3	S1	C1	M2	21	S2	C2	M3
4	S2	C1	M3	22	S1	C2	M2
5	S2	C1	M1	23	S1	C1	M3
6	S2	C1	M2	24	S2	C1	M3
7	S2	C2	M1	25	S2	C2	M2
8	S1	C1	M1	26	S2	C1	M1
9	S1	C2	M3	27	S2	C1	M3
10	S2	C2	M2	28	S2	C1	M2
11	S1	C1	M3	29	S1	C2	M1
12	S2	C1	M2	30	S1	C2	M2
13	S1	C2	M2	31	S1	C1	M2
14	S2	C2	M3	32	S1	C1	M3
15	S1	C2	M3	33	S2	C2	M3
16	S2	C2	M2	34	S1	C2	M3
17	S1	C1	M2	35	S1	C1	M1
18	S2	C2	M1	36	S2	C2	M1

S1= -8 km/h from posted speed. S2= +8 km/h from posted speed. C1= cellphone 1. C2= cellphone 2. M1= mount 1. M2= mount 2. M3= mount 3.

3.3.1 Study Locations

Three locations in the city of Phoenix where chosen for this study: Glendale Avenue, Van Buren Street and 44th Street. Glendale Avenue section from between 7th St. and Central Avenue, is a hot mix asphalt pavement (HMA) arterial 2-lane road which was overlaid two weeks prior to the data collection. The section did not show any major distress, Figure 3-6 (a). Van Buren Street from 28th Street and 32nd Street section is a 2-lane urban arterial consisting of HMA pavement. Some of the distresses found in this location were moderate block and edge cracking extending about 60% of the entire section, small potholes and rutting, Figure 3-6 (b). The pavement section on 44 Street runs from Thomas Road to Indian School Road is a 3-lane arterial with HMA pavement. The pavement in this location did not show any visible distress, Figure 3-6 (c). The description for each section is summarized in Table 3-3.

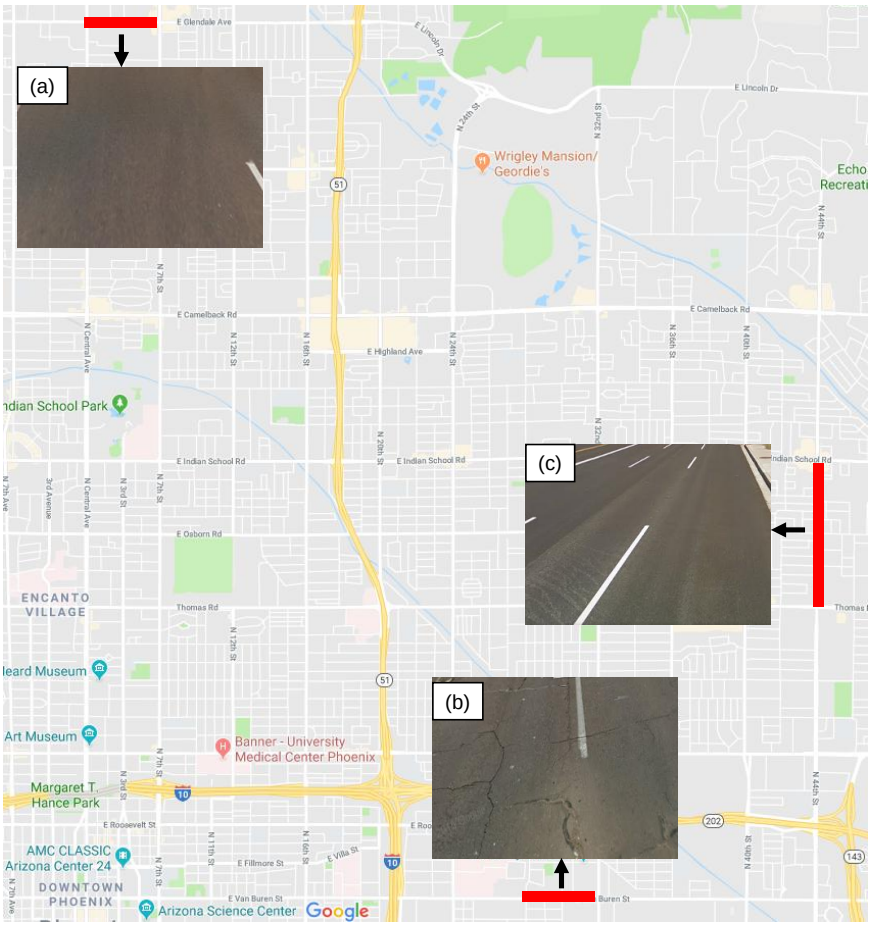

Figure 3-6. Map and Pavement Condition. (a) Glendale Ave.; (b) Van Buren St.; (c) 44th St.

Table 3-3. Summary Description of Each Location.

Section	Length (m)	Pavement Type	Classification	Speed Limit (km/h)	Distresses
Glendale Ave.	800	HMA	Arterial	72	No visible distresses
Van Buren St.	800	HMA	Arterial	56	Block cracking, potholes, rutting, edge cracking
44th St.	1600	HMA	Arterial	72	No visible distresses

3.3.2 Study Factors

A single, 2013 Hyundai Elantra with a vehicle gross weight rating of 1720 kg, was used for the preliminary study. More details about the vehicle are given in Table 3-4.

Table 3-4. Summary of Vehicle Information

Make	Model	Year	VGW (kg)	Tires	Tire Pressure MPa
Hyundai	Elantra	2013	1720	P205-55R16 89H	241

VGW= vehicle gross weight

Aside from the vehicle the factors evaluated included; 1) two smartphones, 2) two speeds at ± 8 km/h from the posted speed limit, and 3) three smartphone mounts. The smartphones selected for the preliminary study were an iPhone 5s and a Motorola Moto G. These two phones were chosen from a pilot study of four smartphones (iPhone 5s, Motorola Moto G, Samsung Galaxy SII, Samsung Galaxy 5s) because they resulted in the most extreme values for RQI measurements. The smartphone applications used to collect the vertical acceleration were the SensorLog and Andro Sensor for the iOS and Android systems respectively. The different mounts used in the preliminary study and cellphones are pictured in Figure 3-7 along with their naming convention. Mounts 1 and 2 were placed in the middle of the windshield, and mount 3 was attached to the dashboard. The selection of mounts 1 and 2 were based on the same pilot study used to select the smartphones, and Mount 3 was arbitrary added in the study.

2013 Elantra

Mount 1 Mount 2 Mount 3

C1 iPhone 5s C2 Mototola Moto G

Figure 3-7. Devices Used for Preliminary Study

3.3.3 Ride Quality Index Analysis and Results

Figure 3-8 to Figure 3-10, show the first 8 runs from the DOE for each location. Included in these figures are the IRI values reported by the City of Phoenix using their ARAN vehicle. Upon first examination, the data from the cellphones show a substantial variation, which suggests some level of calibration is needed. What many researchers have suggest when looking at results like these is that such calibration is needed to yield an equivalent profile to the IRI. It is important to mention that results showing in these figures are the results from individual runs. It is also important to note that although GPS coordinates was recorded for each run, it was not possible to precisely align the starting position in each run.

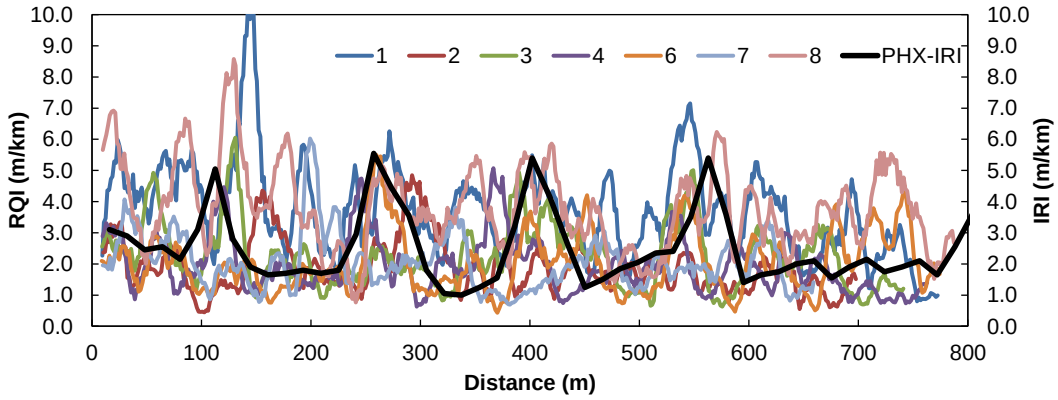

Figure 3-8. Glendale Avenue Individual RQI Measurements.

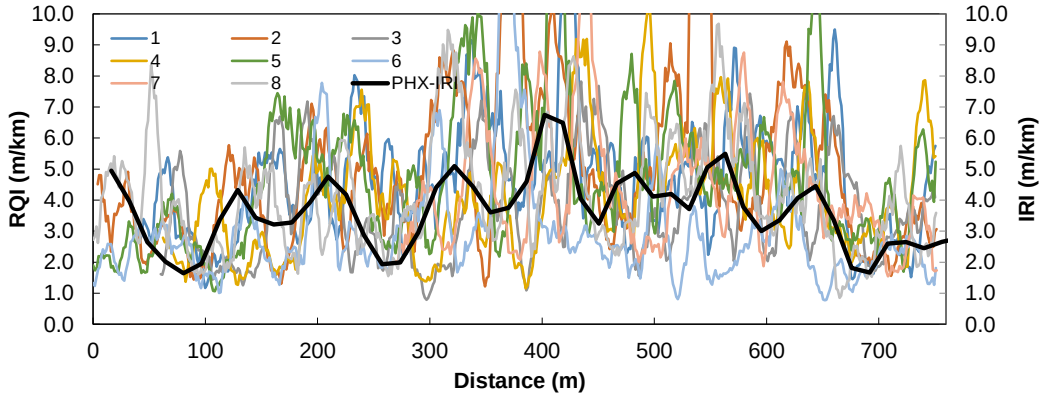

Figure 3-9. Van Buren Street Individual RQI Measurements.

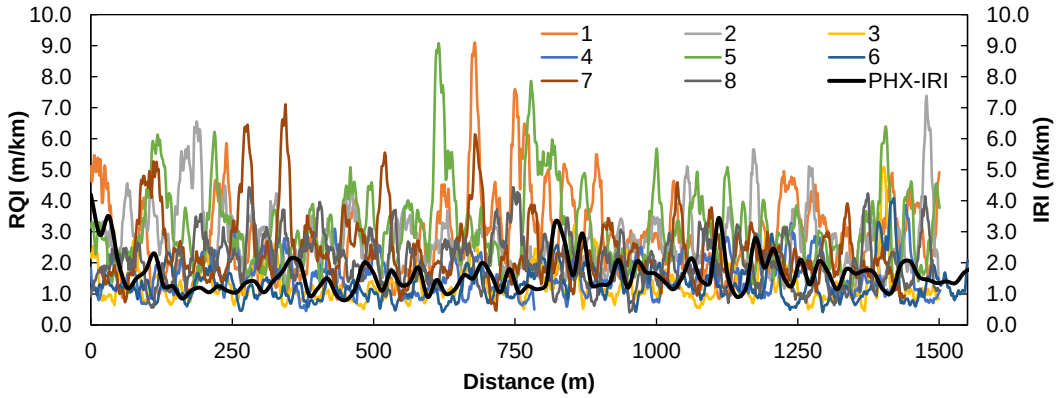

Figure 3-10. 44th Street Individual RQI Measurements.

However, once the individual profiles are combined to generate a single profile, the combined RQI profile smoothens with an increased number of samples. Figure 3-11

to Figure 3-13 shows the combined RQI profiles after different number of runs. The IRI from the City of Phoenix are included in these figures as a reference measure and not necessarily as a comparison.

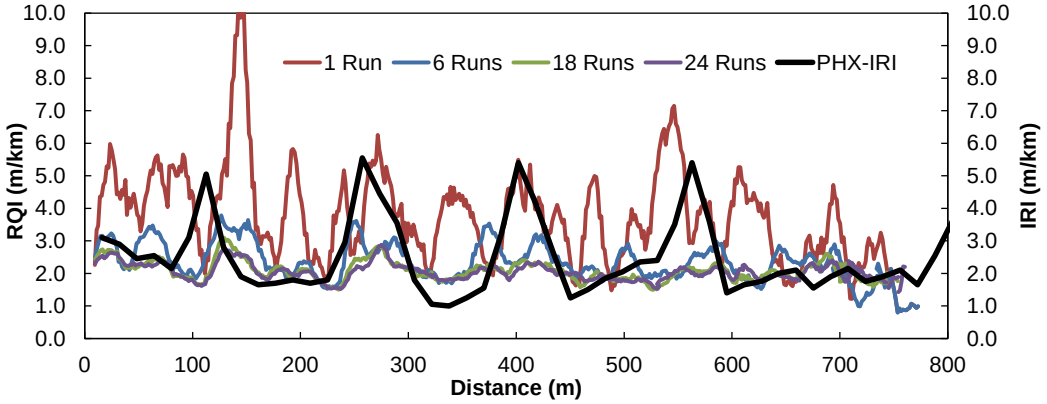

Figure 3-11. RQI Profile Combination Glendale Ave.

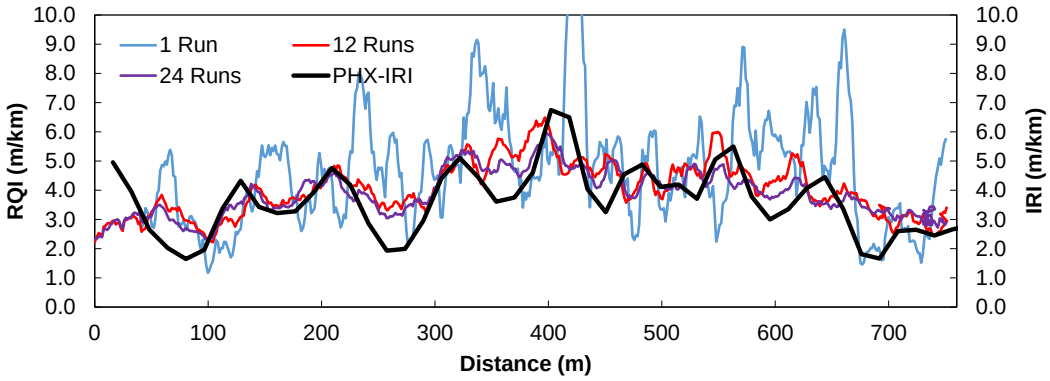

Figure 3-12. RQI Profile Combination Van Buren St.

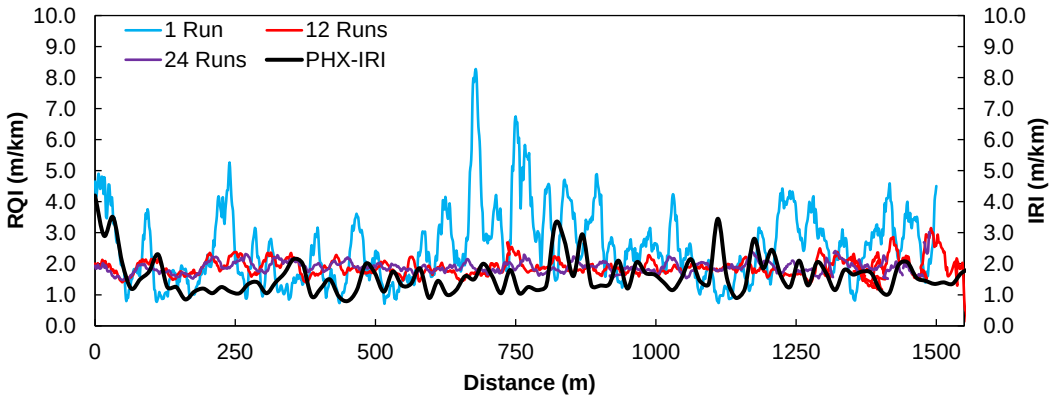

Figure 3-13. RQI Profile Combination 44th St.

To more clearly demonstrate the convergent nature of the data, Figure 3-14 (a), (b) and (c) show the average RQI from the Glendale Ave., Van Buren St., the 44th St. sections respectively, and the dotted line represents the average IRI from the City of Phoenix measurements. From the figures as the number of runs increases, the RQI cumulative average start to converge (after approximately 6-12 runs) into a single value that is similar to the measured reference IRI value. The individual results for this study can be found in APPENDIX C.

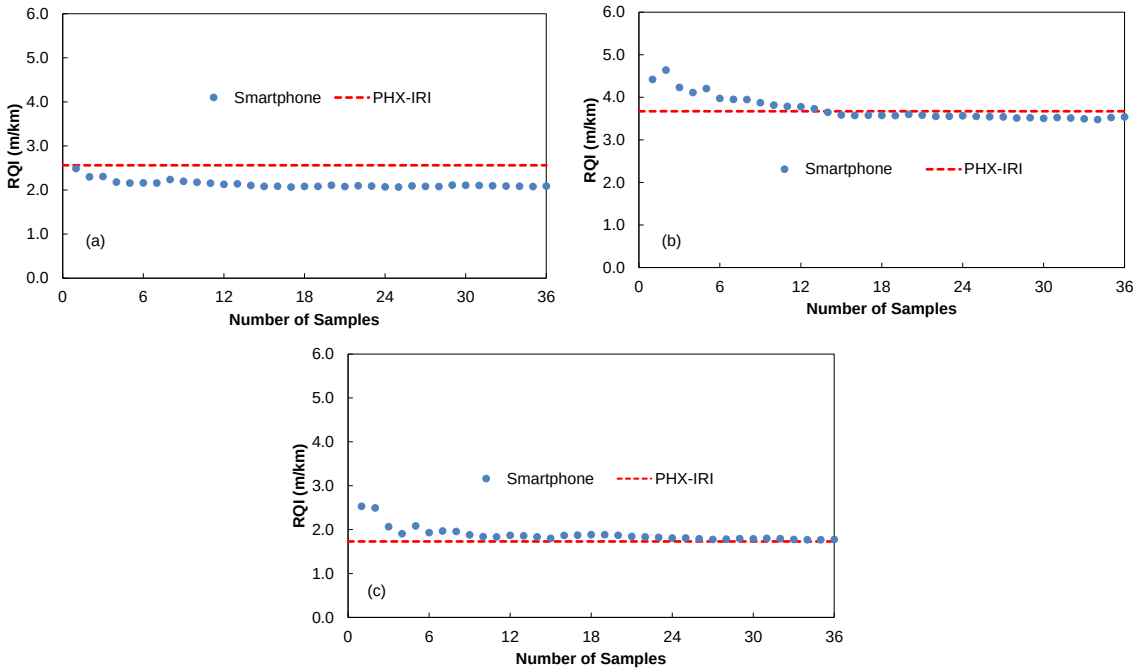

Figure 3-14. Average RQI for Three Locations. (a) Glendale Avenue; (b) Van Buren Street; (c) 44th Street.

Typically the city will report the IRI measurements as an average of the entire section. The average from the 36 runs and the IRI measurements from the City of Phoenix are summarized in Table 3-5.

Table 3-5. Summary of RQI Results from Smartphone Measurements.

Location	RQI (m/km)			IRI (m/km)
	Avg.	Min.	Max.	City of Phoenix
Glendale Ave.	2.1	1.5	3.0	2.6
Van Buren St.	3.5	2.6	5.2	3.7
44th St.	1.8	1.2	2.9	1.7

3.3.4 Multi-factor Statistical Analysis

Before starting with the multifactor statistical analysis, the first thing was to identify the probability distribution from the RQI measurements. . It is important to

understand the distribution of the data collected so proper statistical test such ANOVA can be used to analyze the results. For this research study the Anderson-Darling test was conducted using Minitab. This test is the default test used by Minitab for normality test, but there are others such as Shapiro-Wilk test, Pearson's chi-squared tests, etc. For normality, the Anderson-Darling statistic (AD) for a 95% confidence has to be less than 0.75 in the case where the population mean and the variance is unknown (91). The description and its use for the Anderson-Darling test is presented elsewhere (92). Table 3-6 summarizes the output from Minitab, and Figure 3-15 shows the histogram from the 3 pavement locations.

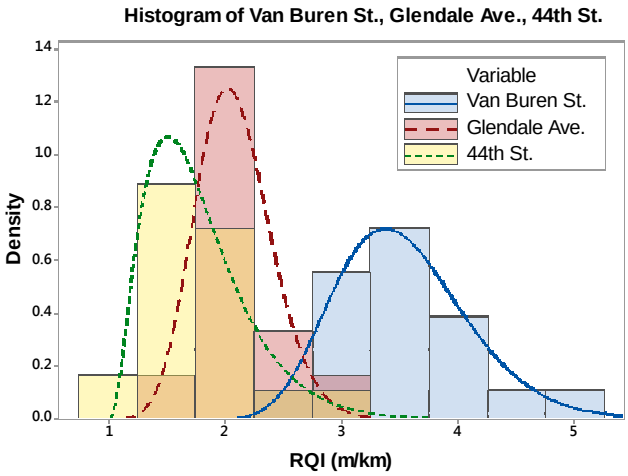

Figure 3-15. Histogram for the Three Locations.

Table 3-6. Normality Test Summary for RQI Measurements.

Probability Distribution	Anderson-Darling		
	Glendale Ave.	Van Buren St.	44th St.
Normal	0.979	**0.495**	**0.571**
Box-Cox Transformation	**0.326**	**0.145**	**0.184**

Table 3-6 shows that the data collected followed normal distribution for the Van Buren St. and the 44th St. locations, and a normal distribution after Box-Cox transformation for the Glendale Ave. location. To make the data normal for the Glendale Ave. location a Box-Cox transform was used using Equation (3-9) (93). Box-Cox transformation is a statistical technique to make the output data *y* normally distributed by changing the parameter λ from -5 to 5. Then properly statistical analysis was made on the data.

$$y_i^{\lambda} = \begin{cases} y_i^{\lambda}; \lambda \neq 0 \\ \log y_i; \lambda = 0 \end{cases} \quad (3\text{-}9)$$

One of the objectives of this Preliminary Study was to identify if the speed, the smartphone and the cellphone mount were significant factors to determine RQI values when a single vehicle was used. Table 3-7 to Table 3-9 show the results from the effect test carried out using the statistical software JMP. The results from the three locations show that the mount has a significant effect in the estimation of RQI index. The type of smartphone showed as significant factor in the Van Buren St. Location, while the speed showed a significant effect on the Glendale Ave. location only. The interaction of the three factors analyzed in this study showed no significant impact in the results.

Table 3-7. ANOVA Results for Glendale Ave.

Factor	Nparm	DF	Sum of Squares	F Ratio	Prob > F
Speed	1	1	0.0173649	7.9101	0.0087
Cell	1	1	0.0014725	0.6484	0.4272
Mount	2	2	0.0691768	15.2296	<.0001
S*C*M	2	2	0.0013191	0.2904	0.7501

Table 3-8. ANOVA Results Van Buren St.

Factor	Nparm	DF	Sum of Squares	F Ratio	Prob > F
Speed	1	1	0.1039701	0.5615	0.4593
Cell	1	1	1.6044444	8.6652	0.0061
Mount	2	2	5.5745257	15.0534	<.0001
S*C*M	2	2	0.1863321	0.4865	0.6197

Table 3-9. ANOVA Results for 44th St.

Factor	Nparm	DF	Sum of Squares	F Ratio	Prob > F
Speed	1	1	0.0106778	0.0737	0.7878
Cell	1	1	0.0009000	0.0062	0.9377
Mount	2	2	2.2356056	7.7201	0.0019
S*C*M	2	2	0.0079056	0.0256	0.9748

A further look into each factor was made to identify any trends in the measurements. The mount was a significant factor in all three locations. It was found that mount 1 gave the highest RQI values. Mount 3 (M3) gave the lowest RQI values, and the results were consistent through all the locations. To continue to investigate this effect, an interaction between mount-cellphone was also analyzed. The results showed that M1 with cellphone 1 (C1- iPhone) gave the highest RQI readings for the Glendale Ave. and Van Buren St. locations. The lowest readings were taken with mount 3 and cellphone 2 (C2- Motorola Moto G). In this controlled scenario, the use of only one of these extremes will under predict or over predict the RQI measurements. The summary of this analysis is shown in Table 3-10 and Table 3-11.

Table 3-10. Results from Mount Effect.

Mount	Glendale Ave.	Van Buren St	44th St.
M1	**2.39**	**4.08**	**2.05**
M2	2.07	3.29	1.83
M3	**1.79**	**3.23**	**1.45**

Table 3-11. Results from Mount-Cellphone Effect

Mount/Cell	Glendale Ave.	Van Buren St.	44th St.
M1C1	**2.45**	**4.27**	1.99
M1C2	2.33	3.90	**2.12**
M2C1	2.03	3.42	1.80
M2C2	2.10	3.17	1.86
NMC1	1.83	3.56	1.54
NMC2	**1.75**	**2.90**	**1.36**

The different cellphone showed to be significant in the Van Buren St. location. The iPhone RQI average was 13 % higher than the Motorola Moto G cellphone. It was also observed with the Glendale Ave. location data that with increasing speed the RQI values were lower than those collected at lower speeds, the difference between collecting data at 14 km/h to 72 km/h can be up to 40 % different. This is similar to studies made by others where specific factors are analyzed an individual calibrations need to be made.

3.3.5 Discussion

This preliminary study gave an insight on three different aspects; 1) the ability of the model to differentiate ride quality characteristic based on different road profiles and conditions; 2) the type of distribution for the data collected; and 3) the statistical significance of using different smartphones, mounts and speeds. Judging from the results collected in this experiment one may agree with other research studies to calibrate the

RQI model for individual factors that affects the RQI measurements (61, 67, 68). The next study, tries to solve the need for a case by case model calibration by looking at a larger population and to evaluate the impact of different vehicle classifications.

3.4 Comprehensive Study

The objective of the comprehensive study is to estimate the variability in ride quality index measurements due to vehicle classification along with other factors such as smartphones, mounts, speed, etc. The intent of this comprehensive study is to get more knowledge on the variability impact from vehicle classification to RQI measurements. This experiment was carried out in the same locations as the preliminary study. A custom design of experiment was created for a single location with a total of 225 runs (Total of 675 runs for all three locations). Out of the 675 runs only 616 (91%) were analyzed, the reason is that either the data output from the smartphone was not recorded properly or there was a missing cellphone. Some researchers suggest that if the missing data is due to random causes, there should not be a problem analyzing and interpreting the data (94). Furthermore, when running ANOVA one of the assumptions is that the variance between the treatments, in this case vehicle classifications, are equal. As a rough estimate, if the ratio between the largest sample variance to the smallest sample variance (F-max) is greater than 9, meaning heterogeneity of the variance, preventive measures should be taken with the data analysis (94). General details of the experiment are shown in Table 3-12 and Table 3-13.

Table 3-12. Factors Used for DOE.

Factors	Quantity
Locations	3
Cellphone	3+1*
Speed	2
Mounts	5
Vehicles/Drivers	45

* 3 base cellphones and 1 from volunteer driver

Table 3-13. Custom DOE for Comprehensive Study

Run	Speed	Driver/Vehicle	Mount	Cell	Run	Speed	Driver/Vehicle	Mount	Cell
1	-1	D2	M1	L1	16	-1	D4	M1	L4
2	-1	D5	M1	L4	17	-1	D3	M2	L2
3	-1	D2	M2	L1	18	-1	D5	M3	L1
4	1	D2	M3	L3	19	-1	D5	M2	L1
5	1	D2	M4	L1	20	1	D5	M4	L4
6	1	D2	M3	L2	21	1	D3	M1	L3
7	1	D3	M4	L2	22	-1	D3	M3	L3
8	1	D4	M4	L3	23	1	D5	M3	L2
9	-1	D1	M2	L2	24	1	D1	M3	L3
10	-1	D1	M4	L1	25	1	D2	M1	L4
11	1	D1	M1	L4	26	-1	D3	M4	L4
12	-1	D2	M3	L4	27	1	D4	M2	L2
13	-1	D3	M4	L3	28	-1	D4	M3	L3
14	-1	D1	M3	L2	29	-1	D1	M3	L4
15	1	D5	M2	L4	30	-1	D3	M3	L1

Table 3-13. (Continuation)

Run	Speed	Driver/Vehicle	Mount	Cell	Run	Speed	Driver/Vehicle	Mount	Cell
31	1	D4	M4	L4	46	1	D1	M4	L3
32	1	D1	M1	L4	47	-1	D1	M1	L3
33	-1	D4	M4	L2	48	-1	D1	M2	L3
34	1	D3	M3	L4	49	1	D5	M1	L2
35	-1	D4	M1	L3	50	-1	D2	M4	L3
36	1	D2	M4	L4	51	-1	D5	M4	L2
37	1	D1	M3	L1	52	1	D5	M4	L1
38	1	D3	M2	L1	53	-1	D2	M1	L2
39	1	D4	M2	L3	54	-1	D3	M1	L1
40	1	D2	M2	L3	55	1	D1	M4	L2
41	1	D4	M1	L1	56	1	D1	M2	L1
42	-1	D4	M4	L1	57	-1	D1	M4	L4
43	1	D3	M2	L4	58	-1	D5	M2	L3
44	1	D4	M3	L2	59	-1	D3	M1	L2
45	-1	D4	M2	L4	60	1	D5	M1	L3

Run	Speed	Driver/Vehicle	Mount	Cell
61	1	D1	NM	L2
62	-1	D5	NM	L2
63	-1	D2	NM	L2
64	-1	D3	NM	L1
65	1	D4	NM	L2
66	1	D5	NM	L1
67	-1	D5	NM	L3
68	1	D3	NM	L2
69	-1	D1	NM	L3
70	-1	D2	NM	L1
71	-1	D2	NM	L3
72	1	D4	NM	L1
73	1	D3	NM	L3
74	1	D1	NM	L1
75	-1	D4	NM	L3

3.4.1 Study Locations

These are the same locations used in the preliminary study. The data collection period lasted for approximately 3 months.

3.4.2 Study Factors

For this comprehensive study a total of 45 vehicles were used. The vehicles were classified as sedan, SUV and minivan, and trucks. Under the FHWA classification, sedan vehicles would be a class 2, and SUV-minivans and trucks as class 3. The total number of vehicles from each classification on every pavement location was five. Table 3-14 to Table 3-16 lists the characteristics of the vehicles used.

Table 3-14. Sedan Description.

Make	Model	Year	VGW (kg)	Tires	Tire Pressure kPa
Dodge	Challenger	2013	2246	P225-60 R18	207
Ford	Focus	2015	1810	215-55 R16 93H	290
Ford	Fusion	2013	1991	P235-50 R17	244
Ford	Fusion	2015	2059	235-45 R18	241
Honda	Accord	2002	1850	P195-65 R15	179
Honda	Accord	2015	1980	P215-65 R16	221
Honda	Civic	2014	1720	P205-55R16 89H	193
Hyundai	Accent	2014	1610	P175-70 R14 84T	262
Hyundai	Elantra	2013	1720	P205-55R16 89H	241
Hyundai	Genesis	2013	1970	245-40 R19 94W	228
Lexus	is 350	2015	2100	P225-45 R17	296
Mitsubishi	Eclipse	2003	1750	P195-65 R15	248
Mitsubishi	Lancer	2014	2060	P205-60 R16	230
Toyota	Camry	2003	1900	P205-65 R15 92T	131
Toyota	Camry	2009	2061	P215-60 R16	234

VGW= Vehicle Gross Weight

Table 3-15. Truck Description

Make	Model	Year	VGW (kg)	Tires	Tire Pressure kPa
Chevy	Colorado	2006	2200	215-75 R15	248
Chevy	Colorado	2007	2200	P225-75 R15	234
Chevy	Silverado 1500	2007	2903	245-70 R17	296
Chevy	Silverado 2500	2001	4173	LT245-75 R16	379
Dodge	Ram 1500	2013	2900	P265-70 R17	290
Ford	F150	2014	3334	P275-65 R18	276
Ford	F-150	2005	3016	P255-65 R17	362
Ford	Ranger	2004	2240	P235-70 R16	255
GMC	Silverado 2500	1991	3266	LT265-75 R16	345
Jeep	Wrangler	2007	2223	R17	255
Jeep	Wrangler	2009	2495	35-12 R17	262
Nissan	Titan	2013	3175	275-55 R20 117H	296
Toyota	Tacoma	2007	2426	265-70 R16	269
Toyota	Tacoma	2017	2545	P265-65 R17	272
Toyota	Tundra	2001	2735	P265-70 R16	296

VGW= Vehicle Gross Weight

Table 3-16. SUV-Minivan Description

Make	Model	Year	VGW (kg)	Tires	Tire Pressure (kPa)
BMW	X3	2013	2330	P245-50 R18	241
Chevrolet	Equinox	2016	2270	P225-65 R17	231
Chrysler	Town n Country	2013	2745	225-65 R17 102H	262
Honda	Odyssey	2016	2730	P235-60 R18	290
Jeep	Cherokee	2009	2586	P245-65 R17	228
Jeep	Cherokee	2015	2291	225-55 R18 98MS	241
Jeep	Grand Cherokee	2008	2727	P245-65 R17	221
Kia	Sorento	2016	2489	235-65 R17 104H	234
Lincoln	Navigator	2011	3737	P275-55 R20 111H	248
MAZda	Cx9	2014	2645	P245-60 R18	290
MAZda	Tribute	2008	2041	P235-70 R16	276
Nissan	Armada	2003	3083	P275-65 R18	248
Nissan	Pathfinder	2016	2715	P235-55 R20	255
Toyota	RAV4	2015	2050	P225-65 R17	172
Toyota	Sienna	2006	2580	P215-65 R16	276

VGW= Vehicle Gross Weight

A total of 45 volunteers participated in the experiment where each volunteer drove one vehicle only, in most of the cases their own vehicle. Each volunteer performed

between 14-17 runs according to the DOE in their assigned location. The only instruction given to the driver was to keep the driving speed and to stay in the corresponding lane (e. g. in a two-lane road drive on the right lane). Table 3-17 gives the ID assigned to all vehicle-drivers for the comprehensive study.

Table 3-17. Driver-Vehicle ID.

ID	Model	Year	ID	Model	Year	ID	Model	Year
D1	Accord	2002	D16	Lancer	2014	D31	Elantra	2013
D2	Genesis	2013	D17	Fusion	2013	D32	Camry	2009
D3	Focus	2015	D18	Camry	2003	D33	Civic	2014
D4	Fusion	2015	D19	is 350	2015	D34	Accord	2015
D5	Accent	2014	D20	Challenger	2013	D35	Eclipse	2003
D6	Silverado 1500	2007	D21	Ranger	2004	D36	Silverado 2500	1991
D7	Titan	2013	D22	Tacoma	2017	D37	Tundra	2001
D8	Tacoma	2007	D23	Colorado	2007	D38	Silverado 2500	2001
D9	F-150	2014	D24	Wrangler	2009	D39	Colorado	2006
D10	Ram 1500	2013	D25	Wrangler	2007	D40	F-150	2005
D11	RAV4	2015	D26	Equinox	2016	D41	Armada	2003
D12	Pathfinder	2016	D27	Navigator	2011	D42	Town n Country	2013
D13	Tribute	2008	D28	Grand Cherokee	2008	D43	Cherokee	2015
D14	Cherokee	2009	D29	Odyssey	2016	D44	Sienna	2006
D15	X3	2013	D30	Sorento	2016	D45	Cx9	2014

The smartphones considered for this study are three base smartphones and one random smartphone belonging to the volunteer driver. The three base phones are the iPhone 5s, Motorola Moto G and the Samsung Galaxy II. In the DOE, the random

smartphone is represented by L4. Sometimes in experiments there are known/unknown, controlled/uncontrolled factors that may have an effect on the response, these are called nuisance factors. These factors can cause the experimental error and the variability to increase. L4 can be considered as a nuisance factor in the sense that is not a controlled factor. The possible undesired variability can be mitigated by randomization (116). These smartphones could be considered as randomly selected from volunteers, minimizing any extra effects on the analysis. Table 3-18 provides a list of the smartphones used based on the operating system. In total, 16 different models were used and a total of 33 devices.

Table 3-18. List of Smartphones Used in the Comprehensive Study.

Android	iOS
Motorola Moto G	iPhone 5s (2)
Galaxy II (2)	iPhone 7 (4)
Galaxy s5	iPhone 7 Plus (3)
Galaxy s6	iPhone 6s (5)
Galaxy s6 Edge	iPhone 6 (6)
Galaxy s7 Edge	iPhone 6 Plus (2)
ZTE	
HTC M10	
1+	
BLU	

Four different smartphone mounts with suction cups were placed in the middle of the windshield (M1-M4), and one mount (M5) was attached to the dashboard, Figure 3-16. Similar to the preliminary study, two speeds at ± 8 km/h from the posted speed limit where considered.

Figure 3-16. Different Mount Types Used in the Comprehensive Study.

3.4.3 Ride Quality Index Analysis and Results

Similar to the Preliminary Study, the cumulative average after every run is shown in Figure 3-17 for all 3 locations. Just by visual inspection of the figures, there seems to be no significant effect on the vehicle classification uses. Furthermore, given the increase in number of random factors and levels, the data starts to converge to a single number after approximately 40 to 45 samples. The cumulative RQI average for the three locations is summarized in Table 3-19. Individual results from this experiment can be found in APPENDIX D.

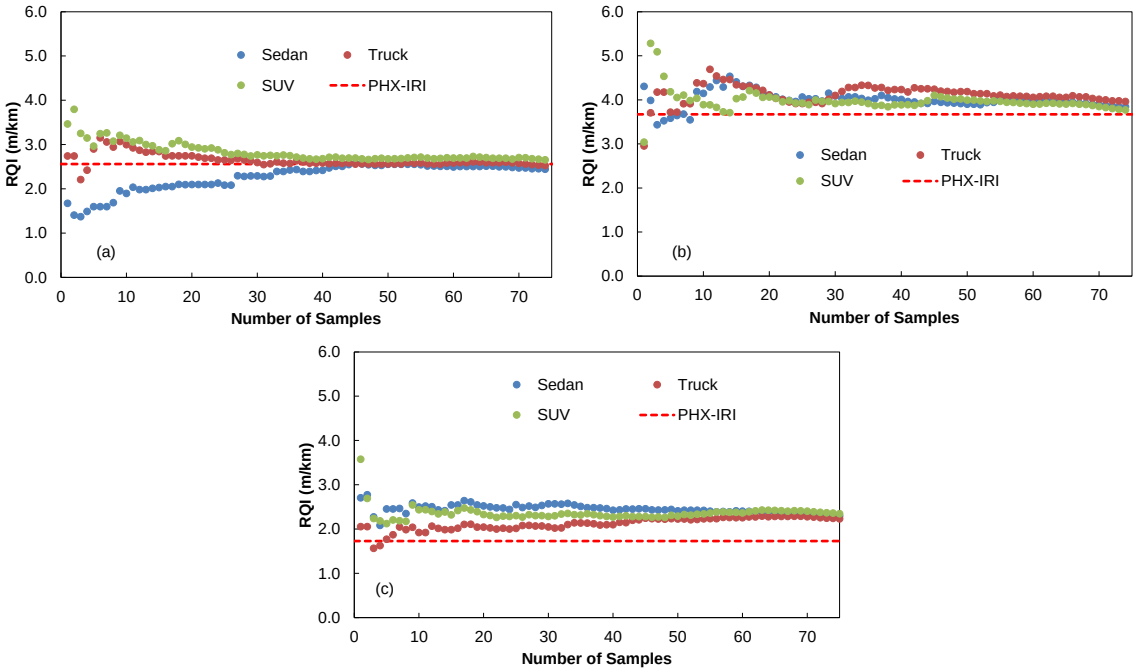

Figure 3-17. Average RQI for Three Locations. (a) Glendale Avenue; (b) Van Buren Street; (c) 44th Street.

Table 3-19. Summary of RQI Results from Smartphone Measurements.

Vehicle Classification	RQI (m/km)		
	Glendale Ave.	Van Buren St.	44th St.
Sedan	2.43	3.82	2.29
Trucks	2.51	3.95	2.23
SUV	2.64	3.76	2.35

3.4.4 Vehicle Classification Comparison

Further statistical analysis was done on this Comprehensive Study to determine if vehicle class will have a significant impact on the RQI measurements. First, to get an overall perspective on the mean and variability by vehicle class, histograms were created for all the RQI measurements. From the histograms shown in Figure 3-18, the data seems to follow a skewed distribution. The Anderson-Darling statistics was used again to determine the type of distribution for the collected data. Table 3-20 to Table 3-22 shows

the summary of the Goodness of Fit Test for all the three sections and all vehicle classification.

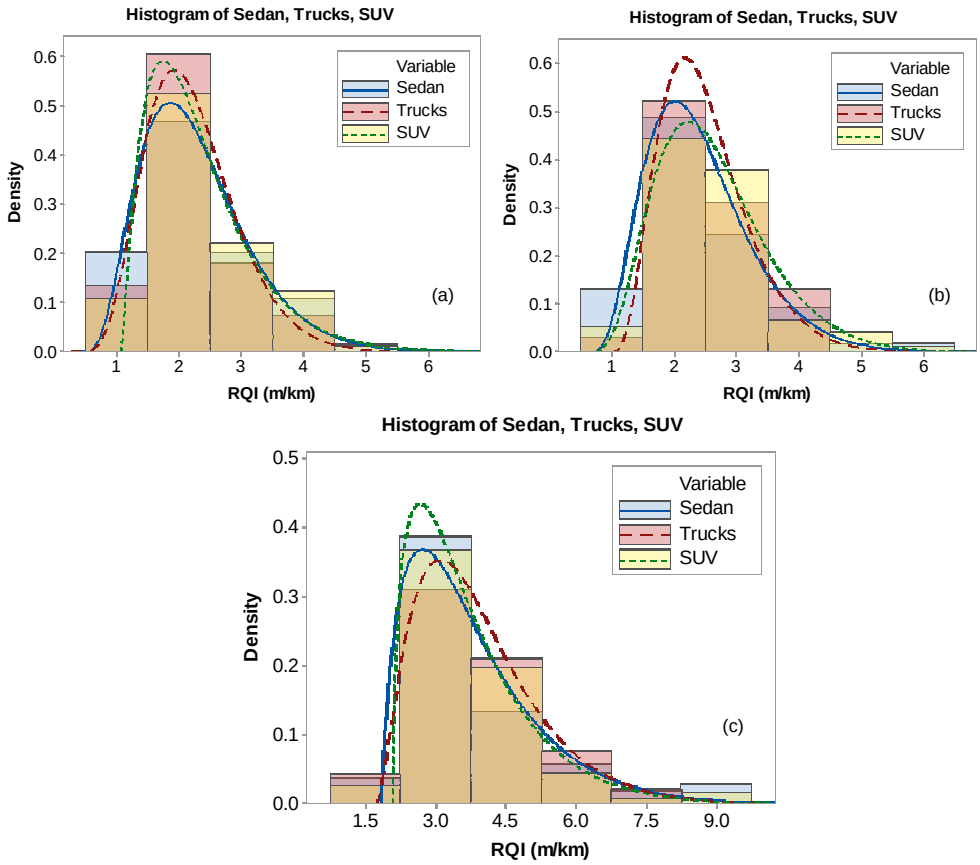

Figure 3-18. Histogram for the Three Locations; (a) Glendale Ave.; (b) Van Buren St.; (c) 44th St.

Table 3-20. Goodness of Fit Test- A-D Statistic for Glendale Ave.

Distribution	Sedan	Trucks	SUV	ALL
Normal	1.504	1.297	1.249	3.391
Box-Cox Transformation	**0.234**	**0.277**	**0.283**	**0.191**
Johnson Transformation	**0.181**	**0.265**	**0.223**	**0.134**

Table 3-21. Goodness of Fit Test- A-D Statistic for Van Buren St.

Distribution	Sedan	Trucks	SUV	ALL
Normal	4.350	1.293	3.345	8.134
Box-Cox Transformation	**0.379**	**0.305**	**0.220**	**0.469**
Johnson Transformation	**0.275**	**0.197**	**0.129**	**0.196**

Table 3-22. Goodness of Fit Test- A-D Statistic for 44th St.

Distribution	Sedan	Trucks	SUV	ALL
Normal	0.778	1.156	2.915	4.013
Box-Cox Transformation	**0.236**	**0.258**	0.958	**0.711**
Johnson Transformation	**0.194**	**0.23**	**0.555**	**0.431**

From the Goodness of Fit Test, the data fallows many statistical distributions. For the interest of this analysis the tables only shows the results for normal after Box-Cox and Johnson transformations. The data was transformed using Box-Cox method for the Glendale Ave. and the Van Buren St. locations, and Johnson method for the 44th St., then ANOVA test was performed on these transforms to see if vehicle class had a significant effect on the measurements. Similar to the Box-Cox transformation, the Johnson transform is another statistical method typically used to make data follow normal distribution. This is a more complex procedure which requires a statistical software to estimate the transform. Basically, the software does an iterative process changing the different parameters and models, and provides de optimal solution to make the data normal. The three models used and parameters are given in Equations (3-10) to (3-12). Where Y is the transformed data, γ,η,ε and λ are the model parameters and x is the original data. More on this transformation can be found elsewhere (95, 96).

$$Y = \gamma + \eta \sinh^{-1}\left(\frac{x-\varepsilon}{\lambda}\right) \tag{3-10}$$

$$Y = \gamma + \eta \log\left(\frac{x-\varepsilon}{\lambda+\varepsilon-x}\right) \tag{3-11}$$

$$Y = \gamma + \eta \log\left(\frac{x-\varepsilon}{\lambda}\right) \tag{3-12}$$

After the proper transformations, the statistical summary for the 3 locations are given in Table 3-23 to Table 3-25. The ANOVA analysis was performed on the vehicle classification, and not on individual parameters or single vehicles. The results showed that there is no statistical significance between sedan, trucks and SUV-minivans. This experiment demonstrated that when looking at a population of vehicles, detailed effects on individual factors becomes not significant. In general, sedan vehicles gave lower RQI than SUV and trucks. Another observation made is that with increasing roughness measures, the variance also increased.

Table 3-23. Statistical Summary for Glendale Ave.

Groups	Count	Sum	Average	Variance
Sedan	65	158.0583	2.43	0.8519
Trucks	72	181.0349	2.51	0.5435
SUV	74	195.4046	2.64	0.8701

ANOVA

Source of Variation	SS	df	MS	F	P-value	F-crit
Between Groups	1.5492	2	0.774612	1.02867	0.3593	3.039
Within Groups	156.6287	208	0.753023			
Total	158.1779	210				

Table 3-24. Statistical Summary for Van Buren St.

Groups	Count	Sum	Average	Variance
Sedan	69	263.6675	3.82	2.7115
Trucks	60	236.8293	3.95	1.8000
SUV	74	278.1570	3.76	2.0511

ANOVA

Source of Variation	SS	df	MS	F	P-value	F-crit
Between Groups	1.1964	2	0.598213	0.27172	0.7623	3.041
Within Groups	440.3128	200	2.201564			
Total	441.5092	202				

Table 3-25. Statistical Summary for 44th St.

Groups	Count	Sum	Average	Variance
Sedan	64	146.8088	2.29	0.7788
Trucks	66	147.1292	2.23	0.5732
SUV	72	168.9377	2.35	0.7882

ANOVA

Source of Variation	SS	df	MS	F	P-value	F-crit
Between Groups	0.4729	2	0.236476	0.33073	0.7187	3.041
Within Groups	142.2863	199	0.715007			
Total	142.75925	201				

3.4.5 Discussion

This Comprehensive Study showed that by combining different factors and conducting a design of experiment with different vehicles and drivers, the effect of a single random factor does not represent a significant impact in the RQI measurements from the population. The increase in random factor levels, increases the variance of the entire experiment resulting in increase of the sample size to determine convergence, which will be explained in the following chapter.

3.5 Extreme Case

The preliminary and comprehensive study focused exclusively on Class 2 and 3 vehicles. A smaller study, named Extreme Case, was conducted with the objective to identify the impact of collecting RQI measurements using heavy duty commercial trucks (Class 4-6) with respect to a typical sedan The motivation for the study was that local agencies might adopt in the future the use of this crowd sourced data collection using their own fleet of vehicles, which may include heavy duty construction trucks, dump trucks, local busses and even waste collector trucks. A total of 23 runs where performed on a single road in both directions, more specific details on the number of runs is given in Table 3-26.

Table 3-26. Experiment for the Extreme Case Study.

Section	Number of Runs	
	Sedan	HD Trucks
Eastbound	8	3
Westbound	8	4

3.5.1 Study Location

This study was carried out on the eastbound and westbound of Honeycutt Rd. in the City of Maricopa Arizona. The measurement was done for the entire 9.9 kilometers of this road. The geometry of the road varies along the entire stretch, and typically in a pavement management system is recommended to split the road into sections whenever there is a change in geometry, traffic or pavement type. For the purpose of this study, sections were created based on the road geometry, and then RQI was estimated for each

subsection as well as for the entire length of the road. The road characteristics is summarized in Table 3-27.

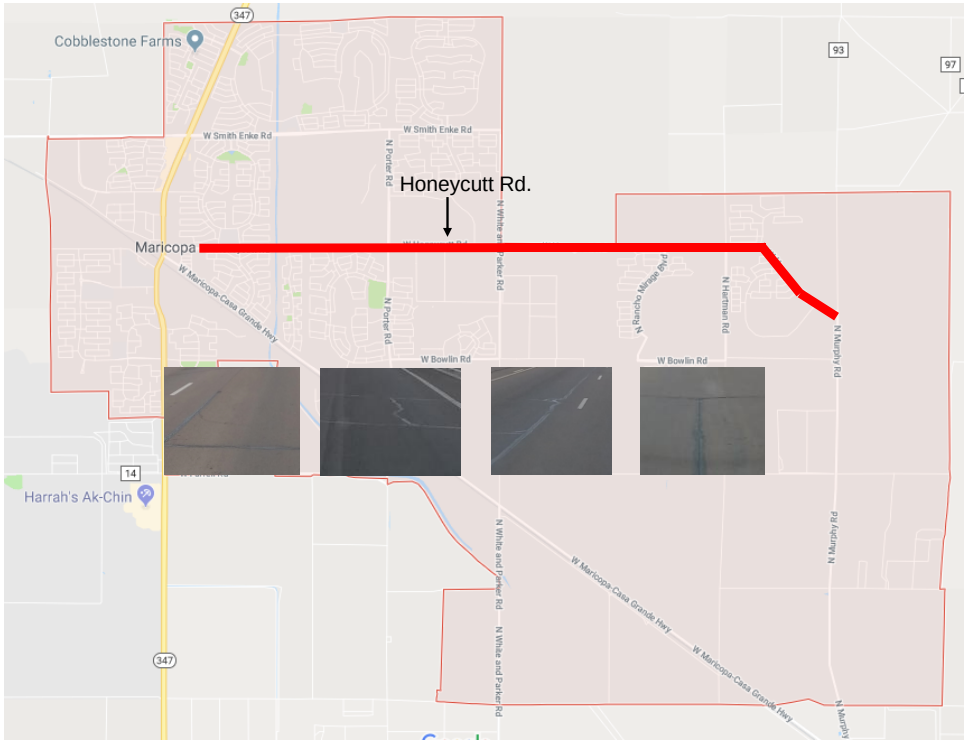

Figure 3-19. Extreme Case Location in City of Maricopa.

Table 3-27. Road Condition Summary.

Section	Length (m)	Pavement Type	Classification	Distresses
Honeycutt Rd.	9900	HMA	Arterial	Some block cracking, depressions, crack sealed, low severity long cracking

3.5.2 Study Factors

The heavy-duty vehicles used for this study were: 1- class 4, 3- class 5 and 2 class 6 vehicles shown in Figure 3-20. The passenger vehicle used was a Hyundai Elantra sedan described in the Preliminary Study.

(a)

(b)

(c)

Figure 3-20. Heavy Duty Commercial Trucks: (a) Class 4; (b) Class 5; (c) Class 6

The measurements from the heavy duty trucks were taken with a single cell phone, a LG G6 Android smartphone, a single cellphone mount, and one driver. The measurements from the sedan were taken using 4 smartphones (Table 3-28, two cellphone mounts and one driver. And finally, the measurements were taken at the speed limit.

Table 3-28. Smartphones Used for Comprehensive Study

Android	iOS
Motorola Moto G Galaxy II (2) LG G6	iPhone 5s

3.5.3 Ride Quality Index Analysis and Results

The measured RQI values from the heavy duty trucks and the sedan were not the same. Figure 3-21 shows a sample of the averaged RQI profile for the first 2000 m from each direction. Even though in some cases the RQI peaks match in some locations, the magnitude of the measurements done by heavy duty truck seems to be higher than those of the sedan. The entire road was split into sections, the summary RQI for all the sections is presented in Table 3-29. The measurements from heavy duty trucks are in average about 50-70 % higher than those measured with a typical sedan.

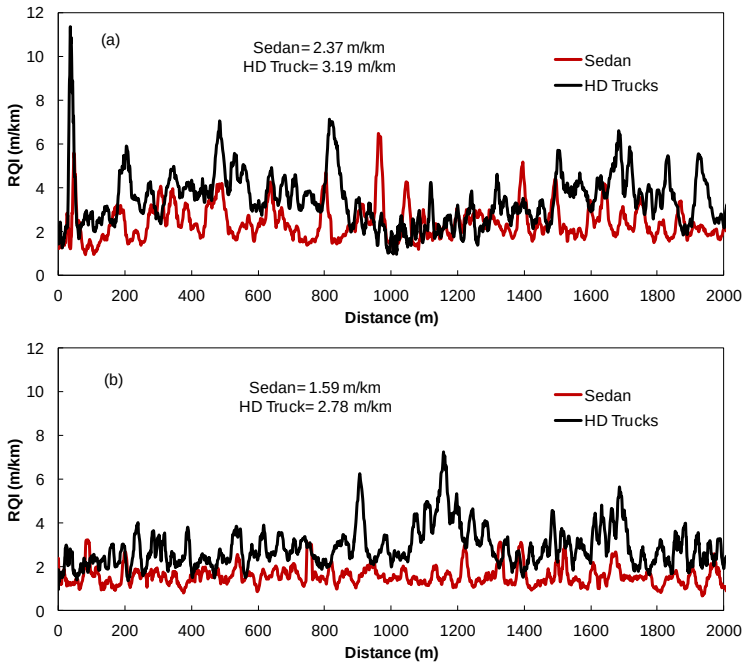

Figure 3-21. RQI Profile for First 2000 m; (a) Eastbound; (b) Westbound.

Table 3-29. RQI Summary for the Entire Road.

Direction	Start (m)	End (m)	RQI (m/km)	
			Sedan	HD Trucks
East	0	350	2.15	3.35
	350	1080	2.52	3.11
	1080	1510	2.43	2.68
	1510	2410	2.13	3.35
	2410	3210	1.48	2.89
	3210	4810	1.74	2.64
	4810	6460	2.06	2.94
	6460	8020	2.42	3.49
	8020	9990	1.82	2.53
	Average		**2.01**	**3.08**
West	0	1990	1.59	2.78
	1990	3550	1.70	2.85
	3550	5200	1.58	3.11
	5200	6800	1.55	2.41
	6800	7600	1.44	2.59
	7600	8500	2.15	3.24
	8500	8930	2.28	3.56
	8930	9660	1.96	3.24
	Average		**1.76**	**3.42**

This study was limited to 6 heavy duty trucks and only 1 sedan, but the ANOVA analysis showed that there is a significant difference between collecting RQI values from heavy duty trucks to sedans. An average increase of 75% for both directions.

Table 3-30. Statistical Summary for Honeycutt Rd Eastbound.

Groups	Count	Sum	Average	Variance
Sedan	8	16.0719	2.01	0.1607
HD Trucks	3	9.2348	3.08	0.4282

ANOVA

Source of Variation	SS	df	MS	F	P-value	F-crit
Between Groups	2.4946	1	2.4946	11.3320	0.0083	5.1174
Within Groups	1.9812	9	0.2201			
Total	4.4758	10				

Table 3-31. Statistical Summary for Honeycutt Rd Westbound.

Groups	Count	Sum	Average	Variance
Sedan	8	14.0938	1.76	0.1904
HD Trucks	4	13.6880	3.42	1.6932

ANOVA

Source of Variation	SS	df	MS	F	P-value	F-crit
Between Groups	7.3507	1	7.3507	11.4636	.0069	4.9646
Within Groups	6.4122	10	0.6412			
Total	13.7629	11				

3.5.4 Discussion

The objective of this Extreme Case study was to determine if collecting RQI values from extreme cases such as sedan and heavy duty trucks make a different in the magnitude of RQI. Results showed that there is a significant difference in the results. Heavy duty trucks RQI values are greater that those measured by sedan vehicles. If using heavy duty trucks for data collection, special calibration may be needed.

3.6 Summary

A mechanical ride quality model to account for the smartphone set up inside the vehicle was developed, and calibrated. One of the main objectives of this study was to create a framework to collect ride quality measurements by relying the data collected from road users. Some of the questions to address by each case study were: 1) Does it matter when using one vehicle? 2) Does it matter when using many vehicles? 3) Or does it matter if using extreme heavy duty commercial vehicles in comparison to typical sedans?

The Preliminary Study aimed to answer the first question, and the results showed that individual random factors that can affect the RQI measurements can be significant. In this case, mount and cellphone showed that are significant factors that can bias the results. The results also showed that the interaction between all the factors was not significant and that the data seemed to converge after 20-30 samples.

The Comprehensive Study showed that when the RQI values from many vehicles of the same classification are averaged and then compared to other vehicle types (sedan-trucks-SUV), there is no significant difference between all of them. There are individual cases that a smartphone-mount-speed-vehicle configuration will give a greater or lower RQI value, but when these cases are combined with many other configurations, the results from this analysis showed that is does not matter, and the difference between vehicle types is not significant. The variance of this experimental study increased in comparison to the Preliminary Study, but the data seemed to converge after 50-60 samples.

Going to the Extreme Case Study, heavy duty commercial trucks showed a significant difference in RQI measurements when compared to a regular sedan. This study was limited by the number of runs that were collected but gave an insight about the difference between those extreme cases.

As a conclusion, if RQI values are evaluated in a case by case basis, there might be a significant difference that will suggest some kind of calibration as has been proposed by many. If the data is analyzed as a whole, meaning not taking one vehicle but instead the entire vehicle spectra, the data shows no significant difference.

Chapter 4 Parametric Assessment of the Factors Affecting Ride Quality Index Estimation and Sample Size Determination

4.1 Introduction

This chapter takes a further step and builds from the results obtained in the case studies presented in Chapter 3. The sequence of these steps is shown in Figure 4-1. First step, a model to incorporate a smartphone device was developed. Second step, a preliminary study was carried out to investigate the effect on individual factors. The results showed that when the measurements are assessed in a case by case basis, the model requires calibration for every particular case. Third step, a comprehensive study involving many factors and many vehicles was carried out to investigate the effect not just on individual factors but instead on a population of different vehicle classifications. The results showed no statistical difference between vehicle classes. Now the next step was to expand the analysis to a broader scenario in which a large vehicle spectra is consider. Since this task would be time consuming, and would require many resources, longitudinal road profiles from the Long Term Pavement Performance (LTPP) InfoPave database were used, and the Monte Carlo method was adopted for RQI estimations.

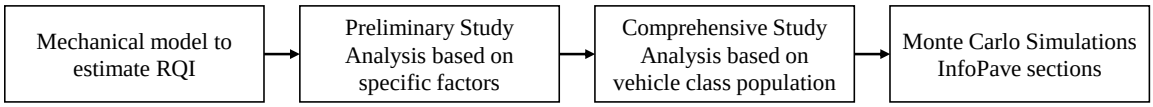

Figure 4-1. Studies Sequence Flowchart.

The following sections presents a description of the road sections from InfoPave database that were used for our RQI simulations, the development of the Monte Carlo simulation approach, the backcalculation of the cellphone mount parameters, and

suspension parameters for different vehicle classification based on literature review. The core of this chapter is the simulations to evaluate the effect of the different vehicle classifications and mixed traffic under three assumptions; 1) vehicles driving in a single lane without wander, 2) vehicles driving in a single lane with wander, and 3) vehicle driving in two lanes without wander. Finally, this chapter concludes with an estimation of the sample size given the traffic spectra and number of lanes from a given road.

4.2 Road Sections from InfoPave

The road sections included in this research study were chosen with the idea of analyzing roads from different states and with different roughness conditions. The Long Term Pavement Performance (LTPP) database InfoPave was used to obtain the information from sections in Arizona, Colorado, California, Minnesota, and New Jersey. A brief description of each sections is given in Table 4-1.

Table 4-1. InfoPave Section Summary.

Section	Lanes	Climate Zone	AADT	IRI (m/km)
AZ-260	2	Dry, Non Freeze	6200	0.88
CO-560	2	Dry, Freeze	3800	1.86
CA-8202	1	Dry, Non Freeze	3900	2.84
MN-1016	2	Wet, Freeze	2300	3.48
NJ-1030	2	Wet, Freeze	4264	5.97

AADT= average annual daily traffic

4.2.1 Arizona

This section is a two lane interstate road on I-10 eastbound at mile post 109, with LTPP id number 04-260. The climatic zone of this region is a dry/non freeze. This road

section has been active for monitoring since 1993. The pavement structure for this location is shown in Figure 4-2, and consist of an unbound granular base of ten centimeters (cm) and an asphalt concrete layer of 24 cm. The elevation profile for this section and the IRI profiles are shown in Figure 4-3. The average IRI for the entire section is 0.88 m/km.

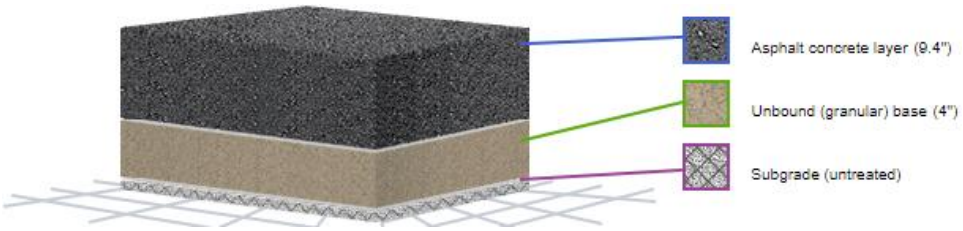

Figure 4-2. Pavement Structure for AZ-260 Section (Source:InfoPave).

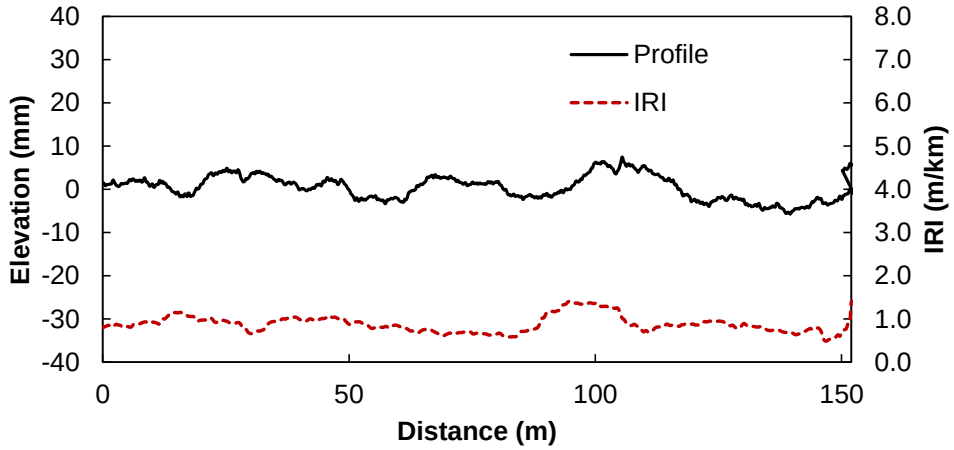

Figure 4-3. Pavement Elevation and IRI Profile for AZ-260.

4.2.2 Colorado

This section in Colorado is a two lane interstate road on I-70 eastbound at mile post 386.4 with LTPP id number 08-0560. The climatic zone for this region is a dry/freeze. This pavement structure of this section consists a 6.3 cm treated base, and 30

cm of asphalt concrete, Figure 4-4. The elevation profile for this section and the IRI profiles are shown in Figure 4-5. The average IRI for the entire section is 1.86 m/km.

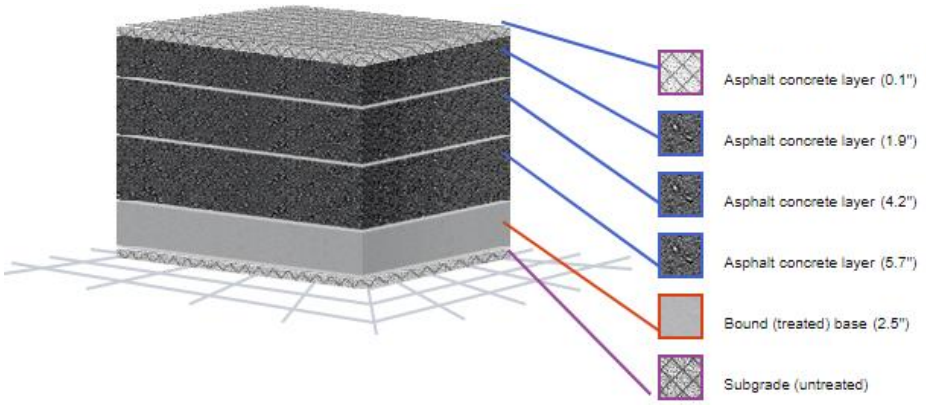

Figure 4-4. Pavement Structure for CO-560 Section (Source:InfoPave).

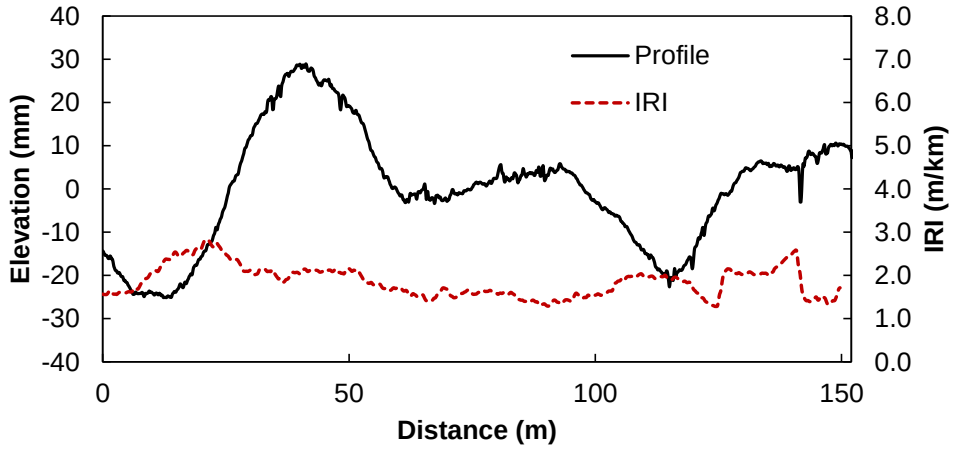

Figure 4-5. Pavement Elevation and IRI Profile for CO-560.

4.2.3 California

Section number 06-8202 in California is a one road on state highway 41 southbound at mile post 37.2. This section is located in a dry/non-freeze climatic region. This test section is no longer active for monitoring. Figure 4-6 shows the structure of the pavement which consists of a bound treated base of 29.5 cm and 13 cm of asphalt

concrete. The elevation profile for this section and the IRI profiles are shown in Figure 4-7. The average IRI for the entire section is 2.84 m/km.

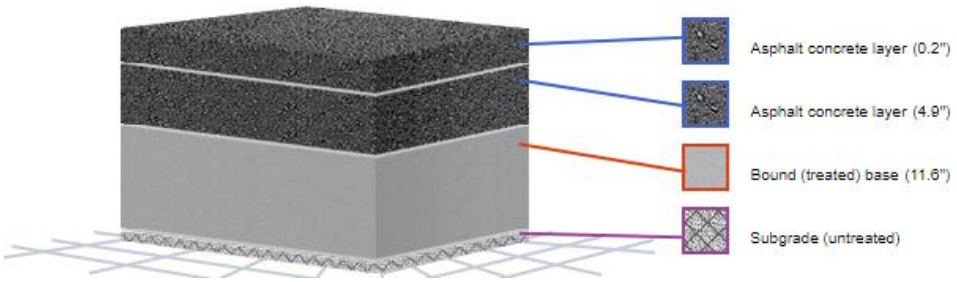

Figure 4-6. Pavement Structure for CA-8202 Section (Source:InfoPave).

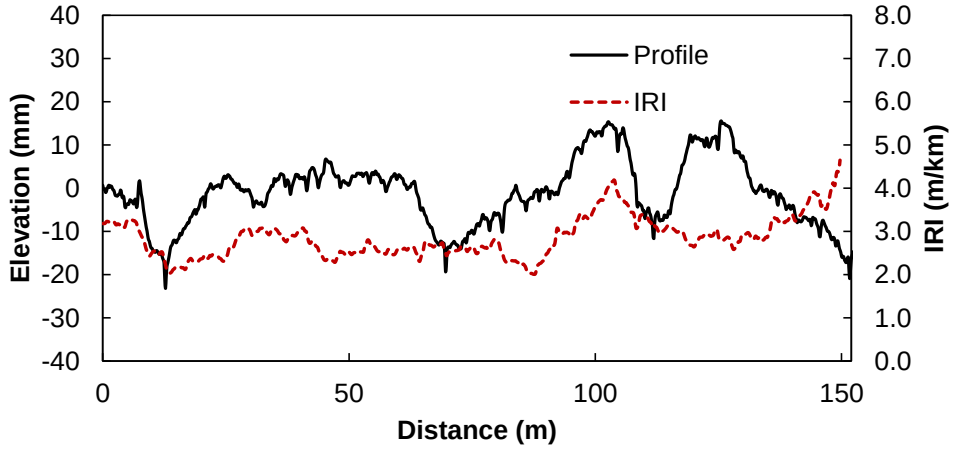

Figure 4-7. Pavement Elevation and IRI Profile for CA-8202.

4.2.4 Minnesota

This section is a two lane principal arterial on U.S.-71 south bound at 313.8 mile post, and with LTPP id number 27-1016. The climatic region for this location is wet/freeze, and this section has been out of the LTPP study since 2003. The pavement structure for this section consists of an 11.4 cm unbound granular base, and 7.6 cm of

asphalt concrete as shown in Figure 4-8. The elevation profile for this section and the IRI profiles are shown in Figure 4-7. The average IRI for the entire section is 3.48 m/km.

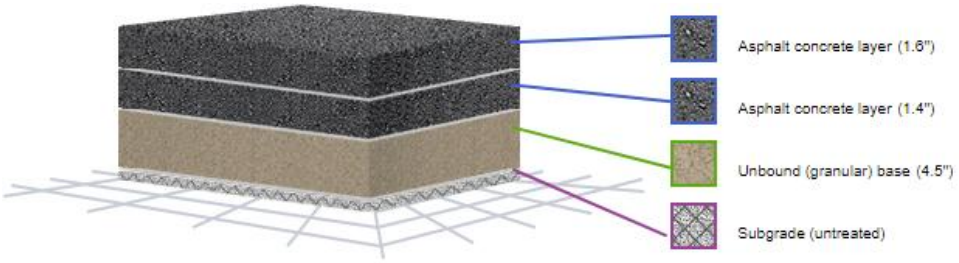

Figure 4-8. Pavement Structure for MN-1016 Section (Source:InfoPave).

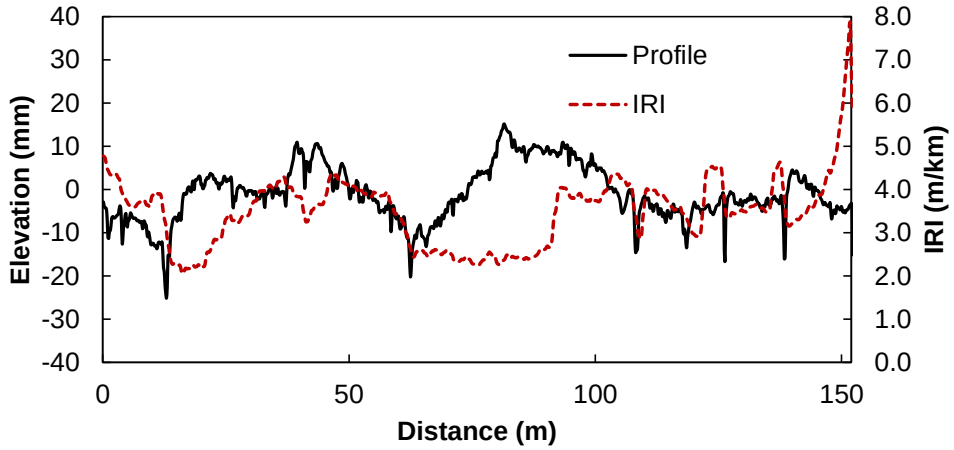

Figure 4-9. Pavement Elevation and IRI Profile for MN-1016.

4.2.5 New Jersey

This section located in south bound direction on state highway 23 at mile post with LTPP id number 34-1030. This location is in a wet/freeze climatic zone. The section is no longer active for monitoring. The pavement structure of this section consists of a 59.5 cm of unbound granular subbase, 17.3 cm of unbound granular base, and 15.2 cm of asphalt concrete, Figure 4-10. The elevation profile for this section and the IRI profiles are shown in Figure 4-11. The average IRI for the entire section is 5.97 m/km.

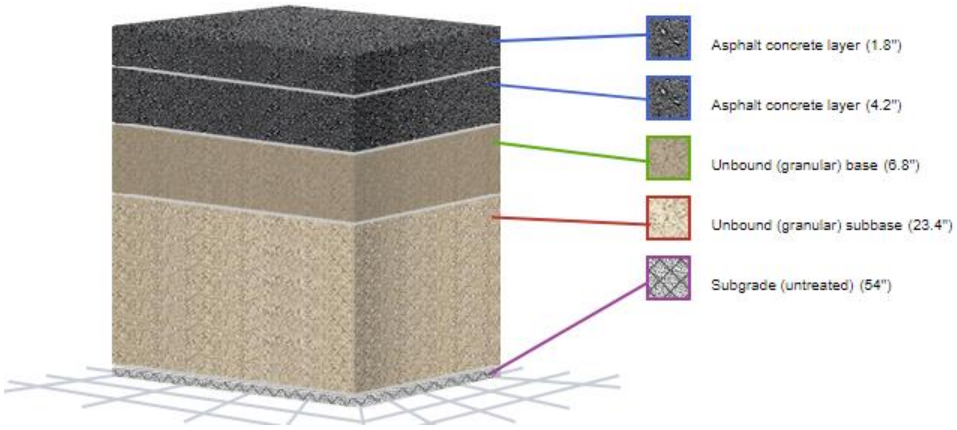

Figure 4-10. Pavement Structure for NJ-1030 Section (Source:InfoPave).

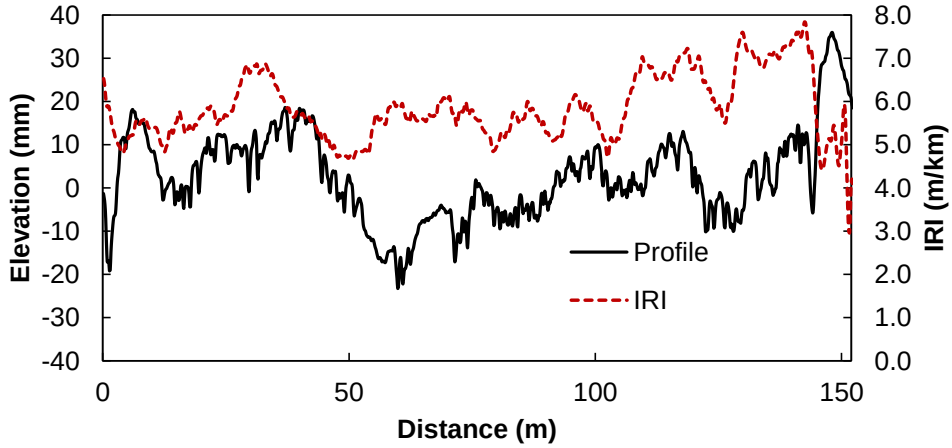

Figure 4-11. Pavement Elevation and IRI Profile for NJ-1030.

4.3 Monte Carlo Simulations

The Monte Carlo method is useful when trying to predict the outcome of an objective function with known input variables statistics and a system dependent (in a predictable way) on the independent statistically varying quantities. The use of Monte Carlo method in this research is demonstrated with the following scenario. Consider the

calculation of RQI using the quarter car filter plus accounting for the cellphone mount as shown in Figure 4-12. The steps are as follow:

1. Define the objective model. In this case the objective model is the mechanical model to estimate RQI presented in Chapter 3.
2. Determine the statistical distribution for the input variable (road profile), and the suspension parameters from the mechanical model.
3. Select the mechanical model parameters randomly based on their individual statistical distributions, and solve the mechanical model.
4. Finally, iterate this procedure for the desire amount of simulations.

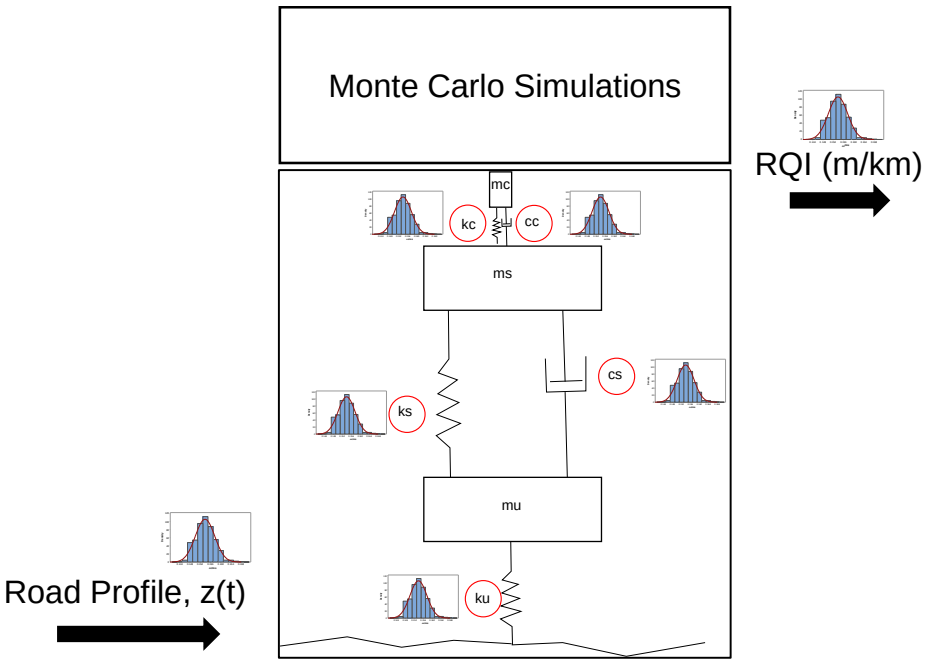

Figure 4-12. Monte Carlo Simulation Schematics.

This is an effective statistical tool because it allows one to identify the relative importance of individual factors, and their statistical uncertainty that can affect the results of a physical system under some imposed perturbation. The proposed methodology is to

collect RQI from randomly selected vehicles with unknown vehicle suspension characteristics, and factors. The key part of Monte Carlo is to include the statistical uncertainty of these factors in the RQI model to evaluate and validate the proposed methodology.

The statistical distributions or uncertainty from the mechanical parameters of the cellphone mount (*kc* and *cc*) were estimated from the case studies presented in Chapter 3, and an experimental method developed in the lab to backcalculate the suspension parameters from the cellphone mount. The description of this method is presented in the next section.

The vehicle suspension parameters for different vehicle classifications were taken from literature review as provided. However, the suspension parameters gave only a range of values, but did not provide a specific statistical distribution. So, in this analysis different statistical distributions were assumed.

Then, to account for wander effects a normal distribution was assumed for the road elevation profile based on experimental data from LTPP InfoPave and MNDOT Road Test database. Once all the parameter distributions are known, a MatLab code was used to perform thousands of simulations by randomly changing the mechanical model parameters using Monte Carlo, and to determine the variance of the RQI estimations so that sample size can be estimated within an acceptable error.

4.4 Backcalculation of Cellphone Mount Response

The statistical distributions or uncertainty from the mechanical parameters of the cellphone mount (*kc* and *cc*) were estimated using two approaches. The first approach

was to use the information from the case studies presented in Chapter 3, Section 3.2.2. In the second approach, an experimental method was developed in the lab to backcalculate the suspension parameters from the cellphone mount.

This second approach to estimate the stiffness and damping characteristics of the cellphone mounts was performed using a load frame specially designed as shown in Figure 4-13. A bicycle cellphone mount (b) was first attached to the actuator (a), then a 3D printed base with a piece of glass was fabricated to simulate a windshield (c-d). After the bicycle mount was set up, finally the windshield cellphone mount (e) with a suction cup was attached to the fabricated base. A total of four cellphone mount and three smartphones (iPhone 5s, Motorola Moto G, and Samsung sII) were used in this experiment, Table 4-2 .

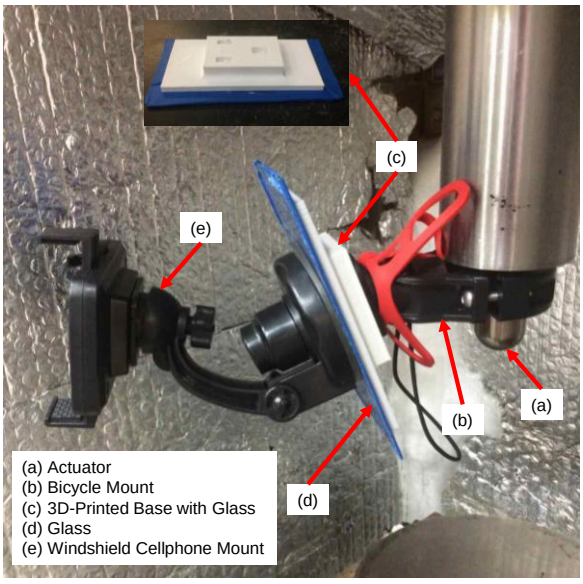

Figure 4-13. Mount Set Up.

Table 4-2. Summary of Experimental Factors.

Factor	Quantity
Cellphone	3
Cellphone Mount	4
Load	1

The schematics of the test procedure is shown in Figure 4-14, and the steps were as follow:

1. First a single pulse load was applied to the mount. The smartphone recorded the vertical acceleration generated by the pulse.
2. The displacement is calculated by double integration of the smartphone vertical acceleration.
3. The estimated vertical displacement is computed using the model of an underdamped system given by Equation (4-1). Where the output response over time is represented by $x(t)$, X_0 is the amplitude of the impulse, ζ is the damping ratio less than one and greater than zero, ω_n is the natural frequency of the system, and ϕ is the phase angle.

$$x(t) = X_0 e^{-\zeta\omega_n t} \sin\left(t\omega_n\sqrt{1-\zeta^2} - \phi\right) \tag{4-1}$$

4. Then, the suspension parameters were backcalculated by minimizing the error between the measured and the estimated displacement using the least squared method.

(a) (b) (c)

Figure 4-14. Schematics of Impulse Response Data Collection; (a) Impulse Input; (b) Cellphone Recording; (c) Response Output.

The results were analyzed and compared to those results from the comprehensive results. The ranges of the resonant frequency, w_c, from the comprehensive study (CS) where between 1.6 to 4.8 rad/s, those from the lab experimental study (Lab) ranged from 0.8 to 5.6 rad/s. The damping, s_c, from the both studies ranged from 0.03 to 0.07 and .01 to .08 for the comprehensive study and lab respectively, Figure 4-15. The larger spread in the data from the lab experiment probably is because only 12 data samples were analyzed as compared with 600 samples from the comprehensive study. Given this information it was decided to use the values and distributions from the comprehensive study to perform the Monte Carlo simulations.

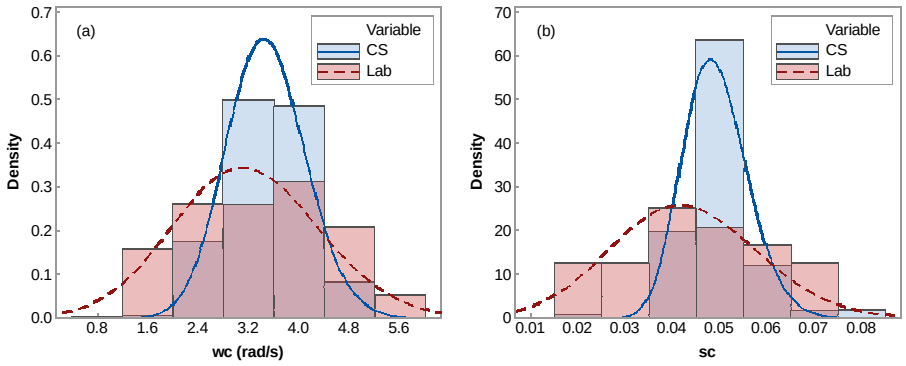

Figure 4-15. Mount Parameters. (a) Stiffness; (b) Damping

4.5 Estimation of Suspension Parameters

The suspension parameters from different vehicle classification was taken from typical suspension values from literature review (18, 45, 97). The range of values of resonant frequencies for the sprung mass (w_s) and un-sprung mass (w_u) and the damping ratio for the sprung mass (s_s) are given in Table 4-3. In this section of the study, the description of a sedan vehicle is equivalent to a Class 2 according to the FHWA vehicle classification which consists in a typical passenger vehicle. SUVs are similar to Class 3 which are a two-axle, four tire vehicle that also includes small trucks and minivans. And Heavy Duty Trucks corresponds to a Class 5 vehicle with two-axle, and six tires. Bridgelall (2015) presented some information on the statistics of suspension parameters for passenger cars from typical vehicles from 2007 (18). The results provided the typical values a long with the standard deviations. However, there was nothing said about the statistical distribution that these parameters follow. Since there was not enough information about the suspension parameters variability and type of statistical distributions among different vehicle classification, and only ranges of values were available, different statistical distributions were assumed for each suspension parameter according to vehicle classification.

Table 4-3. Suspension Parameters Ranges.

Parameter	Vehicle Classification		
	Passenger Car	SUV	Heavy Duty Trucks
w_s (rad/s)	6.9-9.7	8.0-13.8	7.4-14.9
w_u (rad/s)	55.3-77.5	57.7-66.6	48.5-68.3
s_s	0.1-0.4	0.2-0.4	0.1-0.3

4.5.1 Normal Distribution Assumption

Figure 4-16 shows the assumed normal distribution for the suspension parameter. The normal distribution curve was constructed using the mean values found in the literature, and the standard deviation was estimated so that the estimated values fall in the range shown in Table 4-3.

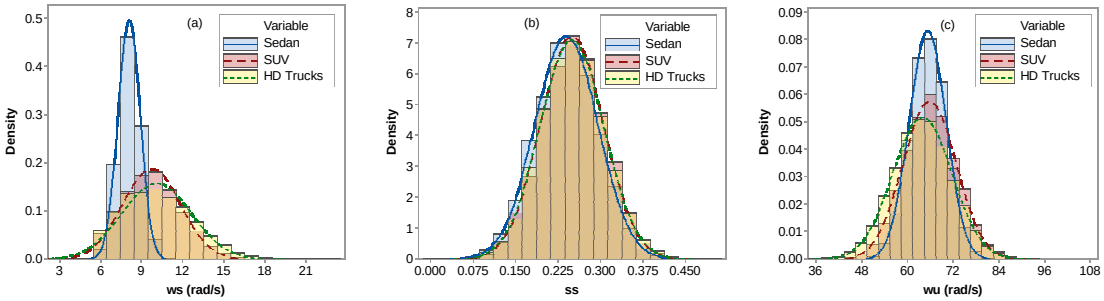

Figure 4-16. Normal Distribution; (a) Sprung Mass Frequency; (b) Sprung Mass Damping Ratio; (c) Un-Sprung Mass Frequency.

4.5.2 Uniform Distribution Assumption

This is a straight forward estimate. The suspension parameters were estimated based on equal probability for each parameter based on the ranges presented before. Figure 4-17 shows the ranges and the histogram for a uniform distribution of the suspension parameters.

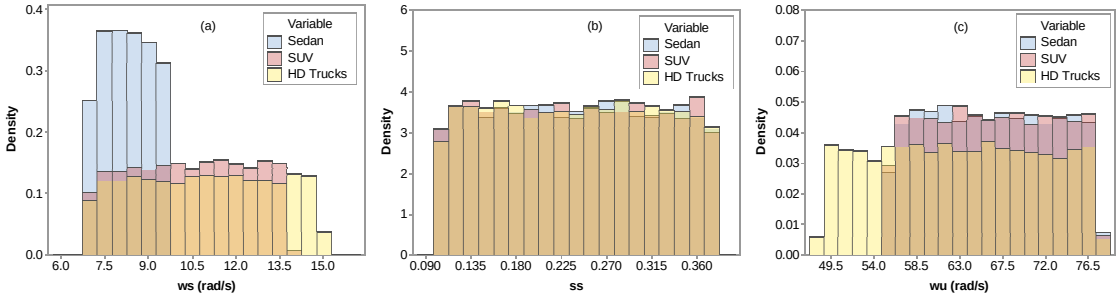

Figure 4-17. Uniform Distribution; (a) Sprung Mass Frequency; (b) Sprung Mass Damping Ratio; (c) Un-Sprung Mass Frequency.

4.5.3 Skewed Distribution Assumption

The estimated suspension parameters for the skewed distribution assumption was calculated using the following Equation (4-2).

$$x = x_{\min} + \left(x_{mean} - x_{\min} \right) \times P\left(Z \right) \tag{4-2}$$

Where x is the estimated parameter, x_{min} is the minimum value for that given suspension parameter from the literature, x_{mean} is taken as the average value, P(Z) is the probability of a random sample Z following a gamma distribution with mean E[Z]=1. In this way, the lower limit, and the mean is controlled based on the known values. By definition, the mean and the skewness of a gamma distribution is given by Equations (4-3) and (4-4) (98). Where k and θ are the shape and scale factors respectively. These parameters where modified by trial and error such that $k\theta$=1 and the skewness of the curve will cover the upper limit from the suspension parameter found in the literature.

$$E[Z] = k\theta \tag{4-3}$$

$$Skewness = \frac{2}{\sqrt{k}} \tag{4-4}$$

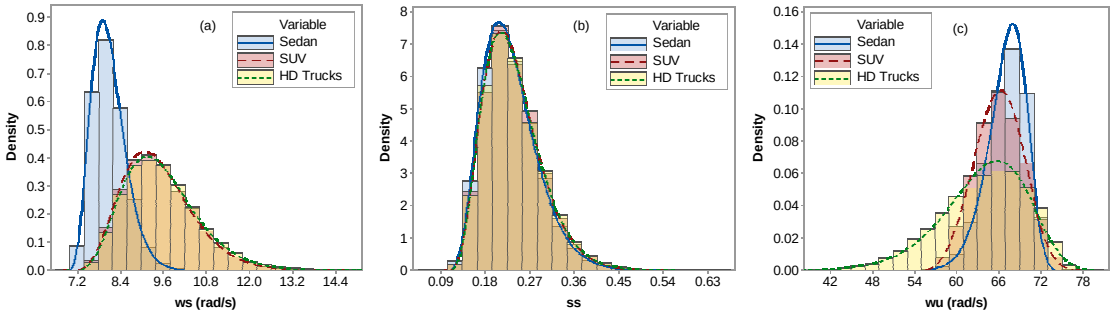

Figure 4-18. Gamma or Beta Distribution; (a) Sprung Mass Frequency; (b) Sprung Mass Damping Ratio; (c) Un-Sprung Mass Frequency.

4.6 Effect of Vehicle Suspension/Classification on Ride Quality Index Estimation

This section presents the analysis that was carried out using the Monte Carlo simulation method with the assumed suspension parameters presented in the previous section on the five road sections from InfoPave.

The RQI simulations where performed following these assumptions.

1. Three different parameter distributions were considered for the suspension parameters: Normal, Uniform, and Skewed.
2. For the cellphone mount parameters, only normal distribution was assumed for all simulations since the results from the comprehensive study in Chapter 3 provided the statistical properties of the data.
3. It was assumed that all suspension parameters would follow similar distributions. In other words, the variability of the manufacturing process of suspension systems

is consistent throughout the different components. Thus, only one probability distribution for all suspension parameter was considered at a time.

The simulations were carried out for three vehicle classifications, and three different vehicle spectra given in Table 4-4. The average percent of each vehicle classifications from a principal arterial, minor arterial, major and minor collectors is represented by traffic Mix 1 (99). Mix 2 is an arbitrary case where the SUV and truck percentages are doubled. Finally, the traffic Mix 3 represents equal percentages for every class.

Table 4-4. Percentages of Every Vehicle Classification.

Vehicle Spectra	Class 2/Sedan	Class 3/SUV	Class 5/Trucks
Mix 1	70	24	6
Mix 2	40	48	12
Mix 3	33	33	33

The total number of simulations were carried for 45 cases; for five pavements, three vehicle classifications and 3 assumed distributions. For each case10,000 simulations were performed for a total of 450,000 simulations. The reason to choose 10,000 was to guarantee that enough simulations were performed for the vehicle class comparison and that the data converges. Figure 4-19 shows the rate of convergence is fast, and after around 300 samples the coefficient of variation of the standard error is 2 % which can be considered an acceptable margin of error.

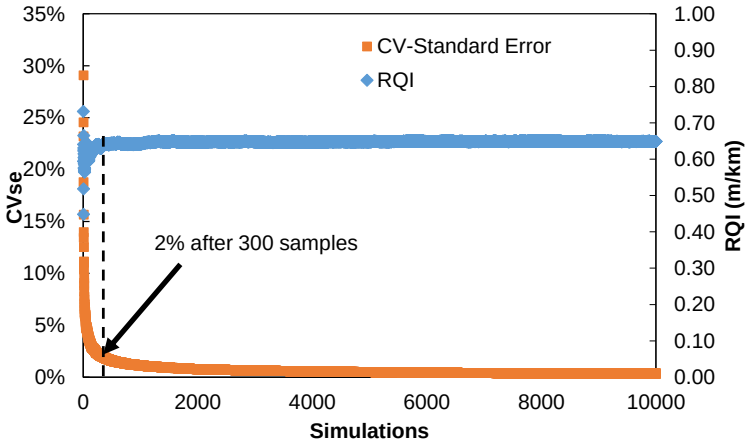

Figure 4-19. RQI and Convergence.

When ANOVA is used to identify the statistical significance between two large datasets (i.e. hundreds or thousands) most of the cases, the null hypothesis H_0 will be rejected when it is false, this is call statistical power. In other words, the statistical power is the likelihood that an effect will be detected if there is an effect to be detected (100). Cohen (1969) proposed a statistical measure commonly refer to as Cohen's d value to study the effect size (ES) between two groups (101). Cohen's d value is calculated using Equation (4-5). Where d is the EF statistic, M_1 and M_2 are the mean from two populations and σ is the standard deviation within populations. What this number tells is how different two populations mean are in term of standard deviations (i.e. d=1 group differs by one standard deviation from the other). Cohen (1962) and Sawilowsky (2009) proposed as a rule of thumb values for d summarized in Table 4-5. To explain this in a different context, a large difference would be an effect that people can perceive easily by the naked eye, and small would be effects that exists but has to be carefully analyzed (102,104).

$$d = \frac{M_1 - M_2}{\sigma} \quad (4\text{-}5)$$

Table 4-5. Effect Size Rule of Thumb Values for d.

Effect	d-statistic
Very Small	0.01
Small	0.20
Medium	0.50
Large	0.80
Very Large	1.20
Huge	2.00

The next analysis was based on both: Cohen's d statistic and visual interpretation of the box plots and the confidence interval. As presented earlier, three distributions where assumed for the Monte Carlo simulations. The comparison between the different statistical distributions using Cohen's d value are shown in Table 4-6. In general, the EF showed a small to medium effect for all cases. These results provided meaningful information as to decide whether or not to use all the assumed distributions for the simulations or just one.

Table 4-6. Cohen d-Statistic on Different Distributions.

Distribution	Arizona	Colorado	California	Minnesota	New Jersey
Norm-Uniform	0.1	0.3	0.5	0.2	0.4
Norm-Skewed	0.3	0.5	0.3	0.1	0.2
Uniform-Skewed	0.2	0.2	0.3	0.3	0.3

The same analysis was performed for all pavement locations, but now to identify the effect of vehicle classification. The overall conclusions from this analysis were that

the effect between individual vehicle classifications is significant. In most of the cases, heavy duty trucks showed significant difference when comparing to sedan and SUV. This EF results for the AZ-260 section are shown in Table 4-7. The EF values from sedan and SUV compared to HD trucks shows that the effect ranges from medium to large, while the comparison between different mixed traffic showed small effect.

Table 4-7. Cohen d-Statistic on Vehicle Classifications, AZ-260.

Vehicle	d-Statistic		
	Normal	Uniform	Skewed
Sedan-SUV	0.1	0.2	0.4
Sedan-HD Trucks	0.4	0.5	0.7
SUV-HD Trucks	0.3	0.7	0.4
Mix1-Mix2	0.0	0.0	0.1
Mix1-Mix3	0.1	0.1	0.2
Mix2-Mix3	0.1	0.1	0.1

The next analysis is to look at the histograms and box plot to get an idea of the statistical characteristics of the data. Figure 4-20 shows the RQI simulation results for AZ-260 section assuming normal distributed parameters, and includes the three vehicle class and three mixed traffic cases. In this section, the plots for only normally distributed factor simulation are included, the plots for the other distributions and pavement locations are shown in APPENDIX E. From visual inspection, the difference between all cases seems to be not significant. Typically, pavements with IRI less than 1 m/km are considered a very smooth pavement, and the results agree with that. The RQI measurements taken from individual vehicles and the mixed traffic cases. It is also observed that outliers exist only in the upper bound and nothing on the lower bound. In

this statistical analysis, the definition of outlier is given in Equation (4-6). Where Q_1 and Q_3 are the quantiles one and three respectively.

$$outlier = \begin{cases} RQI < Q_1 - 2\times(Q_3 - Q_1) \\ RQI > Q_3 + 2\times(Q_3 - Q_1) \end{cases} \quad (4\text{-}6)$$

The reason for this might be because the RQI measurements, similar to IRI, will never have negative values. The interpretation of this in terms of vehicle suspension is that brand new vehicles will have "good" suspension (assuming car companies follows standards for suspension system manufacturing), and that the suspension systems will deteriorate over time (i.e. old vehicles). This phenomena is more clearly seen in the mixed traffic cases. As the percentage trucks increases, the number of outliers goes up, since those vehicles will typically have a stiffer suspension.

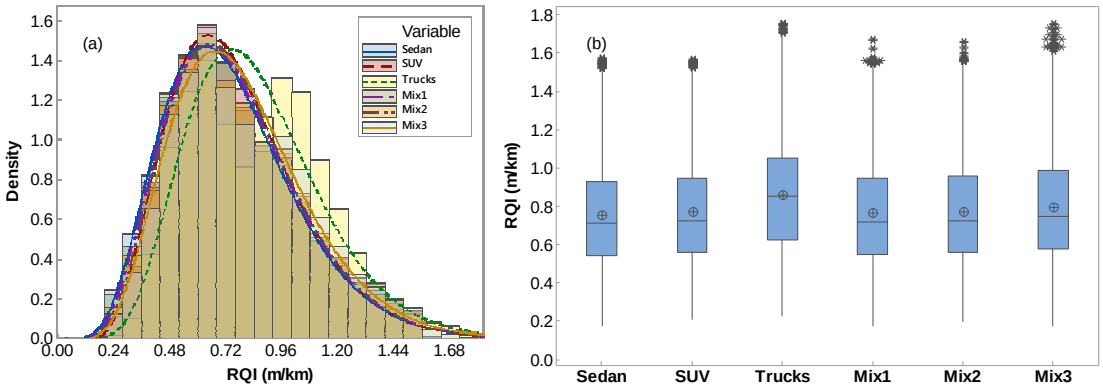

Figure 4-20. Results from Simulations on AZ-260 Assuming Normal Distribution for Suspension Parameters. (a) Data Presented in a Histogram, and (b) in a Box Plot.

The average RQI values from the three vehicle classes and the mixed traffic are summarized Table 4-8. In this case, sedan vehicles showed the lowest RQI while heavy duty trucks the highest. A more realistic scenario would be mixed traffic one (Mix 1) with RQI of 0.75 m/km.

Table 4-8. Summary of RQI Values for AZ-260.

Vehicle	RQI (m/km)		
	Normal	Uniform	Skewed
Sedan	0.73	0.70	0.66
SUV	0.75	0.66	0.75
HD Trucks	0.84	0.80	0.84
Mix 1	0.75	0.69	0.69
Mix 2	0.75	0.70	0.72
Mix 3	0.78	0.73	0.75

The results from CO-560 section showed that there is a medium to large effect between sedan and SUV with respect to heavy duty trucks, and also large effect between Sedan and SUV when assuming a skew distribution. The general trend for the mixed traffic comparison is that the effect between them is small. However, the Mix1-Mix3 under the skewed distribution assumption, showed a medium effect. The summary is shown in Table 4-9.

Table 4-9. Cohen d-Statistic on Vehicle Classifications, CO-560.

Vehicle	d-Statistic		
	Normal	Uniform	Skewed
Sedan-SUV	0.1	0.4	0.7
Sedan-HD Trucks	0.5	0.8	1.0
SUV-HD Trucks	0.4	0.4	0.5
Mix1-Mix2	0.1	0.1	0.2
Mix1-Mix3	0.2	0.3	0.4
Mix2-Mix3	0.1	0.1	0.2

To complement the previous results, the histogram and box plot for normal distributed factors is shown in Figure 4-21. Similar to the Arizona section, the RQI average from the three vehicle classifications are significant, but the mixed traffic where not significant.

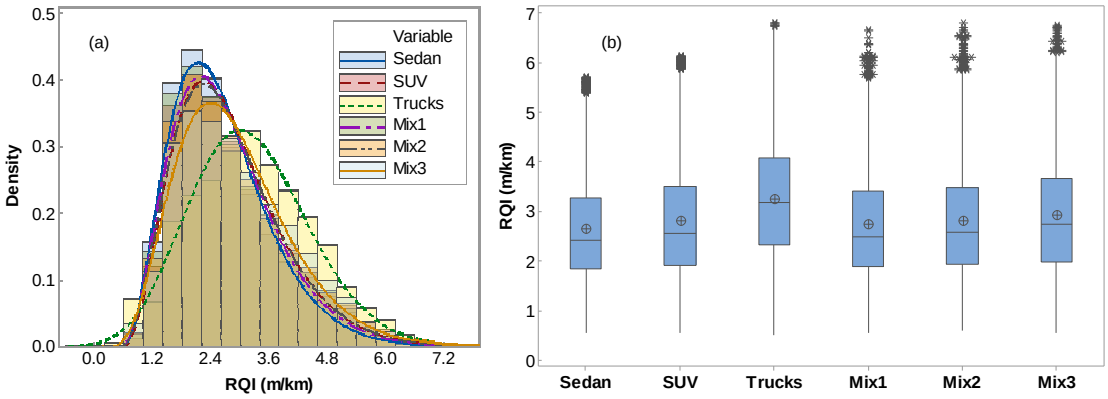

Figure 4-21. Results from Simulations on CO-560 Assuming Normal Distribution for Suspension Parameters. (a) Data Presented in a Histogram, and (b) in a Box Plot.

The RQI average results are summarized in Table 4-10. The RQI values ranged from 2.17 to 3.18 m/km for the vehicle classes and 2.34 to 2.85 m/km for the mixed traffic. The larger range seen within the vehicle class is mainly because the results are from extreme cases, smooth suspension from sedans or stiff suspension from trucks. The

ranges of values simulated for the mixed traffic is because tin real life situations, the data lies in between the extremes.

Table 4-10. Summary of RQI Values for CO-560.

Vehicle	RQI (m/km)		
	Normal	Uniform	Skewed
Sedan	2.55	2.31	2.17
SUV	2.75	2.70	2.66
HD Trucks	3.18	3.15	3.13
Mix 1	2.66	2.47	2.34
Mix 2	2.71	2.67	2.52
Mix 3	2.85	2.71	2.64

The Cohen test results showed small effect from all vehicle classification comparisons assuming a normal distribution. The results from the uniform and skewed distribution assumptions, the results showed a medium to high effect. Again, in a more real life scenarios represented by the mixed traffic cases, the results showed low effect. The summary of this analysis is presented in Table 4-11.

Table 4-11. Cohen d-Statistic on Vehicle Classifications, CA-8202.

Vehicle	d-Statistic		
	Normal	Uniform	Skewed
Sedan-SUV	0.3	0.7	1.0
Sedan-HD Trucks	0.1	0.6	0.5
SUV- HD Trucks	0.2	0.0	0.5
Mix1-Mix2	0.1	0.2	0.3
Mix1-Mix3	0.0	0.3	0.2
Mix2-Mix3	0.1	0.1	0.0

Now, by visually inspecting Figure 4-22, the histogram and box plot shows no significance between vehicle classifications. However, it is observed that SUV RQI

average is slightly higher than the other two vehicle classification. A similar observation was made in the Comprehensive Study for the 44th St. and the Glendale Ave. sections with RQI values lower than 3 m/km. The possible reason for this is that the quarter car filter magnifies or attenuates frequencies within a certain range, and most likely the suspension response from SUV to this profile is more susceptible than other vehicles.

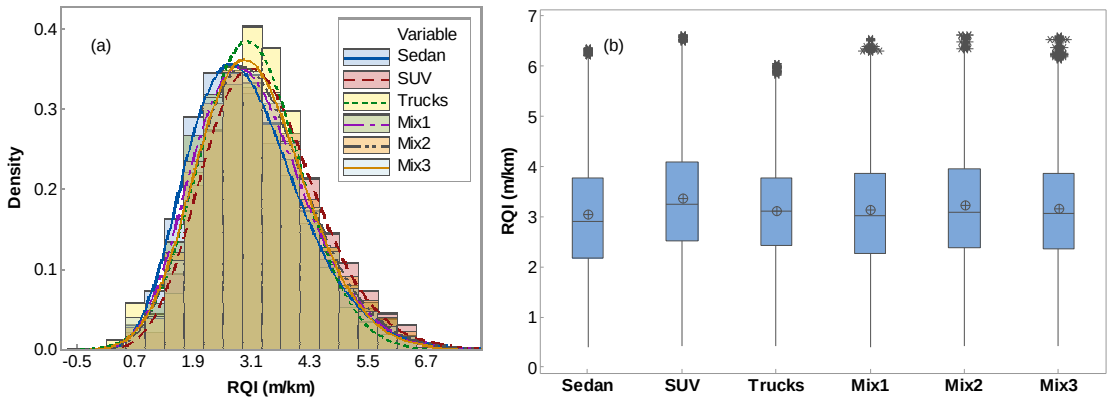

Figure 4-22. Results from Simulations on CA-8202 Assuming Normal Distribution for Suspension Parameters. (a) Data Presented in a Histogram, and (b) in a Box Plot.

The average RQI values of all simulations are shown in

Table 4-12. In this pavement location, sedan vehicles showed the lowest RQI measurements with 2.71 m/km while SUV the largest with 3.60 m/km.

Table 4-12. Summary of RQI Values for CA-8202.

Vehicle	RQI (m/km)		
	Normal	Uniform	Skewed
Sedan	2.91	2.46	2.71
SUV	3.34	3.04	3.60
HD Trucks	3.09	3.14	3.04
Mix 1	3.03	2.63	2.97
Mix 2	3.13	2.81	3.20
Mix 3	3.07	2.90	3.15

The Minnesota section MN-1016 with an IRI values of 3.54 m/km showed a significant difference between vehicle classifications clearly seen in Figure 4-23. These results can by corroborated in Table 4-13, where the effect sedan and SUV to heavy duty trucks is large to very large. The three cases for mix traffic showed no statistical significance, which represents a more realistic situation. In this case, the impact of heavy duty trucks would not be significant.

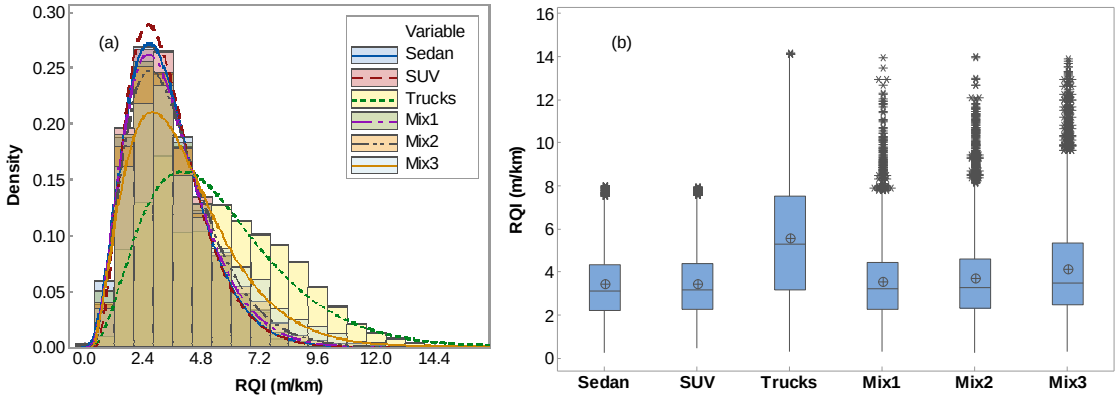

Figure 4-23. Results from Simulations on MN-1016 Assuming Normal Distribution for Suspension Parameters. (a) Data Presented in a Histogram, and (b) in a Box Plot.

Table 4-13. Cohen d-Statistic on Vehicle Classification, MN-1016

Vehicle	d-Statistic		
	Normal	Uniform	Skewed
Sedan-SUV	0.0	0.0	0.6
Sedan-HD Trucks	1.0	1.0	0.8
SUV-HD Trucks	1.0	1.1	1.2
Mix1-Mix2	0.1	0.1	0.0
Mix1-Mix3	0.3	0.3	0.2
Mix2-Mix3	0.2	0.3	0.2

The RQI summary for this location is given in Table 4-14. Sedan and SUV were not significant but heavy duty trucks showed a difference of approximately 60 % to both

sedan and SUV. However, the percentage difference between mixed traffic was from 11 % to 21 %.

Table 4-14, Summary of RQI Values for MN-1016.

Vehicle	RQI (m/km)		
	Normal	Uniform	Skewed
Sedan	3.41	3.09	3.45
SUV	3.37	3.03	2.82
HD Trucks	5.39	5.49	5.06
Mix 1	3.48	3.22	3.40
Mix 2	3.65	3.34	3.33
Mix 3	4.00	3.92	3.82

The last section in this simulation study with a very high roughness showed a statistical difference between vehicle classifications and no difference between mixed traffic, Figure 4-24. At this level of roughness, the pavement can be considered as very poor or failed and is captured by all types of vehicles. This section was milled and overlaid the following year, and that conclusion could be obtained from any vehicle. The RQI results from this section are presented in Table 4-15, along with Cohen's d-statistic in Table 4-16. The trend is similar to all previous sections, heavy duty trucks showed the highest RQI values.

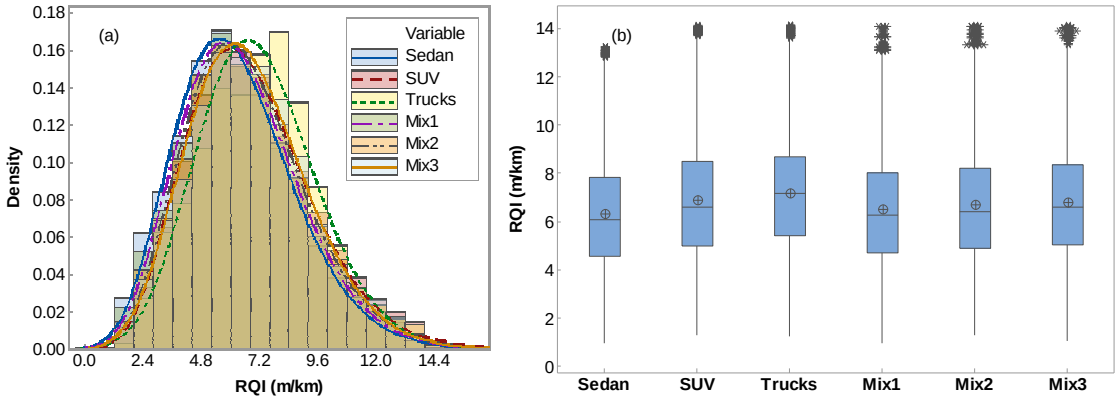

Figure 4-24. Results from Simulations on NJ-1030 Assuming Normal Distribution for Suspension Parameters. (a) Data Presented in a Histogram, and (b) in a Box Plot.

Table 4-15. Summary of RQI Values for NJ-1030.

Vehicle	RQI (m/km)		
	Normal	Uniform	Skewed
Sedan	6.34	5.30	5.93
SUV	6.60	6.14	6.94
HD Trucks	6.86	7.36	7.01
Mix 1	6.37	5.53	6.25
Mix 2	6.59	5.93	6.50
Mix 3	6.74	6.31	6.73

Table 4-16. Cohen d-Statistic on Vehicle Classification, NJ-1030.

Vehicle	d-Statistic		
	Normal	Uniform	Skewed
Sedan-SUV	0.2	0.5	0.5
Sedan-HD Trucks	0.4	0.9	0.5
SUV-HD Trucks	0.1	0.5	0.0
Mix1-Mix2	0.1	0.2	0.1
Mix1-Mix3	0.1	0.3	0.2
Mix2-Mix3	0.0	0.1	0.1

The overall results from this section showed that there was no relative effect on results from a particular assumed distribution. Table 4-17 shows the ranges of RQI values from the normal and skewed distribution assumption, along with IRI values for each

section. For the case of the Arizona section, regardless of the distribution, the range of RQI values fall under a very good payment. The Colorado and California sections, falls under the poor pavement category. And the Minnesota and New Jersey are completely failed pavements. Thus, regardless of the distribution chosen, the outcome conclusion is the same.

Table 4-17. Normal-Skewed Distribution RQI Ranges.

Section	RQI Range (m/km)	IRI (m/km)
Arizona	0.6-0.8	0.9
Colorado	1.9-2.7	1.9
California	2.5-3.0	2.8
Minnesota	3.1-3.4	3.5
New Jersey	5.7-6.3	6.0

All assumed distributions found a statistical effects on vehicle classifications, and in most of the cases, heavy duty trucks gave the higher RQI values. This was expected since typically heavy duty trucks will have a rougher ride quality. The other important outcome from this analysis is that in all cases, the different mixed traffic analyzed gave no statistical significance. Even in the worst case where the traffic spectra consists of 33 % heavy duty trucks, the results showed no statistical difference to typical vehicle class distribution.

Another observation made was that as the pavement roughness increased, the variance in the measurement increased as well. Figure 4-25 shows the plot for the RQI vs the average standard deviation for all locations.

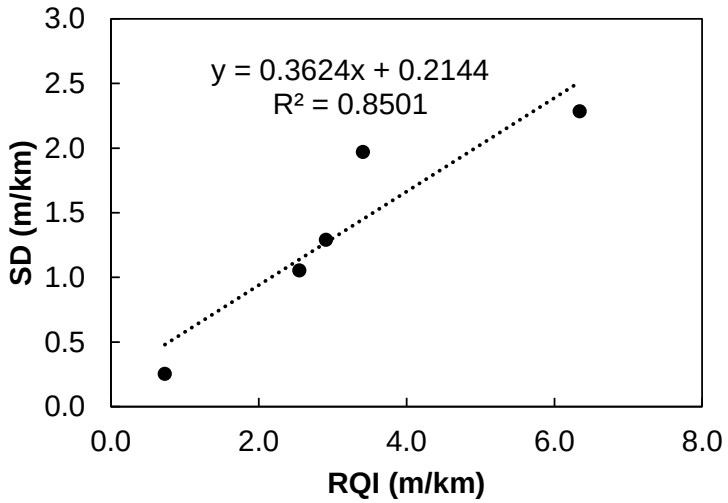

Figure 4-25. Plot RQI vs Standard Deviation for All Pavement Locations.

4.7 Convergence and Sample Size

One key component in this investigation is to estimate the minimum number of random samples necessary to yield a reliable estimate of the mean ride quality for a given pavement, i.e., to identify the conditions necessary for convergence. Since the data contains multiple factors that can induce variability in the results, the hypothesis is that, by collecting a sample large enough, the results will converge to a unique value. In general, convergence is defined by Equation (4-7). As the sample size increases, the data will approach to a convergent value A. Since this study takes random sampling of RQI measurements, there is not an exactly deterministic result. For this study, an acceptable error has to be set to determine the sample size for a given section. The error parameter adopted for this study is the coefficient of variation of the standard error (CV_{SE}) given by Equations (4-8) and (4-9).

$$\lim_{x\to\infty} A(t) = A \tag{4-7}$$

$$CV_{SE} = \frac{se}{E[RQI]}$$

(4-8)

$$se = \frac{RMSE}{\sqrt{n}} \tag{4-9}$$

An example of estimating the sample size based on the acceptable error is shown in Figure 4-26. The RQI plot shows the expected RQI value, *E[RQI]*, after every simulation. Re-arranging and combining Equations (4-8) and (4-9) the sample size for a given error can be calculated using Equation (4-10). Given these formulations, the coefficient of variation of variation of the standard error is plotted vs the number of simulations. For this particular example, the total number of samples required to reach convergence at CV_{se} of 5%, 2%, and 1% are about 50, 250, and 910 samples respectively.

$$n = \sqrt{\frac{RMSE \times E[RQI]}{CV_{se}}} \tag{4-10}$$

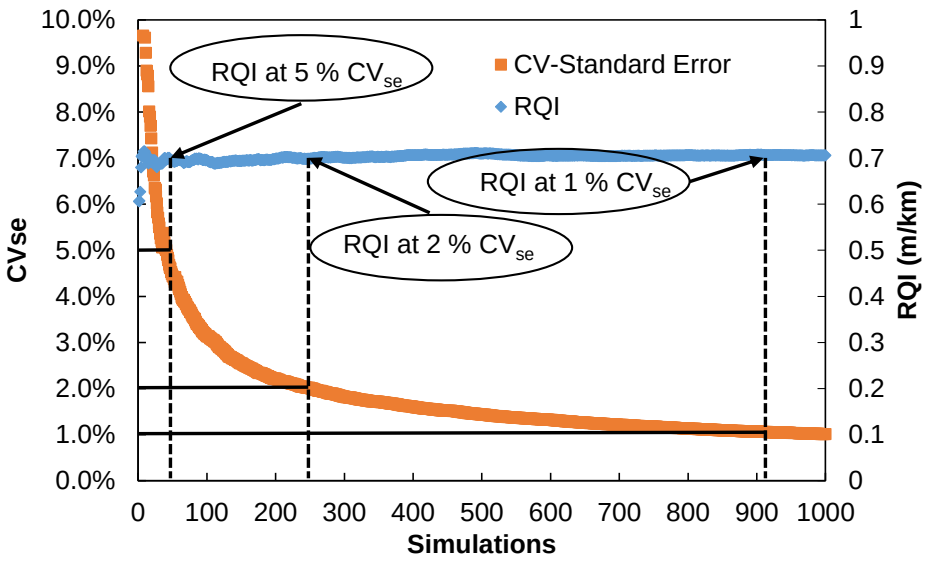

Figure 4-26. Example

Three different scenarios were considered: 1) perform simulation analysis assuming that the vehicle is driving on a single lane with no wander; 2) the second case is assuming a single lane with wander, and 3) considers the increase in variability if two lane plus wander are considered. This is an important analysis to determine if there is a significant difference in sample size required to estimate RQI.

4.7.1 Single lane – no wander

This case assumes that all vehicles will drive exactly the same location every time and no wander. The suspension parameters were only changed and not the road profile. The results from these simulations were shown in the previous section. From those results, the estimated sample size to reach convergence given different acceptable error is shown in Table 4-18. This table shows the average for all vehicles and sections, individual results are shown in Appendix 4-2.

Table 4-18. Sample Size Average for All Cases.

CV (%)	Sample Size		
	Normal	Unifom	Skewed
10	11	11	8
5	50	50	38
2	328	319	250
1	1240	1113	970

4.7.2 Single lane – wander

This section tries to account for wander effect on the RQI readings and specially in estimating the sample size this effect can be considered by recognizing that with wander the profile will change slightly. The wander effect refers to the transverse position or the deviation within lane markings while driving in a single lane. The wander effect is typically modeled as a normal distribution, with the edge of the tire 37.5 cm from the lane markings and a standard deviation of 25 cm (105). No studies were found on the impacts of wander effect to wheel path longitudinal profiles, but some literature was found on the variability of IRI measurements from a single wheel path. It is assumed that this variability in IRI measurements are due to the wander effect during data collection. A recent study by Jia et. al. (2018) showed that the range of standard deviation values for road sections with IRI ranging from 1.58 to 2.37 m/km can be between 0.03 and 0.05 m/km and this variance will increase with increase in IRI (106). Other researchers have found that typical coefficient of variation between IRI measurements are around 5 % and this value also agrees with measurements taken by the City of Phoenix ARAN (61).

In the previous Monte Carlo simulations, only the mount and suspension parameters were randomly changed base on different distributions. Now, to include the

wander effect on the Monte Carlo simulations, the elevation profile was randomly changed. This change was assumed to be normal as it is with the wander effect. The known elevation profile was modified using Equation (4-11). Where $z_p(t)$ is the elevation profile after modification, $z_{p0}(t)$ is the known elevation profile, and Z is a factor normal distributed with a mean value of 1. The standard deviation for the normal distribution of factor Z was modified such that the simulated RQI values gave a coefficient of variation of 5%.

$$z_p(t) = z_{p0}(t) \times Z \tag{4-11}$$

Base on this information, simulations were performed, but now adding a normal distributed random factor to the road profile. The mount and suspension parameters were also assumed to be normally distributed since the previous analysis in Section 4.6 showed not significant effect between the other distributions.

Table 4-19 shows the average sample size across the different vehicle classification and mixed traffic. The relative difference in sample size from vehicle to vehicle is relative small. When comparing these numbers with a single lane and no wander, the sample size increased from 328 to 342 at a 2 % CV. More detailed information on sample size for each vehicle and section are found in APPENDIX G.

Table 4-19. Average Sample Size for a Single Lane and Wander.

CV (%)	Sedan	SUV	HD Trucks	Mix 1	Mix 2	Mix 3	Average
10	13	11	12	14	12	13	13
5	62	58	54	66	60	66	61
2	408	382	361	418	404	426	400
1	1305	1511	1389	1570	1534	1528	1473

4.7.3 Two lanes – wander

The idea of this framework is to collect data from random road users. In a multi-lane arterial road it will be hard to identify the lane that the vehicle is driving, thus is important to consider what would be the variability in RQI from lane to lane and to account for wander as well. Is common practice to only take IRI measurements from a single lane, and no literature was found on IRI differences between driving lane and passing lane. To get more insight on this, the Minnesota Test Road database was used to analyze the IRI differences between single lane wheel paths, and between driving to passing lanes based on 16 sections from the Mn Road Test section database. The difference from wheel path in the driving lane left wheel path was 10 % smoother than the right wheel path, while the passing lane right wheel path was smoother than the left wheel path by a difference of 6 %. The analysis on these sections also showed that the passing lane was on average 10 % smoother than the driving lane. The summary of these results are shown in Table 4-20.

Table 4-20. Variability Within a Single Lane and Between Driving and Passing Lane.

Criteria	Measurements	CV (%)	Avg. Difference
Driving Lane LWP-RWP	1049	12	10
Passing Lane LWP-RWP	1026	10	6
Driving-Passing	1026	14	10

The simulations were performed using the following approach:

- Normal distribution for suspension parameters.
- Run simulations with original road profile accounting for 12% coefficient of variation in RQI measurements.
- Run simulations again with the same profile but considering the 10 % smoother and with a coefficient of variation of 14 %.
- Run the analysis considering individual vehicle classification with a 50-50 lane distribution. Sometimes it is consider a 90-10/80-20, the reason to choose a 50-50 was because this would be an extreme case in the simulations. Having 50% driving in the passing lane, which most of the time is smother, the results could have a significant effect on the RQI and sample size calculations.
- Run the analysis with the three mixed traffic scenarios and assuming 50-50 lane distribution.
- The simulations where performed on the Arizona and New Jersey sections.

Figure 4-27 (a) shows the average sample size results for the Arizona section considering the three cases: single lane- no wander (S-NW), single lane- wander (S-W), and two lane- wander (D-W). The sample size increases about 3 % when introducing wander effects, and about 30% when considering two lanes and wander. The RQI results showed no statistical difference when analyzed case by base. The New Jersey section results presented in Figure 4-27 (b) showed similar results than the Arizona section, an increase in sample size of 6 % and 40 % compared to S-W and D-W respectively. The RQI values compared to the S-NW simulations showed a reduction of approximately 6 % with the difference being not significant. Complete results for both sections are shown in Appendix 4-2.

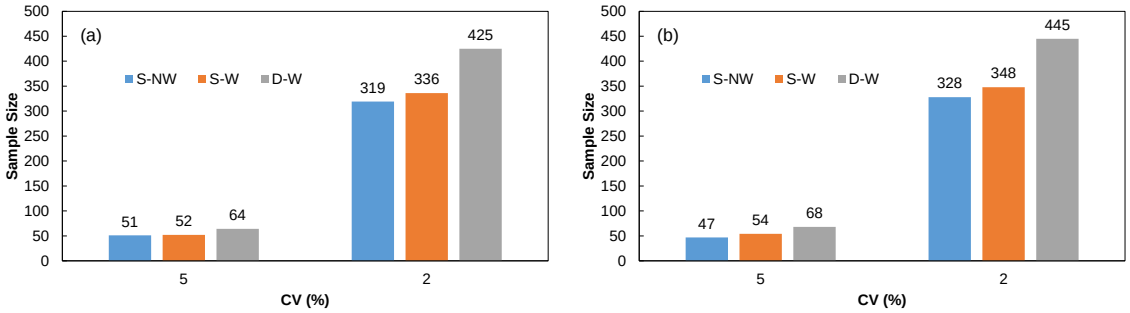

Figure 4-27. Sample Size for Different Cases at Two Error Thresholds. (a) AZ-260, (b) Nj-1030.

4.8 Summary

The objective of this chapter / part of the study was to replicate the results obtained from the field studies by analyzing five road profiles from InfoPave database. Suspension parameters from literature were assumed with different statistical distributions to determine the impact of vehicle classification on the RQI measurements utilizing the Monte Carlo simulation method. Further analysis was performed to estimate the minimum sample size required to estimate an RQI value within an acceptable error. More specific conclusions from this chapter are as follow:

- 900,000 Monte Carlos simulations were performed to identify the effects of vehicle classification on RQI estimates. In most of the cases, the assumed probability distribution for the suspension parameters did not show a significant effect on RQI results.
- Within a given distribution analysis, in most of the cases heavy duty trucks showed a significant difference when compared to sedan and SUV. However, in more realistic scenarios in which a mixed traffic was considered, there was no significant effect on RQI results.

- This simulation analysis was carried out by assuming that the road profile was exactly the same for all simulations. In more realistic cases, there would be wander effects that may or may not affect the RQI values. To address this problem, a normal distribution variability was assumed for the road profile. From literature review, a 6 % coefficient of variation on the road profile was assume to account for wander effects. 300,000 simulations were run for this analysis assuming only normal distribution for suspension parameters since the previous analysis showed no significant effect between the other statistical distributions. The average increase in sample size was from 328 samples to 403 which represents a 23 % increase.
- The two lane plus wander scenario was analyzed by adding the variability caused by wander effects within a lane and the variability from lane to lane. This variability was measured from Minnesota Road Test database. Results showed from this analysis showed that the CV within a lane was 10 to 12 %, and from lane to lane 14 %. The results also showed that in average the passing lane was about 10% smoother than the driving lane.
- A total of 120,000 Monte Carlo simulations for this last case were run only on the Arizona and New Jersey sections. The average number of samples from both sections, required for RQI convergence within 2 % CVSE, was 435 samples which represents a 33 % increase.
- The overall conclusion from this chapter is that there are significant difference between vehicle classifications with respect to heavy commercial trucks, no

statistical significance between mixed traffic cases, and increase in sample size when wander and two lane variability are considered in the analysis.

- Based on this analysis, a conservative sample size estimate of 300 to 400 samples would be recommended to reach convergence at an acceptable level of error (2.5 – 2.0 % CV_{se}). As a network level pavement ride quality assessment, this error is small enough that would not change the outcome in a decision making process.

Chapter 5 Integration of Ride Quality Index (RQI) into Pavement Management System (PMS)

5.1 Introduction

Any pavement condition index by itself probably not fully useful, and a PMS without some kind of condition index becomes just a database. Pavement condition indices and models are used in pavement management systems to develop a multi-year maintenance and rehabilitation plan. So far, one additional focus of this research study is to develop a reliable pavement performance model so that pavement condition data collected can be used effectively in a pavement management system. This part of the research study selects the RQI as a metric for pavement condition modeling and to be used as part of a PMS.

This chapter proceeds in explaining the use of the sigmoidal model and shifting approach proposed by Sotil and Kaloush (2004) to create Pavement Condition Index (PCI) master curves. The PCI master curve is useful as, typically, no complete pavement condition data exist or recorded for road sections without maintenance. In addition, road condition data for various road segments may only be available for a part of their service life (17). Beckley (2016) also used the same approach to create master curves to characterize the pavement performance of a road network using the International Roughness Index (IRI) (107). Furthermore, relationships between PCI and RQI were explored, developed and RQI threshold values were established for the purpose of using them in pavement management analysis and establishing maintenance programs.

5.2 LTPP InfoPave Arizona Sections

Using the Long Term Pavement Performance (LTPP) InfoPave database (108), a total of 40 pavement sections from Arizona with a dry-non freeze climatic region were used to create the master curves for PCI and RQI. The pavement structure for all sections consists of flexible pavement and the functional class is rural principal arterial. Table 5-1 shows the number of pavement sections included from each highway or state route.

Table 5-1. Number of Sections for Each Route.

Route	No. Sections
I-10	4
I-19	5
I-40	5
I-8	9
S-68	1
S-85	1
S-95	1
US-93	14

5.3 PCI Master Curve

Many researchers agree that a good mathematical representation of pavement performance is a sigmoidal function or model represented by an "S" shape curve. The concept of superposition used to construct dynamic modulus master curves has been adopted in pavement management deterministic models to characterize pavement condition (17, 109). The rate of deterioration of a pavement with respect to time, measured in PCI, can be simulated by a sigmoidal function using boundary conditions with lower limit of 0 and upper limit 100. Data from some Arizona sections was used to demonstrate the shifting process to create PCI master curves, Figure 5-1. First, PCI data

from road segments throughout the years are collated individually; they are separated in segments before a major maintenance or rehabilitation is done, as shown in Figure 5-1 (a). Then, superposition of time is applied to predict the life of a pavement, represented by the sigmoidal function, which usually ranges from 20-30 years, Figure 5-1 (b). Figure 5-1 (c) shows the final master curve using an optimization technique for a family of road segments. The sigmoidal model for PCI is given in Equation (5-1).

$$PCI = a_1 + \frac{a_2}{1 + e^{(a_3 \times T + a_4)}} \tag{5-1}$$

Where, PCI= Pavement Condition Index, T_{PCI}= Reduced time calculated by Equation (5-2), a_1,a_2,a_3,a_4= Parameters describing the shape and limits of the sigmoidal model.

$$T = t + \alpha_{(PCI)} \tag{5-2}$$

Where, t= Time since last reconstruction, rehabilitation, maintenance or first available date and α= Shift factor of PCI value.

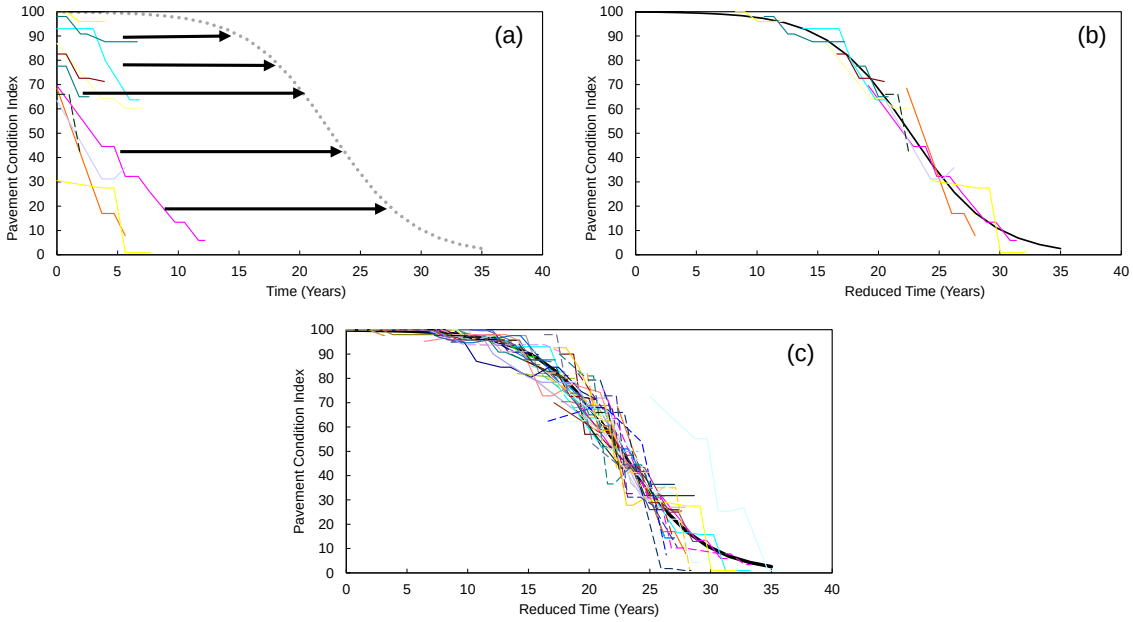

Figure 5-1. Shifting Process for PCI Master Curves. (a) Historical PCI; (b) Time Superposition; (c) Master Curve.

5.3.1 LTPP PCI Analysis and Results

In the optimization process, the coefficient of determination (R^2) is used to determine the number of shifting years that gives the best fit. The data is optimized several times by shifting the data to a maximum of 15, 20, 25, and 30 years. Once the difference in R^2 from one shifting year to another is less than a threshold of 0.005, then the data shifting is considered at optimum; it can also be concluded that the network level pavement life is equal to the maximum shifting years. For the LTPP data, Figure 5-2 (a) shows the PCI master curve with all the observed pavement condition shifted to maximum of 25 years according to Figure 5-2 (b). Finally, Figure 5-2 (c) shows the comparison between the predicted and measured PCI. Table 5-2 gives a summary of the

coefficient of determination for different maximum shifting years. The best fit was estimated to be 25 years with R^2 of 0.976.

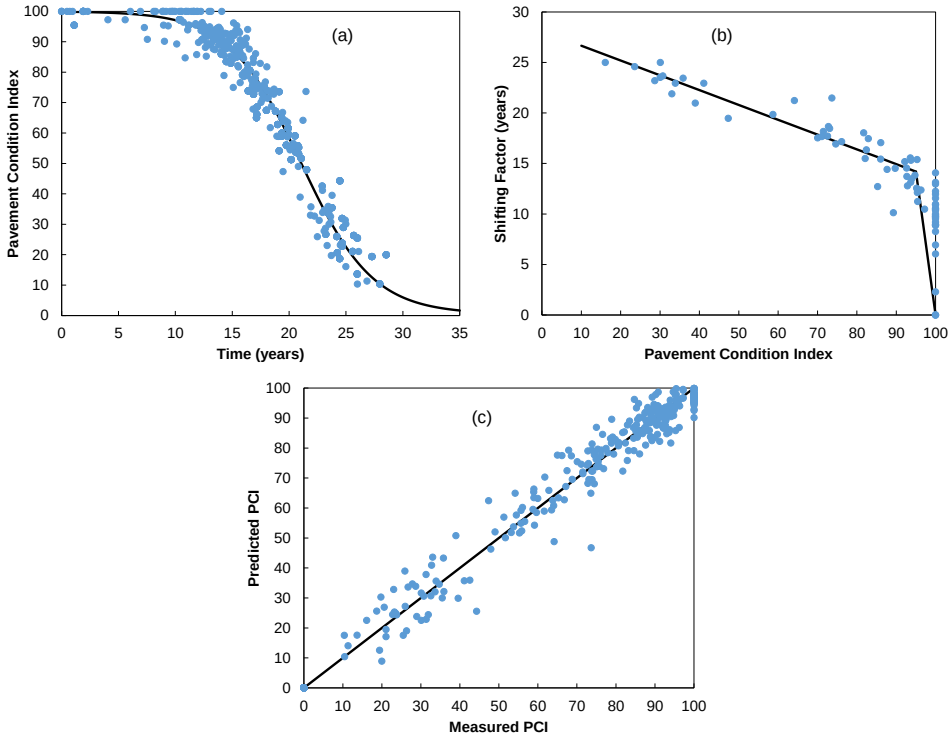

Figure 5-2. Arizona LTPP Sections; (a) PCI Master Curve. (b) Shifting Factors. (c) Predicted vs Measured PCI.

Table 5-2. Coefficient of Determination Summary for PCI Master Curves.

Year Shift	R^2
15	0.935
20	0.967
25	**0.976**
30	0.977

5.4 RQI Master Curve

Similarly to PCI, IRI can be also characterized as a sigmoidal function. Beckley used the same idea to develop IRI master curve using an overturned sigmodial function

(107). Since IRI and RQI values increases with time, and to reverse the shape of the function, the parameter *c* must be simply negative. This approach was similarly implemented to RQI data analysis. The new form is expressed as:

$$RQI = b_1 + \frac{b_2}{1 + e^{(-b_3 \times T + b_4)}} \tag{5-3}$$

Where, *RQI*= Ride Quality Index (m/km), b_1,b_2,b_3 and b_4= Fitting parameters to determine minimum, maximum and shape of the function, and T_{RQI}= Reduced Time given by Equation (5-4).

$$T = t + \alpha_{(RQI)} \tag{5-4}$$

Where, *t*= Time since last reconstruction/rehabilitation or first available date and α= Shift factor of RQI value.

5.4.1 LTPP RQI Analysis and Results

The elevation profiles for each section were analyzed using the RQI model presented in Chapter 3. Again, 10,000 Monte Carlo simulations were performed for each road profile assuming a normal distribution of suspension parameters for sedan vehicles explained in Chapter 4. Once all RQI values were calculated, similar to the PCI master curve analysis, RQI data was shifted to 15, 20, 25 and 30 years to determine the best fit. From the optimization process, a maximum shifting of 25 years was determined as best fit. Based

on this information, if the Ride Quality Index is used as a pavement performance measure, the life of this family of pavement sections would be 25 years. Figure 5-3 shows the master curves with the shifted RQI data, the shifting factors plot, and the comparison between predicted and calculated RQI with a R^2 of 0.945. The R2 values for the other year shifts are shown in Table 5-3.

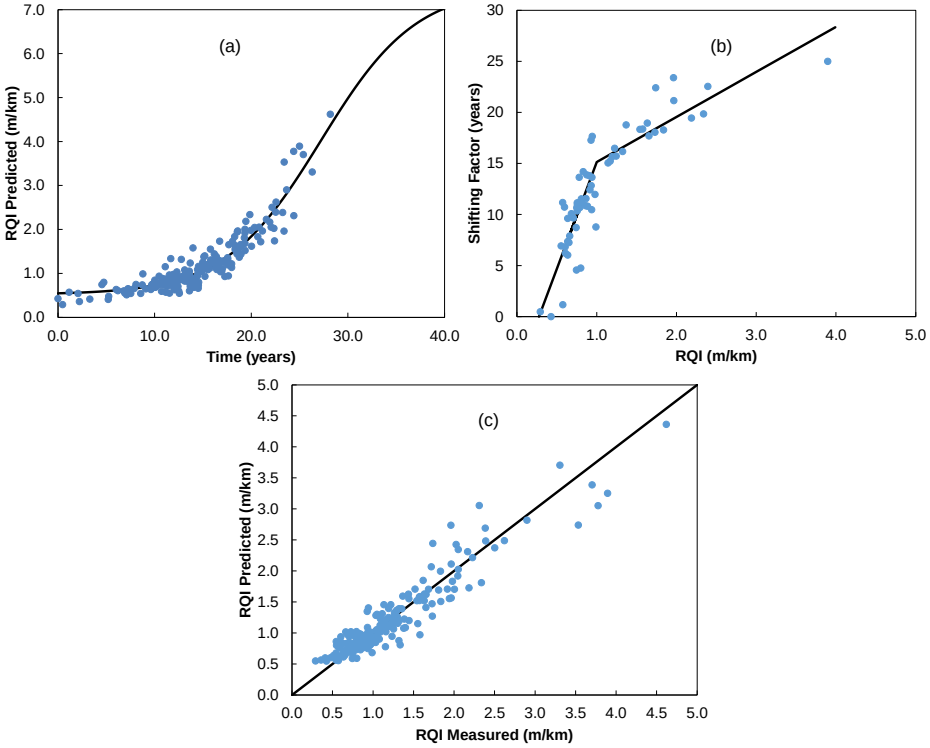

Figure 5-3. Arizona Sections RQI. (a) RQI Master Curve. (b) Shifting Factors. (c) Predicted vs Measured RQI.

Table 5-3. Coefficient of Determination Summary for RQI Master Curves

Year Shift	R^2
15	0.886
20	0.934
25	**0.945**
30	0.946

5.5 Development of a Relationship between PCI and RQI

In the previous two sections, PCI and RQI master curves where developed based on Arizona LTPP data. This section attempts developing a framework on how to relate these two performance measures. The calculation of PCI is straight forward, based on distress type, severity and extent, a deduct value is assign and deducted from 100 in a 0 to 100 scale (100 meaning new pavement with no distress). In contrast with RQI (or IRI), these measures depend on the unevenness of the longitudinal pavement profile after construction. In real life, brand new pavements can have an IRI of 0.5 m/km or up to 1.5 to 2.0 m/km. This represents a problem when trying to establish a relationship between PCI and RQI. To overcome this, initial PCI should be known and track the change in RQI over time. The methodology to establish this relationship is by using the PCI and RQI master curves following four steps.

Step 1. Estimate the initial PCI condition for a specific road section and calculate the corresponding reduced time T_{PCI} using Equation (5-5). Step 1 is similar to indexing the initial condition for that section.

$$T_{PCI} = \frac{\ln\left[\frac{a_2}{PCI_0 - a_1} - 1\right] - a_4}{a_3} \tag{5-5}$$

Where, ln is natural logarithm, PCI_o is the initial PCI, a_i are regression parameters.

Step 2. Use T_{PCI} to estimate the base RQI_{PCI} as shown in Figure 5-4 (b). This RQI value will be used as the initial RQI. RQI_{PCI} is the corresponding RQI to the time at PCI_0 on the mastercurve.

Step 3. Estimate ΔRQI by Equation (5-6), where ΔRQI is the difference between initial RQI and RQI at time *t*. Then estimate the new $RQI_{\Delta TRQI}$ by adding the initial RQI_{PCI} and ΔRQI (Figure 5-4 (c)).

$$\Delta RQI = RQI_t - RQI_0 \tag{5-6}$$

$$RQI_{\Delta TRQI} = RQI_{PCI} + \Delta RQI \tag{5-7}$$

Step 4. From the RQI master curve, back-calculate T_{RQI} given in Equation (5-8). Finally use T_{RQI} to estimate the final $PCI_{\Delta}t$ (Figure 5-4 (d)).

$$T_{RQI} = -\frac{\ln\left[\frac{b_2}{RQI_{\Delta TRQI} - b_1} - 1\right] + b_4}{b_3} \tag{5-8}$$

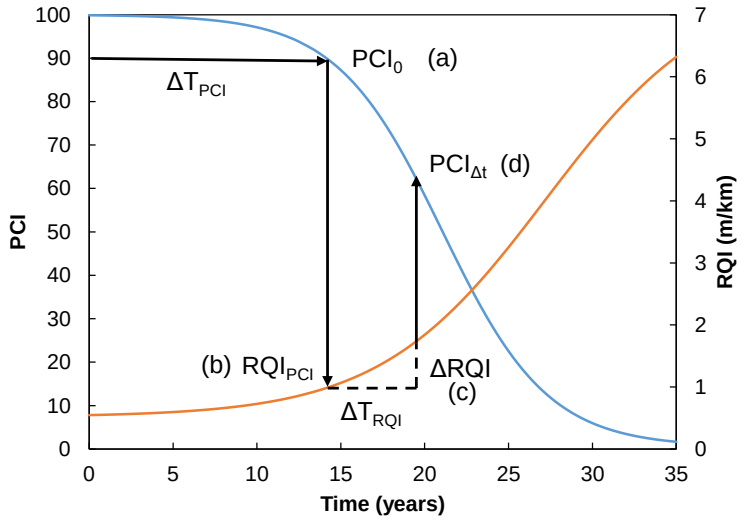

Figure 5-4. Relationship Between PCI and RQI.

Setting the initial conditions is important, because in practice initial roughness can vary from project to project, especially for collectors and local roads where there is no specification on initial roughness. Once initial conditions are set, the change in RQI/IRI is tracked over time, and that change can be related to PCI. Following this methodology, the PCI was predicted using RQI values from each Arizona LTPP section. Figure 5-5 (a) shows the measured PCI vs RQI, and the solid line represents the mathematical relationship from PCI and RQI master curves given by Equation (5-9). This mathematical expression comes from substituting T in Equation (5-1) for Equation (5-8). The PCI predictions showed good correlation to the observed PCI values with a R^2 of 0.85, Figure 5-5 (b).

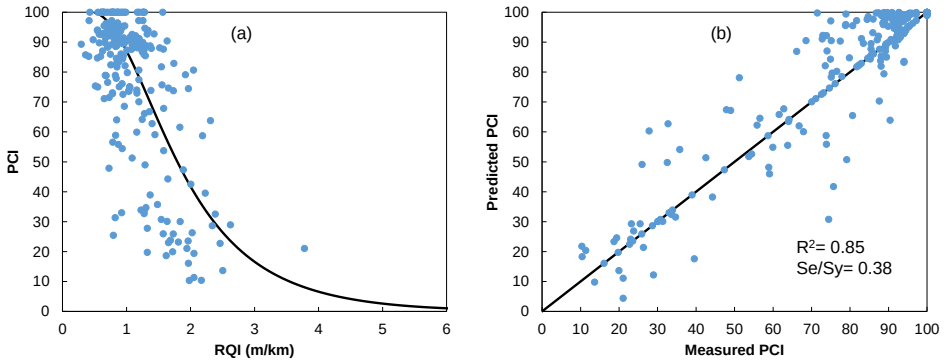

Figure 5-5. Predicted vs Measured PCI

$$PCI = a_1 + \frac{a_2}{1 + e^{(a_3 \times - \frac{\ln\left[\frac{b_2}{RQI_{\Delta TRQI} - b_1} - 1\right] + b_4}{b_3} + a_4)}} \tag{5-9}$$

5.6 RQI Threshold Limits

There are well known IRI threshold limits recommended by the Federal Highway Administration (FHWA), the National Highway System (NHS), the World Bank, and other research studies (56, 107, 110). These values are shown in Table 5-4.

Table 5-4. IRI Threshold Limits.

Condition	IRI (m/km)				
	FHWA			World Bank	70 km/hr Urban
	Interstate	Other	NHS		
Very Good	< 1.0	< 1.0	Acceptable 0 - 2.0	< 2.5	< 1.63
Good	1.0 - 1.5	1.0 - 1.5		2.5 - 3.5	1.6 - 2.7
Fair	1.5 - 1.9	1.5 - 2.0		3.5 - 6.0	2.7 - 3.3
Poor	1.9 - 2.0	2.0 - 3.5		6.0 - 10.0	3.3 - 4.6
Failed	> 2.0	> 3.5		> 10.0	> 4.6

Since this part of the research study focused on Arizona LTPP sections, the results presented next would be mainly applicable to those sections. The threshold limits for Interstate were set by comparing to general PCI threshold limits (111). The Urban thresholds were set by shifting the Interstate threshold limits to match the results from the comprehensive study in Chapter 3 made on the arterial roads. These results are shown in Table 5-5.

Table 5-5. RQI Threshold Limits.

Condition	RQI (m/km)		PCI
	Interstate	Urban	
Very Good	< 1.0	< 1.7	> 95
Good	1.0 - 1.5	1.7 – 3.0	65 - 95
Fair	1.5 – 1.8	3.0 - 3.3	50 - 65
Poor	1.8 – 2.6	3.3 - 4.1	25 - 50
Failed	> 2.6	> 4.1	0 - 25

5.7 Case Study: City of Maricopa

5.7.1 Introduction

This section demonstrates the use of the previously developed models and relationships into practice with a case study for the City of Maricopa, Arizona. The sub-sections to follow will describe the general information about the City and its pavement network. The results of the pavement condition windshield survey conducted will be presented along with the results from RQI measurements using iOS and Android devices. Finally, a cost analysis of the maintenance programs using both (PCI and RQI) approaches will be compared and discussed on how they would fit into a Pavement Management System (PMS).

5.7.2 City of Maricopa General Information

The City of Maricopa is located in south central Arizona in Pinal County. There are currently 47,000 residents living in the city (112). Its location is shown in the vicinity map in Figure 5-6.

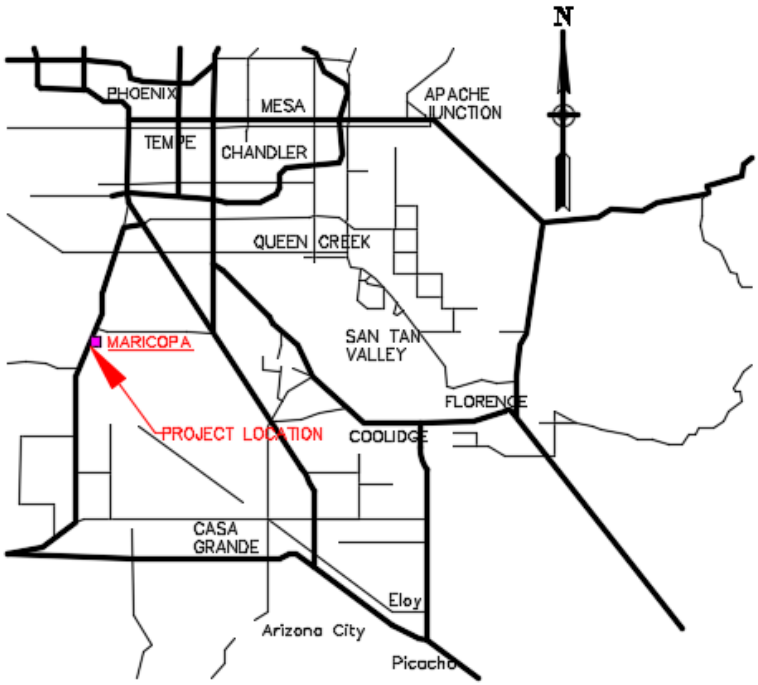

Figure 5-6. Vicinity Map.

The road network consists of 217 centerline miles and it is divided into 3,007 sections. Table 5-6 shows a summary of the road sections by road class and jurisdiction. This case study was conducted only on the sections that are owned by the city.

Table 5-6. Number of Sections per Road Class.

Class	All	State	City	Private
Collector	312	0	300	12
Local	3071	1	2705	365
Main	109	94	2	13

5.7.3 Pavement Condition Survey

A windshield pavement condition survey was carried out by students as part of their class project in a pavement management course. After initial training, the students were split into 13 groups to cover specific zones of the city. The city was divided into 18 zones as shown in Figure 5-7, and each group were assigned one or two zones based on the number of road sections in each zone.

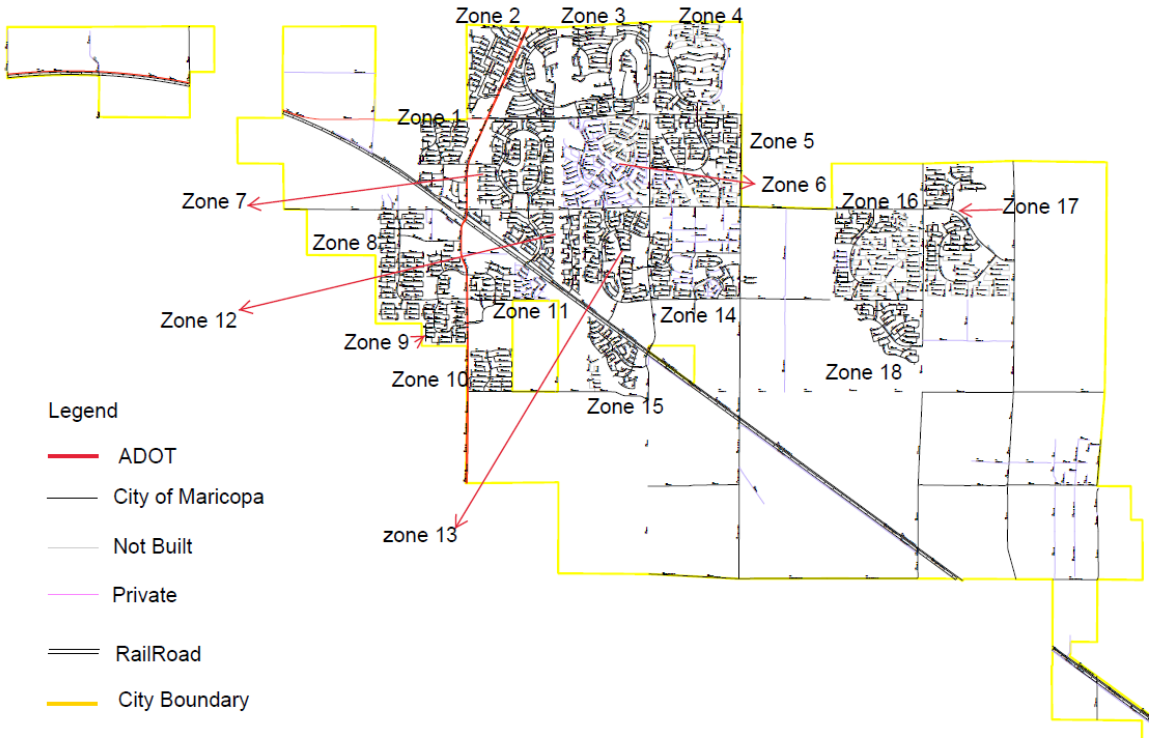

Figure 5-7. Map of City of Maricopa.

The current pavement management practice is to perform the condition survey using a template and distresses designed for flexible pavements, as shown in Figure 5-8. One of the objectives of this task was to provide the City of Maricopa with an overall

pavement condition assessment to use in their newly acquired PMS, and utilize the results in developing a cost-benefit approach to their maintenance planning.

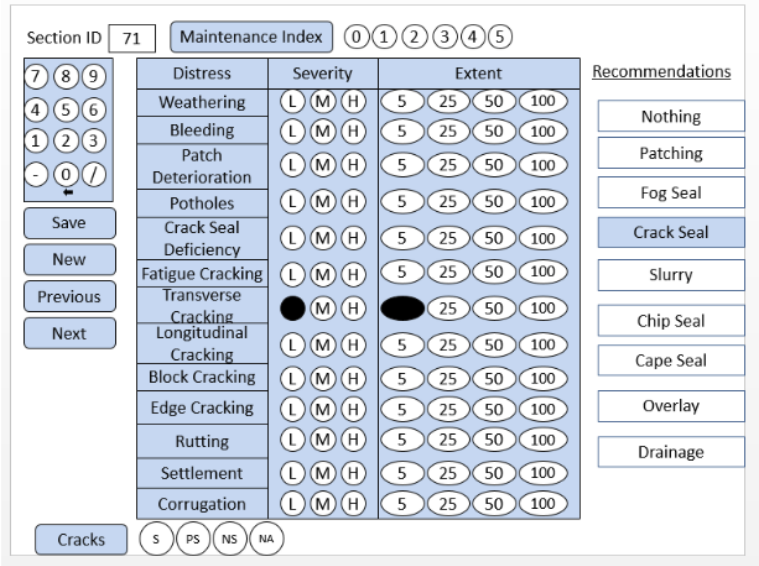

Figure 5-8. Typical Survey Template for Flexible Pavements.

In addition to the windshield pavement condition survey, the students were asked to drive one more time on their road sections and record RQI using their smartphones. The RQI data collection used either one of the same smartphone applications from the field studies in Chapter 3 (AndroSensor and SensorLog). The data was then processed using the RQI model also explained in Chapter 3.

5.7.3.1 Pavement Condition Index

As mentioned before, the pavement condition surveys were carried out by the students with basic training as part of their course. Zones: 1, 2, 4, 5, 8, 9, 10, 11, 12, 14, 15, 16, 17 and 18 were only considered for this analysis since data was available for both

PCI and RQI. This included 1088 road sections out of the total 3007. According to this windshield survey, the overall PCI for these sections was 79, which can be considered as very good condition. The recommended maintenance will dependent on the type of distress and the PCI value for each road section. The recommended maintenance treatment given the PCI range that is currently used by the City of Maricopa are shown in Table 5-7 (111).

Table 5-7. Maintenance Treatment Based on PCI.

PCI	Possible Maintenance
95 - 100	A1
65 - 94.9	A
50 - 64.9	B
25 - 49.9	D
0 - 24.9	E

Where, *A1*= no maintenance required, *A*= routine maintenance, *B*= preventive maintenance, *D*= rehabilitation, and *E*= reconstruction. Routine maintenance would include crack sealing, a seal coat, matching and other minor maintenance. Preventive maintenance would include heavier surface treatment such as microsurfacing and thin overlays. Figure 5-9 shows the percentage of the network that requires the specific maintenance treatment. The results shows that most of the network falls under routine (72.2%) and preventive (10%) maintenance. Based on this quick windshield survey conducted by the students, the results suggest that it would be a good time to implement a cost-benefit analysis to this network, since some of the sections that requires preventive maintenance may soon deteriorate and additional major rehabilitation will be needed in the near future.

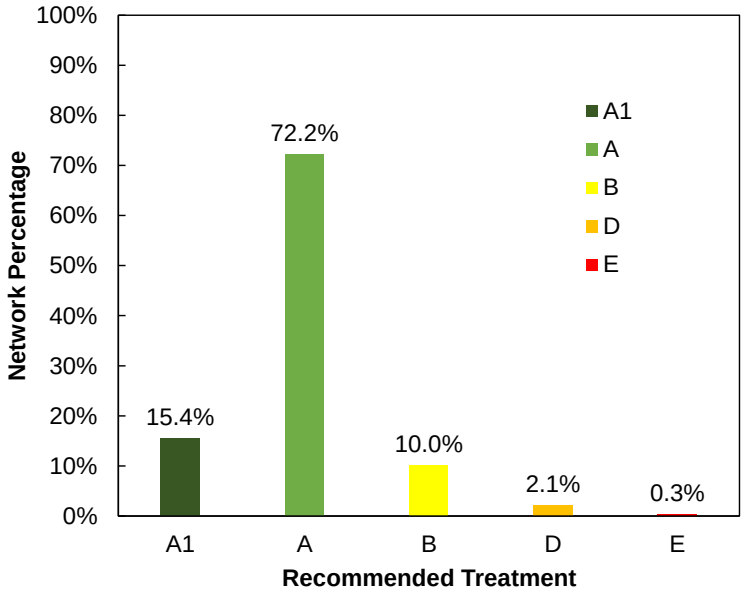

Figure 5-9. Percentage of Network by Recommended Treatment Based on PCI.

5.7.3.2 Ride Quality Index

The approach proposed in this research study (Chapters 3 and 4) is based on collecting data from a minimum sample size to determine reliable RQI values. The limitation in this City of Maricopa case study was that only one measurement from each road section was taken. However, the results from these RQI measurements are presented in this section to demonstrate the implementation process of using and comparing PCI and RQI results. The average RQI for the 1088 sections was 2.50 m/km. Table 5-8 shows a slightly modified RQI ranges from Table 5-5 for maintenance strategies based on urban roads such as arterials, collectors and local roads. Since construction practices and specifications will vary from city to city, some adjustments in RQI ranges may be needed for each specific network.

Table 5-8. Recommended Maintenance Treatment Based on RQI.

RQI	Possible Maintenance
< 1.72	A1
1.72 - 3.20	A
3.20 - 3.80	B
3.80 – 5.80	D
> 5.80	E

Using the RQI maintenance criteria shown above, the results (again, based on only one RQI measurement) are shown in Figure 5-10. Based on RQI values, most of the network requires no maintenance (20.3%), routine maintenance (59.7%) or preventive maintenance (10.9%).

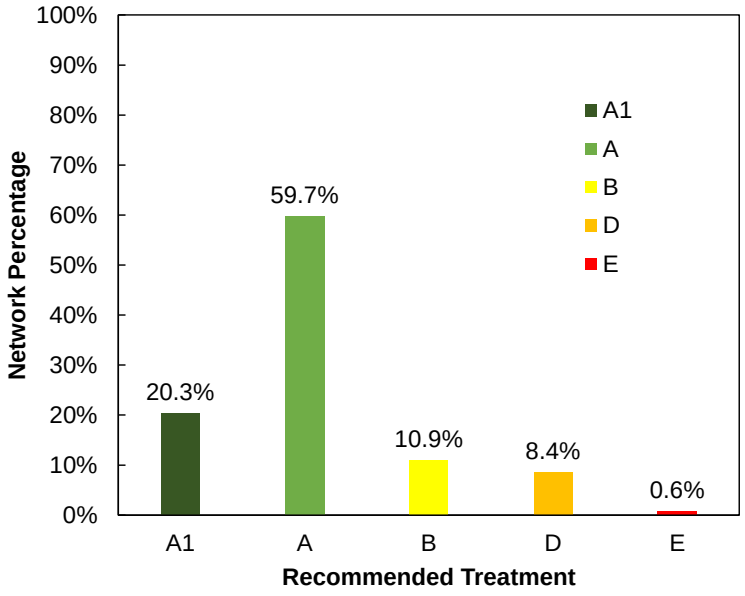

Figure 5-10. Percentage of Network by Recommended Maintenance Treatment Based on RQI.

5.7.3.3 PCI and RQI Comparison

When comparing the PCI to RQI results for all maintenance categories, they are generally in overall agreement/trend, but of course differ in some of the sections as

shown in Figure 5-11. There might be several reasons for this difference. The first reason comes from the fact that windshield condition surveys were carried out by student volunteers with no previous experience collecting distress data. That is, not all distress were picked up during the survey. The second reason could also come from the RQI measurements collected from different vehicles. Based on the results from the experimental studies presented in Chapter 3, RQI measurements can differ by more than 100 % when comparing single measurements. The third reason could come from the combination of both, less accurate windshield distress surveys and vehicles with variable suspension to accurately pick RQI data. Despite all of these issues, out of 1088 sections included in this analysis, 549 matched the proposed maintenance treatment based on the established PCI and RQI ranges. This means a 50 % match given the criteria set in Table 5-7 and Table 5-8. It is believed that the percentage of matching sections could increase if a larger sample size for RQI measurements is collected, and a more reliable windshield survey is performed.

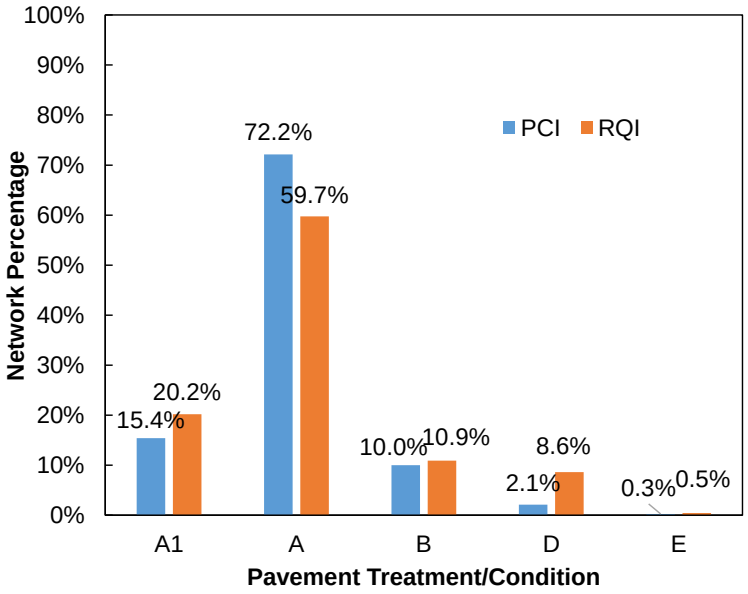

Figure 5-11. PCI and RQI Comparison for All 1088 Sections.

5.7.4 Cost Analysis

The network level maintenance cost estimation for both cases based on PCI, and RQI are presented in this section for the 1088 road sections. The cost analysis was based on average cost for different treatment strategies per the City of Maricopa PMS. These cost are summarized in Table 5-9.

Table 5-9. Average Treatment Cost.

Treatment	Cost ($/yd2)
A1	$ -
A	$ 0.72
B	$ 2.00
D	$ 19.00
E	$ 133.00

5.7.4.1 Pavement Condition Index Based Cost Analysis

The results from the pavement condition windshield surveys, shown in Figure 5-12, estimated that 0.41 Myd^2 needs no maintenance, 1.33 Myd^2 needs a crack seal or a light routine maintenance, 0.17 Myd^2 require some preventive maintenance such as chip/slurry seal, thin overlay, 0.11 Myd^2 needs a rehabilitation treatment, perhaps a mill and overlay, and 0.01 Myd^2 requires full reconstruction. The estimated total cost to bring the pavements from these 12 zones back to excellent condition is around $4.4 million dollars.

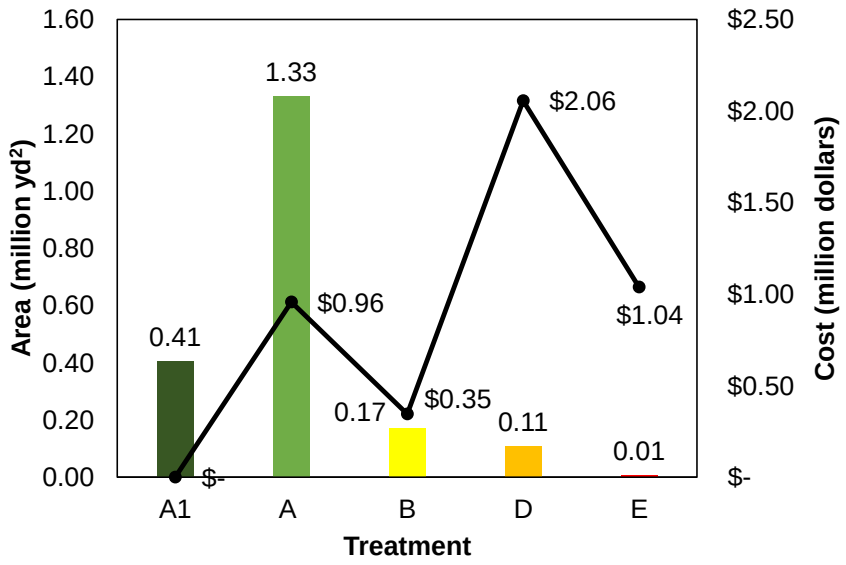

Figure 5-12. Total Area and Cost Estimates by Pavement Treatment for a PCI Based Analysis.

5.7.4.2 Ride Quality Index Based Cost Analysis

This sections provides a summary of the cost analysis based on the collected RQI measurements. Based on this analysis, the results shows that 0.66 Myd2 are in excellent condition and do not require any maintenance, 1.05 Myd2 are under the routine

maintenance category, only 0.17 Myd2 requires preventive maintenance, 0.14 Myd2 needs probably a mill an overlay, and 0.01 Myd2 requires full reconstruction, Figure 5-13. The total cost to bring the studied locations to an excellent ride-ability is $4.7 million dollars.

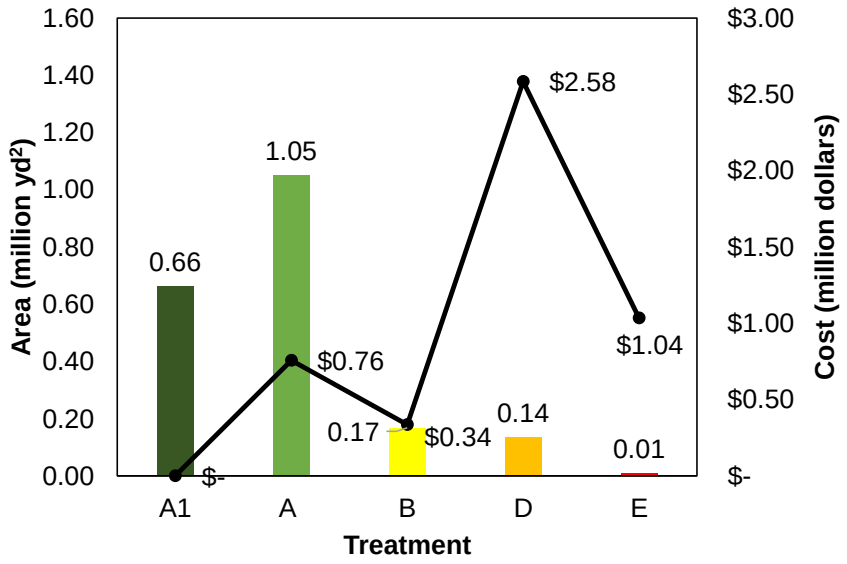

Figure 5-13. Total Area and Cost Estimates by Pavement Treatment for a RQI Based Analysis.

5.7.4.3 Discussion

There are some differences from PCI based to RQI based maintenance cost estimation; however, the results compared really well. Regardless of the quality of the data issues discussed previously, the estimated costs differed by around $300,000, as shown in Table 5-10. This was considered excellent comparison for a network level PMS, keeping in mind that a light treatment such a fog seal or a slurry seal may address surface related distresses, but not necessarily solve smoothness problems (113, 114). A research by McGhee and Gillespie (2006) showed that smoothness specifications for

initial construction may increase initial cost 5 to 10% but increases the life of the pavement by 9 years with savings up to 27 % (115).

Table 5-10. Cost Summary Results for the City of Maricopa.

Treatment	PCI		RQI	
	Area (yd^2)	Cost	Area (yd^2)	Cost
A1	406498	$ -	662873	$ -
A	1329973	$ 957,580.90	1050607	$ 756,437.07
B	172942	$ 345,883.33	168152	$ 336,303.75
D	108232	$ 2,056,408.07	136037	$ 2,584,712.11
E	7809	$ 1,038,625.98	7784.33	$ 1,035,316.43
Total	**2025454**	**$ 4,398,498.28**	**2025454**	**$ 4,712,769.36**

5.8 Summary

The objective of this chapter / part of the study was to develop a relationship between PCI and RQI, and to create RQI threshold limits that can be used in a pavement management system. Historical data from 40 LTPP flexible pavement sections from Arizona dry-non freeze climatic region were used to create PCI master curves using the sigmoidal model and methodology proposed by Sotil and Kaloush, and modified by Beckley to create IRI master curves. Some specific conclusions are as follow:

- Based on the PCI master curve developed, the estimated life of these pavement sections was 25 years; which was based on the best fit for the historical data with R^2 of 0.976.
- Based on RQI master curve, the best optimization with R^2 of 0.945 was also found at 25 year maximum shifting, the same as PCI. From this network level analysis, the average initial RQI is about 0.50 m/km with a PCI of 100.

- The developed methodology to combine both master curves was successful; the results gave good comparative statistics with R^2 of 0.85 and Se/Sy of 0.38.
- Based on pavement sections for this Arizona LTPP network, some RQI threshold limits were proposed for interstate highways and urban local arterials.

5.8.1 City of Maricopa

The objective of the City of Maricopa case study was to put in practice RQI data collection using ordinary vehicles, and to provide the City an assessment of their road network condition based on windshield distress surveys so that it can be implemented in their pavement management system. The city was divided into 18 zones, and student volunteers were assigned one or two zones to carryout windshield surveys and collect RQI data from their vehicles. Some specific outcomes from this case study are as follow:

- The windshield pavement condition survey results showed that 87.6 % of the pavement sections was in excellent and very good condition, with a PCI average of 79.
- The RQI results from a single vehicle run showed that 80.0 % of the road sections were in excellent to very good condition. The RQI average was 2.50 m/km for the 1088 road sections used in the comparison.
- Despite of the windshield distress survey collected by student volunteers with limited training, and only one RQI measurement collected for each road section, the results had very good to excellent match in recommended maintenance for 549 sections out of 1088.

- The estimated cost based on PCI survey was $4.4 million dollars while the cost based on RQI was estimated to be $4.7 million dollars. This was concluded to be excellent for a network level pavement management system analysis.

RQI based pavement management system is definitely promising and could be considered as an alternative for network level evaluation.

Chapter 6 Summary, Conclusions and Future Work

6.1 Summary and Conclusions

The pavement infrastructure network is a valuable asset that needs to be preserved, using limited resources, in the best cost-effective way. Pavement management systems and pavement distress assessment have been implemented in many countries for decades to evaluate the condition of a pavement at a network and project levels. One issue with current survey practices is that it requires qualified raters to carry out manual pavement distress surveys. Despite the availability of a guide to rate the condition of pavements, there is always some kind of subjectivity involved. Another tool used for assessing pavement condition is the use of automated vehicles. The problem with this type of equipment is that it is costly and not all agencies can afford to purchase it. This study intended to address these limitations by developing a simple and feasible method to continually and systematically quantify pavement condition of the entire road network by using technologies already embedded in new cars and smart phones. With the surge of big data and crowdsourcing techniques, this study presented a methodology to implement this data collection into a pavement management system (PMS) with the goal of achieving 100% automation.

There are many performance indices used in PMS. One that is of importance for this research was the IRI as a measure of pavement roughness. IRI is a widely accepted performance index; it has been used by many researchers to characterize pavement roughness using inertial sensors, and in the recent past, embedded in smartphones. Most of existing technologies build a ride quality model with limited information, controlled

set up, and calibrate the model to a specific setting. There are two additional things that are lacking; 1) the variability from many factors such as different vehicles, driver, speed, cellphone and other, and 2) they do not provide a number of how large the dataset needs to be in order to reach convergence in their roughness measurements.

While the idea of using inertial sensors in smartphone is novel, the proposed uses of this technologies falls short in establishing a framework where ride quality measurements, represented by Ride Quality Index (RQI), can be randomly collected from a vehicle spectra, and how it can be integrated into a pavement management system. The following sections present a summary and conclusions from this research effort.

6.1.1 Smartphone Data Collection Field Studies

- A mechanical model to account for the smartphone set up inside the vehicle was developed, and calibrated. Questions addressed by each of the case study were: Does it matter when using one vehicle? Does it matter when using many vehicles? Or does it matter if using extreme heavy duty commercial vehicles in comparison to typical sedans?
- The Preliminary Study: Effect on Single Factors
    - ✓ Individual random factors, such as cellphone, mount, and speed, affecting the RQI measurements can be significant.
    - ✓ Cellphone and mount were significant factors that can bias the results in a case by case comparison.
    - ✓ The interaction between all factors was not significant.

- ✓ By minimizing the sources of variability (i.e. less mounts and cellphones), the data can converge fast. Typically around 20-30 samples.

- The Comprehensive Study: Effect of a Population of Different Vehicle Classifications
  - ✓ RQI values from many vehicles of the same classification had no significant difference between them.
  - ✓ There are individual cases that a smartphone-mount-speed-vehicle configuration will give a greater or lower RQI value, but when these cases are combined with many other configurations, the results from this analysis showed that it does not matter, and the difference between vehicle classes is not significant.
  - ✓ The variance of this experimental study increased in comparison to the Preliminary Study, but the data seemed to converge after 50-60 samples.
- The Extreme Case Study: Effect of Sedan vs Heavy Duty Commercial Trucks
  - ✓ Heavy duty commercial trucks showed a significant difference in RQI measurements when compared to a regular sedan.
- As a conclusion, if RQI values are evaluated in a case by case basis, there might be a significant difference that would suggest some kind of calibration, as has been proposed by others.
- If the data is analyzed as a whole, meaning not taking one vehicle but instead a population of vehicles, the data showed no significant difference.

6.1.2 Parametric Assessment of the Factors Affecting Ride Quality Index Estimation and Sample Size Determination

- 900,000 Monte Carlos simulations were performed to identify the effects of vehicle classification on RQI estimates. In most of the cases, the assumed probability distribution for the suspension parameters did not show a significant effect on RQI results.
- Within a given distribution analysis, in most of the cases heavy duty trucks showed a significant difference when compared to sedan and SUV. However, in more realistic scenarios in which a mixed traffic was considered, there was no significant effect on RQI results.
- Simulation analysis was carried out by assuming that the road profile was exactly the same for all simulations. In more realistic cases, there would be wander effects that may or may not affect the RQI values. To address this problem, a normal distribution variability was assumed for the road profile. From literature review, a 6 % coefficient of variation on the road profile was assume to account for wander effects. 300,000 simulations were run for this analysis assuming only normal distribution for suspension parameters since the previous analysis showed no significant effect between the other statistical distributions. The average increase in sample size was from 328 samples to 400 which represents a 23 % increase.
- The two lane plus wander scenario was analyzed by adding the variability caused by wander effects within a lane and the variability from driving lane to passing lane. This variability study was measured from Minnesota Road Test database.

Results from this analysis showed that the CV within a lane was 10 to 12 %, and from lane to lane 14 %. The results also showed that, on average, the passing lane was about 10% smoother than the driving lane.

- A total of 120,000 Monte Carlo simulations for this last case were run only on the Arizona and New Jersey sections. The average number of samples from both sections, required for RQI convergence within 2 % CVSE, was 435 samples which represents a 33 % increase in sample size from the original case (single lane – no wander).
- The overall conclusion from this part of the study was that there are significant difference between vehicle classifications with respect to heavy commercial trucks. However there was no statistical significance between mixed traffic cases on RQI values, and increase in sample size was observed when wander and two lane variability are considered in the analysis.
- Based on this analysis, a conservative sample size estimate of 300 to 400 samples would be recommended to reach convergence at an acceptable level of error (2.5 – 2.0 % CV_{se}). As a network level pavement ride quality assessment, this error is small enough that would not change the outcome in a decision making process.

6.1.3 Integration of Ride Quality Index (RQI) into Pavement Management System (PMS)

- Based on the PCI master curve developed, the estimated life of these pavement sections was 25 years; which was based on the best fit for the historical data with R^2 of 0.976.
- Based on RQI master curve, the best optimization with R^2 of 0.945 was also found at 25 year maximum shifting, the same as PCI. From this network level analysis, the average initial RQI is about 0.50 m/km with a PCI of 100.
- The developed methodology to combine both master curves was successful; the results gave good comparative statistics with R^2 of 0.85 and Se/Sy of 0.38.
- Based on pavement sections for this Arizona LTPP network, some RQI threshold limits were proposed for interstate highways and urban local arterials.

6.1.4 City of Maricopa

- The windshield pavement condition survey results showed that 87.6 % of the pavement sections was in excellent and very good condition, with a PCI average of 79.
- The RQI results from a single vehicle run showed that 80.0 % of the road sections were in excellent to very good condition. The RQI average was 2.50 m/km for the 1088 road sections used in the comparison.
- Despite of the windshield distress survey collected by student volunteers with limited training, and only one RQI measurement collected for each road section,

the results had very good to excellent match in recommended maintenance for 549 sections out of 1088.

- The estimated cost based on PCI survey was $4.4 million dollars while the cost based on RQI was estimated to be $4.7 million dollars. This was concluded to be excellent for a network level pavement management system analysis.
- RQI based pavement management system is definitely promising and could be considered as an alternative for network level evaluation.

6.1.5 General Conclusions

- From the experimental studies and the Monte Carlo simulations it was shown that the data converges into a single value within an acceptable level of error.
- The speed of data convergence will depend on the number of different vehicles and factors (i.e. mounts, speed, and cellphones) which increases variability in the results.
- With typical average daily traffic for arterials and collectors, if this methodology is fully implemented, a pavement condition assessment of the entire network based on RQI can be accomplished in one or two days.
- RQI data collection approach is an easy and inexpensive way to estimate network-level pavement performance and maintenance costs.
- RQI threshold limits has to be adjusted for individual networks, and based on road classification.

- The limitation of using RQI as an index for pavement management system is that it cannot give detailed information about specific surface distresses, but provides and overall insight of the pavement conditions at a network level.

6.1.6 Implementation Strategies

- The data collection approach developed in this study can be implemented by agencies, using their own vehicle fleet, the smaller the vehicle fleet is the less number of samples will be required for data convergence.
- The implementation can be further extended by using Uber or Lyft drivers to collect RQI. These companies already have hundreds of thousands of drivers in their network which provides millions of rides a day. With this kind of a driver/vehicle network, this approach can be readily implemented by these companies.

6.2 Future Work

This study provided a new methodology to assess pavement condition at a network level through a ride quality index using crowdsourcing. Future and follow up work recommendations are as follows:

- Full scale implementation of this cowdsourcing data collection.
- Investigation of the effects of seasonal variations such as frost heave on RQI measurements, and implications to assessing network level condition in a pavement management system.

- Expand the RQI analysis for more pavement conditions and rigid pavements. Develop thresholds for rigid pavements in urban settings.
- Development of a crowdsource methodology to quantify cracking. Cracks in a pavement can be induced by fatigue or thermal cracking. A methodology need to be developed to quantify all the surface cracks in a pavement section using image processing; also following ASTM D6433 to calculate a crack based PCI and the minimum sample units required. This will complement the RQI approach and give a more detailed overview of the road network in terms of pavement condition.
- Development of rolling weight deflectometer system that can be used in typical freight semi-trucks to estimate the pavement structural capacity using crowdsourcing techniques.
- Development of a complete pavement management system based on crowdsourcing data collection to calculate RQI, PCI-crack, and structural number indices.

References

1. 2011-15: U.S. Department of Transportation, Federal Highway Administration, Highway Statistics (Washington, DC: Annual issues), table HM-12, available at http://www.fhwa.dot.gov/policyinformation/statistics.cfm as of Apr. 14, 2017.

2. 2015: U.S. Department of Transportation, Federal Highway Administration, Highway Statistics (Washington, DC: Annual issues), table DISB-C, available at https://www.fhwa.dot.gov/policyinformation/statistics/2015/ as of Mar. 6, 2018.

3. Robbins, Mary M., and Nam Tran. "Literature review: the effect of pavement roughness on vehicle operating costs." (2015).

4. Zaabar, Imen, and Karim Chatti. "Identification of localized roughness features and their impact on vehicle durability." HVTT11, International Heavy Vehicle Symposium: Balancing Competing Needs in Heavy Vehicle Transport Technology. 2010.

5. Golabi, Kamal, Ram B. Kulkarni, and George B. Way. "A statewide pavement management system." Interfaces 12.6 (1982): 5-21.

6. Finn, Fred. "Pavement management systems--Past, present, and future." Public Roads 62.1 (1998).

7. Kulkarni, Ram, and Richard Miller. "Pavement management systems: Past, present, and future." Transportation Research Record: Journal of the Transportation Research Board 1853 (2003): 65-71.

8. FHWA. Pavement Management Systems Document.

9. Haider, Syed, et al. "Effect of frequency of pavement condition data collection on performance prediction." Transportation Research Record: Journal of the Transportation Research Board 2153 (2010): 67-80.

10. Rada, Gonzalo R., Jossef Perl, and Matthew W. Witczak. "Integrated model for project-level management of flexible pavements." Journal of Transportation Engineering 112.4 (1986): 381-399.

11. Shahin, Mohamed Y., and Starr D. Kohn. Pavement maintenance management for roads and parking lots. No. CERL-TR-M-294. CONSTRUCTION ENGINEERING RESEARCH LAB (ARMY) CHAMPAIGN IL, 1981.

12. Shahin, Mohamed Y., and J. A. Walther. Pavement maintenance management for roads and streets using the PAVER system. No. CERL-TR-M-90/05.

CONSTRUCTION ENGINEERING RESEARCH LAB (ARMY) CHAMPAIGN IL, 1990.

13. NCHRP Synthesis 501. Pavement Management Systems: Putting Data to Work. (2017).

14. Gowda, S., Jain, S., Patil, K. S., Biligiri, K. P., & Prabhakar, B. E. (2015). Development of a Budget-Prioritized Pavement Management System based on Engineering Criteria. International Journal of Pavement Research & Technology, 8(3).

15. Camahan, J. V., et al. "Optimal maintenance decisions for pavement management." Journal of Transportation Engineering 113.5 (1987): 554-572.

16. Bianchini, A. (2012). Fuzzy representation of pavement condition for efficient pavement management. Computer- Aided Civil and Infrastructure Engineering, 27(8), 608-619.

17. Sotil, A., and K. E. Kaloush. "Development of pavement performance models for Delhi township, Ohio pavement management system." Compendium of Papers CD-ROM 83rd Annual Meeting of the Transportation Research Board. 2004.

18. Bridgelall, Rajinder. Pavement performance evaluation using connected vehicles. Diss. North Dakota State University, 2015.

19. Lytton, Robert L. "Concepts of pavement performance prediction and modeling." Proc., 2nd North American Conference on Managing Pavements. Vol. 2. 1987.

20. Haas, Ralph, W. Ronald Hudson, and John P. Zaniewski. Modern pavement management. 1994.

21. Butt, Abbas A., et al. Pavement performance prediction model using the Markov process. No. 1123. 1987.

22. Ningyuan, L., R. Haas, and W. Xie. "Investigation of the Relationship between Deterministic and Probabilistic Models in Pavement Management." Washington, DC (1997).

23. Solorio Murillo, J. R., et al. "Aplicacion de Metodos Markovianos en el Modelado del Deterioro de Carreteras." Publicacion Tecnica 396 (2014).

24. Li, Ningyuan, Wei-Chau Xie, and Ralph Haas. "Reliability-based processing of Markov chains for modeling pavement network deterioration." Transportation

Research Record: Journal of the Transportation Research Board 1524 (1996): 203-213.

25. Shalaby, Ahmed, and Alan Reggin. "Optimization of data collection needs for manual and automated network-level pavement condition ratings based on transverse variability and neural networks." Canadian Journal of Civil Engineering 34.2 (2007): 139-146.

26. Fu, Pengcheng, et al. "Comprehensive evaluation of automated pavement condition survey service providers' technical competence." International Journal of Pavement Engineering 14.1 (2013): 36-49.

27. Radopoulou, Stefania C., and Ioannis Brilakis. "Automated detection of multiple pavement defects." Journal of Computing in Civil Engineering 31.2 (2016): 04016057.

28. Wang, Kelvin CP. "Designs and implementations of automated systems for pavement surface distress survey." Journal of Infrastructure Systems 6.1 (2000): 24-32.

29. Bridgelall, Raj, and Denver Tolliver. "Accuracy enhancement of roadway anomaly localization using connected vehicles." International Journal of Pavement Engineering 19.1 (2018): 75-81.

30. Terzi, Serdal. "Modeling the pavement serviceability ratio of flexible highway pavements by artificial neural networks." Construction and Building Materials 21.3 (2007): 590-593.

31. ASTM (2011). "Standard Practice for Roads and Parking Lots Pavement Condition Index Surveys." ASTM D6433-11, West Conshohocken, PA.

32. Shahin, Mohamed Y., Michael I. Darter, and Starr D. Kohn. Development of a Pavement Maintenance Management System. Volume I. Airfield Pavement Condition Rating. No. CERL-TR-C-76-VOL-1. CONSTRUCTION ENGINEERING RESEARCH LAB (ARMY) CHAMPAIGN ILL, 1977.

33. Elbagalati, Omar, et al. "Prediction of In-Service Pavement Structural Capacity Based on Traffic-Speed Deflection Measurements." Journal of Transportation Engineering 142.11 (2016): 04016058.

34. Rohde, Gustav T. "Determining pavement structural number from FWD testing." Transportation Research Record 1448 (1994).

35. Smith, K. D., et al. "Using Falling Weight Deflectometer Data with Mechanistic-Empirical Design and Analysis, Volume 1: Final Report." Federal Highway Administration (2017).

36. Transportation Officials. AASHTO Guide for Design of Pavement Structures, 1993. Vol. 1. AASHTO, 1993.

37. Elbagalati, Omar, et al. "Development of the pavement structural health index based on falling weight deflectometer testing." International Journal of Pavement Engineering (2016): 1-8.

38. Sayers, Michael W., and Steven M. Karamihas. "The little book of profiling." University of Michigan (1998).

39. Janoff, M. S., et al. "National Cooperative Highway Research Program (NCHRP) Report 275: Pavement Roughness and Rideability." Transportation Research Board, National Research Council, Washington, DC (1985).

40. Kelly, L. S., T. G. Leslie, and D. E. Lynn. "Pavement Smoothness Index Relationships: Final Report." Publication No. FHWA-RD-02-057, US Department of Transportation, Federal Highway Administration, Research, Development, and Technology, Turner-Fairbank Highway Research Center(2002).

41. Janoff, Michael S. "National Cooperative Highway Research Program (NCHRP) Report 308: Pavement Roughness and Rideability Field Evaluation." Transportation Research Board, National Research Council, Washington, DC (1988).

42. Zamora Alvarez, Eric Jose. A Discrete Roughness Index for Longitudinal Road Profiles. Diss. Virginia Tech, 2016.

43. California Department of Transportation (Caltrans). 2012. Method of Test for Operation of California Highway Profilograph and Evaluation of Profiles. California Department of Transportation, Sacramento, CA.

44. Smith, Kurt, and Prashant Ram. Measuring and Specifying Pavement Smoothness. Tech brief no. FHWA-HIF-16-032. 2016.

45. Capuruço, Renato, et al. "Full-car roughness index as summary roughness statistic." Transportation Research Record: Journal of the Transportation Research Board 1905 (2005): 148-156.

46. Múčka, Peter. "Current approaches to quantify the longitudinal road roughness." International Journal of Pavement Engineering 17.8 (2016): 659-679.

47. Smoothness Specifications Online [online]. 2012. The Transtec Group, Austin, Texas, USA, Available from:http://www.smoothpavements.com [Accessed March 7, 2018].

48. Perera, R. W., and S. D. Kohn. "Issues in pavement smoothness." Transportation Research Board, Washington, DC (2002).

49. Merritt, David K., George K. Chang, and Jennifer L. Rutledge. Best practices for achieving and measuring pavement smoothness, a synthesis of state-of-practice. No. FHWA/LA. 14/550. 2015.

50. Sayers, Michael W. "Two quarter-car models for defining road roughness: IRI and HRI." Transportation Research Record1215 (1989).

51. Minnesota Department of Transportation, Introduction to the International Roughness Index. Bituminous Smoothness Training Workshop. (2007).

52. Gillespie, T. D., M. W. Sayers, and L. Segel. "Calibration of Response Type Road Roughness Systems." NCHRP Report228.

53. Sayers, Michael W. "Guidelines for conducting and calibrating road roughness measurements." (1986).

54. Al-Omari, Bashar, and Michael I. Darter. "Relationships between international roughness index and present serviceability rating." Transportation Research Record 1435 (1994).

55. Paterson, William. "International roughness index: Relationship to other measures of roughness and riding quality." Transportation Research Record 1084 (1986).
56. Archondo-Callao, Rodrigo. "Applying the HDM-4 model to strategic planning of road works." (2008).

57. Kerali, H. R., R. Robinson, and W. D. O. Paterson. "Role of the new HDM-4 in highway management." 4th International Conference on Managing Pavements. 1998.

58. Willett, M., G. Magnusson, and B. W. Ferne. "FILTER experiment-Theoretical study of indices." FEHRL TECHNICAL NOTE 2000/02 (2000).

59. Delanne, Yves, and Paulo Pereira. "Advantages and limits of different road roughness profile signal-processing procedures applied in Europe." Transportation Research Record: Journal of the Transportation Research Board 1764 (2001): 254-259.

60. Múčka, Peter. "International Roughness Index specifications around the world." Road Materials and Pavement Design 18.4 (2017): 929-965.

61. Islam, Shahidul, et al. "Measurement of pavement roughness using android-based smartphone application." Transportation Research Record: Journal of the Transportation Research Board 2457 (2014): 30-38.

62. McGhee, K. H. "Automated Pavement Distress Collection Techniques. NCHRP Synthesis 334. National Cooperative Highway Research Program." Transportation Research Board, Washington DC (2004).

63. 2015: Arizona Department of Transportation: Multimodal Planning Division Geographic Information System Section, 2015 State Highway System Log: Table II Centerline Miles of Road by Route, available at https://www.AZdot.gov/docs/default-source/planning/2015msbooklet.pdf?sfvrsn=2 as of Mar. 10, 2018.

64. Stevens, Ryan. "City of Phoenix Pavement Management System". Arizona Pavements and Materials Conference, 15 November 2017, Arizona State University, Tempe, AZ. Conference Presentation.

65. Bridgelall, Raj. "A participatory sensing approach to characterize ride quality." SPIE Smart Structures and Materials+ Nondestructive Evaluation and Health Monitoring. International Society for Optics and Photonics, 2014.

66. Bridgelall, Raj, Jill Hough, and Denver Tolliver. "Characterising pavement roughness at non-uniform speeds using connected vehicles." International Journal of Pavement Engineering(2017): 1-7.

67. Islam, Md Shahidul. Development of a smartphone application to measure pavement roughness and to identify surface irregularities. Diss. University of Illinois at Urbana-Champaign, 2015.

68. Chen, Chih-Sheng, Chia-Pei Chou, and Ai-Chin Chen. Viscoelastic Model for Estimating the International Roughness Index by Smartphone Sensors. No. 17-04217. 2017.

69. Wang, Winnie, and Feng Guo. RoadLab: Revamping Road Condition and Road Safety Monitoring by Crowdsourcing with Smartphone App. No. 16-2116. 2016.

70. Forslöf, Lars, and Hans Jones. "Roadroid: Continuous road condition monitoring with smart phones." Journal of Civil Engineering and Architecture 9.4 (2015): 485-496.

71. Forslöf, Lars. "Roadroid–smartphone road quality monitoring." Proceedings of the 19th ITS World Congress. 2012.

72. 2013-18: Roadroid, available at http://www.roadroid.com/common/References/Roadroid%20reference%20projects%200.5.pdf as of Mar. 10, 2018.

73. AYDIN, Metin Mutlu, Mehmet Sinan YILDIRIM, and Lars FORSLOF. "The Use of Smart Phones to Estimate Road Roughness: A Case Study in Turkey." International Conference on Advanced Engineering Technologies (ICADET 2017). Vol. 21. 2017.

74. Scholotjes, M., A. Visser, and C. Bennett. "Evaluation of a smartphone roughness meter." Proceedings of The 33rd Southern African Transport Conference (SATC 2014). 2014.

75. YAGI, Koichi CEO. "2 nd IRF Asia Regional Congress & Exhibition."

76. Eriksson, Jakob, et al. "The pothole patrol: using a mobile sensor network for road surface monitoring." Proceedings of the 6th international conference on Mobile systems, applications, and services. ACM, 2008.

77. Mednis, Artis, et al. "Real time pothole detection using android smartphones with accelerometers." Distributed Computing in Sensor Systems and Workshops (DCOSS), 2011 International Conference on. IEEE, 2011.

78. Koch, Christian, Gauri M. Jog, and Ioannis Brilakis. "Automated pothole distress assessment using asphalt pavement video data." Journal of Computing in Civil Engineering 27.4 (2012): 370-378.

79. Initiative, NSF-NIH Interagency. "Core Techniques and Technologies for Advancing Big Data Science and Engineering (BIGDATA)." URL: http://grants. nih. gov/grants/guide/notice-files/NOT-GM-12-109. html [accessed 2018-03-11].

80. Gartner. (2016). "IT Glossary." Available at: https://www.gartner.com/it-glossary/big-data as of March 11, 2018.

81. McAfee, Andrew, et al. "Big data: the management revolution." Harvard business review 90.10 (2012): 60-68.

82. Edwards, John S., and Eduardo Rodriguez Taborda. "Using knowledge management to give context to analytics and big data and reduce strategic risk." Procedia Computer Science99 (2016): 36-49.

83. HAZen, Benjamin T., et al. "Back in business: Operations research in support of big data analytics for operations and supply chain management." Annals of Operations Research (2016): 1-11.

84. Wamba, Samuel Fosso, et al. "Big data analytics and firm performance: Effects of dynamic capabilities." Journal of Business Research 70 (2017): 356-365.

85. Misra, Aditi, et al. "Crowdsourcing and its application to transportation data collection and management." Transportation Research Record: Journal of the Transportation Research Board 2414 (2014): 1-8.

86. Goodchild, Michael F. "Assertion and authority: the science of user-generated geographic content." (2008).

87. Irwin, Mark (2016). "Convergence in Distribution Central Limit Theorem". Available at: http://www2.stat.duke.edu/~sayan/230/2017/Section53.pdf as of March 11, 2018.

88. Bagui, Subhash C., and K. L. Mehra. "Convergence of binomial, Poisson, negative-binomial, and gamma to normal distribution: Moment generating functions technique." American Journal of Mathematics and Statistics 6.3 (2016): 115-121.

89. Landau, David P., and Kurt Binder. A guide to Monte Carlo simulations in statistical physics. Cambridge university press, 2014.

90. Sawilowsky, Shlomo S. "You think you've got trivials?." Journal of Modern Applied Statistical Methods 2.1 (2003): 21.

91. Stephens, Michael A. "EDF statistics for goodness of fit and some comparisons." Journal of the American statistical Association 69.347 (1974): 730-737.

92. Anderson, Theodore W., and Donald A. Darling. "A test of goodness of fit." Journal of the American statistical association49.268 (1954): 765-769.

93. Sakia, R. M. "The Box-Cox transformation technique: a review." The statistician (1992): 169-178.

94. Keppel, G., and T. D. Wickens. "The linear model and its assumptions." Design and Analysis: A Researcher's Handbook (2004): 153-155.

95. Johnson, Norman L. "Systems of frequency curves generated by methods of translation." Biometrika 36.1/2 (1949): 149-176.

96. Johnson, Norman L. "Bivariate distributions based on simple translation systems." Biometrika 36.3/4 (1949): 297-304.

97. Kropáč, O., and P. Múčka. "Effects of longitudinal road waviness on vehicle vibration response." Vehicle System Dynamics 47.2 (2009): 135-153.

98. Thom, Herbert CS. "A note on the gamma distribution." Monthly Weather Review 86.4 (1958): 117-122.

99. 2015: Maryland State Highway Administration, Vehicle Class Distribution. Available at www.roads.maryland.gov/oppen/Vehicle_Class.pdf as of Mar. 17, 2018.

100. Cohen, Jacob. "Statistical power analysis." Current directions in psychological science 1.3 (1992): 98-101.

101. Cohen, Jacob. "The statistical power of abnormal-social psychological research: a review." The Journal of Abnormal and Social Psychology 65.3 (1962): 145.

102. Cohen, Jacob. "A power primer." Psychological bulletin 112.1 (1992): 155.

103. Rice, Marnie E., and Grant T. Harris. "Comparing effect sizes in follow-up studies: ROC Area, Cohen's d, and r." Law and human behavior 29.5 (2005): 615.

104. Sawilowsky, Shlomo S. "New effect size rules of thumb." (2009).

105. Noorvand, Hossein, Guru Karnati, and B. Shane Underwood. "Autonomous Vehicles: Assessment of the Implications of Truck Positioning on Flexible Pavement Performance and Design." Transportation Research Record: Journal of the Transportation Research Board 2640 (2017): 21-28.

106. Jia, Xiaoyang, et al. "Influence of Measurement Variability of International Roughness Index on Uncertainty of Network-Level Pavement Evaluation." Journal of Transportation Engineering, Part B: Pavements 144.2 (2018): 04018007.

107. Beckley, Michelle Elizabeth. Pavement Deterioration Modeling Using Historical Roughness Data. Arizona State University, 2016.

108. ": Data." LTPP InfoPave - Data Selection and Download, infopave.fhwa.dot.gov/Data/DataSelection. [Accessed 2018-01-10].

109. Wu, Kan. Development of PCI-based Pavement Performance Model for Management of Road Infrastructure System. Arizona State University, 2015.

110. Abudinen, Daniel, Luis G. Fuentes, and Juan S. Carvajal Muñoz. "Travel Quality Assessment of Urban Roads Based on International Roughness Index: Case Study in Colombia." Transportation Research Record: Journal of the Transportation Research Board 2612 (2017): 1-10.

111. Kaloush, Kamil,.Highway Consulting Services Inc.

112. City and Town Population Totals: 2010-2016. US Census Bureau, https://www.census.gov/data/tables/2016/demo/popest/total-cities-and-towns.html. [Accessed 2018-03-10].

113. Hall, Kathleen, Carlos Correa, and Amy Simpson. "Performance of flexible pavement rehabilitation treatments in the long-term pavement performance SPS-5 experiment." Transportation Research Record: Journal of the Transportation Research Board 1823 (2003): 93-101.

114. Serigos, Pedro A., Andre Smit, and Jorge A. Prozzi. Performance of Preventive Maintenance Treatments for Flexible Pavements in Texas. No. FHWA/TX-16/0-6878-2. TxDOT Technical Report No: 0-6878-2. Center for Transportation Research, UT Austin, 2017.

115. McGhee, Kevin K., and James S. Gillespie. Impact of a Smoothness Incentive/Disincentive on Hot-Mix Asphalt Maintenance Resurfacing Costs. No. FHWA/VTRC 06-R28. 2006.

116. Montgomery, Douglas C. Design and analysis of experiments. John wiley & sons, 2017.

APPENDIX A

FULL-CAR RESPONSE MODEL

The equation of motion for a Full-Car Model is as follow.

$$\dot{g} = Ag + Bf \tag{A-1}$$

$$\dot{g} \begin{bmatrix} z \\ z_5 \\ z_6 \\ z_7 \\ z_8 \\ w_9 \\ w_{10} \\ w_{11} \\ w_{12} \\ w \\ \varphi \\ p \\ \theta \\ q \end{bmatrix}$$

Where z is the body displacement, z_5 is the left front-wheel displacement, z_6 is the right front-wheel displacement, z_7 is the right rear-wheel displacement, z_8 is the left rear-wheel displacement, w_9 is the left front-wheel velocity, w_{10} is the right front-wheel velocity, w_{11} is the right rear-wheel velocity, w_{12} is the left rear-wheel velocity, w is the body velocity, φ is the roll angle, p is the roll velocity, Θ is the pitch angle, and q is the pitch velocity.

Matrix A is:

$$A = \begin{vmatrix}
0 & 0 & 0 & 0 & 0 & 0 & 0 & 0 & 0 & 1 & 0 & 0 & 0 & 0 \\
0 & 0 & 0 & 0 & 0 & 1 & 0 & 0 & 0 & 0 & 0 & 0 & 0 & 0 \\
0 & 0 & 0 & 0 & 0 & 0 & 1 & 0 & 0 & 0 & 0 & 0 & 0 & 0 \\
0 & 0 & 0 & 0 & 0 & 0 & 0 & 1 & 0 & 0 & 0 & 0 & 0 & 0 \\
0 & 0 & 0 & 0 & 0 & 0 & 0 & 0 & 1 & 0 & 0 & 0 & 0 & 0 \\
\frac{k_1}{m_2} & \frac{(k_1+k_2)}{m_2} & 0 & 0 & 0 & \frac{-c_1}{m_2} & 0 & 0 & 0 & \frac{c_1}{m_2} & \frac{-k_{1b}}{2m_2} & \frac{-c_1 b}{2m_2} & \frac{-k_1 L}{2m_2} & \frac{-c_1 L}{2m_2} \\
\frac{k_1}{m_2} & 0 & \frac{(k_1+k_2)}{m_2} & 0 & 0 & 0 & \frac{-c_1}{m_2} & 0 & 0 & \frac{c_1}{m_2} & \frac{k_{1b}}{2m_2} & \frac{c_1 b}{2m_2} & \frac{-k_1 L}{2m_2} & \frac{-c_1 L}{2m_2} \\
\frac{k_1}{m_2} & 0 & 0 & \frac{(k_1+k_2)}{m_2} & 0 & 0 & 0 & \frac{-c_1}{m_2} & 0 & \frac{c_1}{m_2} & \frac{k_{1b}}{2m_2} & \frac{c_1 b}{2m_2} & \frac{k_1 L}{2m_2} & \frac{c_1 L}{2m_2} \\
\frac{k_1}{m_2} & 0 & 0 & 0 & \frac{(k_1+k_2)}{m_2} & 0 & 0 & 0 & \frac{-c_1}{m_2} & \frac{c_1}{m_2} & \frac{-k_{1b}}{2m_2} & \frac{-c_1 b}{2m_2} & \frac{k_1 L}{2m_2} & \frac{c_1 L}{2m_2} \\
\frac{-4k_1}{m_f} & \frac{k_1}{m_f} & \frac{k_1}{m_f} & \frac{k_1}{m_f} & \frac{k_1}{m_f} & \frac{c_1}{m_f} & \frac{c_1}{m_f} & \frac{c_1}{m_f} & \frac{c_1}{m_f} & \frac{-4c_1}{m_f} & 0 & 0 & 0 & 0 \\
0 & 0 & 0 & 0 & 0 & 0 & 0 & 0 & 0 & 0 & 0 & 1 & 0 & 0 \\
0 & \frac{-k_1 b}{2I_x} & \frac{k_1 b}{2I_x} & \frac{k_1 b}{2I_x} & \frac{-k_1 b}{2I_x} & \frac{-c_1 b}{2I_x} & \frac{c_1 b}{2I_x} & \frac{c_1 b}{2I_x} & \frac{-c_1 b}{2I_x} & 0 & \frac{-k_1 b^2}{I_x} & \frac{-c_1 b^2}{I_x} & 0 & 0 \\
0 & 0 & 0 & 0 & 0 & 0 & 0 & 0 & 0 & 0 & 0 & 0 & 0 & 1 \\
0 & \frac{-k_1 L}{2I_y} & \frac{-k_1 L}{2I_y} & \frac{k_1 L}{2I_y} & \frac{k_1 L}{2I_y} & \frac{-c_1 L}{2I_y} & \frac{-c_1 L}{2I_y} & \frac{c_1 L}{2I_y} & \frac{c_1 L}{2I_y} & 0 & 0 & 0 & \frac{-k_1 L^2}{I_y} & \frac{-c_1 L^2}{I_y}
\end{vmatrix}$$

(A-2)

Where k_1 and k_2 are the vehicle spring constant and the tire stiffness, c_1 and c_2 are the damping of the suspension system and the tire, m_f and m_2 are the body mass and the axle wheel mass, L is the length from the front to the rear axle, b is the width of the vehicle and I_x and I_y are the moment of inertia with respect to the x and y axis.

The matrix B is:

$$B = \begin{vmatrix} 0 & 0 & 0 & 0 \\ 0 & 0 & 0 & 0 \\ 0 & 0 & 0 & 0 \\ 0 & 0 & 0 & 0 \\ \frac{k_2}{m_2} & 0 & 0 & 0 \\ 0 & \frac{k_2}{m_2} & 0 & 0 \\ 0 & 0 & \frac{k_2}{m_2} & 0 \\ 0 & 0 & 0 & \frac{k_2}{m_2} \\ 0 & 0 & 0 & 0 \\ 0 & 0 & 0 & 0 \\ 0 & 0 & 0 & 0 \\ 0 & 0 & 0 & 0 \\ 0 & 0 & 0 & 0 \\ 0 & 0 & 0 & 0 \end{vmatrix} \quad \text{(A-3)}$$

The input vector f is:

$$f = \begin{vmatrix} z_{p1} \\ z_{p2} \\ z_{p3} \\ z_{p4} \end{vmatrix} \quad \text{(A-4)}$$

Where z_{p1} and z_{p2} are the double track profiles, and z_{p3} and z_{p4} delays of z_{p1} and z_{p2}.

APPENDIX B

HALF-CAR RESPONSE MODEL

The equations of motion for the Hal-Car model are as follow.

$$\begin{vmatrix} \dot{z}_1 \\ \dot{z}_2 \\ \dot{z}_3 \\ w_1 \\ w_2 \\ w_3 \\ \varphi_1 \\ p_1 \end{vmatrix} = [A] \begin{vmatrix} z_1 \\ z_2 \\ z_3 \\ w_1 \\ w_2 \\ w_3 \\ \varphi_1 \\ p_1 \end{vmatrix} + [B] \begin{vmatrix} z_{p1} \\ z_{p2} \end{vmatrix} \tag{B-1}$$

$$w_1 = \dot{z}_1 - \frac{c_2}{\left(m_2 + 0.5m_a\right)} z_{p1}$$

$$w_1 = \dot{z}_2 - \frac{c_2}{\left(m_2 + 0.5m_a\right)} z_{p2}$$

$$w_3 = \dot{z}_3$$

Where $\dot{z}_1$, $\dot{z}_2$ and $\dot{z}_3$ are the left, right body and axle velocity, m_2 is the axle-wheel mass, m_a is the axle mass, φ_1 and p_1 are the roll rotation and velocity of the body, z_{p1} and z_{p2} are the road profile from the left-wheel and right-wheel path.

The relative motion, Z', between the sprung mass and the un-sprung mass is defined as:

$$Z' = z_3 - \frac{z_1 + z_2}{2} \tag{B-2}$$

The matrix A is:

$$A=\begin{vmatrix} 0 & 0 & 0 & 1 & 0 & 0 & 0 & 0 \\ 0 & 0 & 0 & 0 & 1 & 0 & 0 & 0 \\ 0 & 0 & 0 & 0 & 0 & 1 & 0 & 0 \\ \frac{-(k_1+k_2)}{(m_2+0.5m_a)} & 0 & \frac{k_1}{(m_2+0.5m_a)} & \frac{-(c_1+c_2)}{(m_2+0.5m_a)} & 0 & \frac{c_1}{(m_2+0.5m_a)} & \frac{-k_1b/2}{(m_2+0.5m_a)} & \frac{-c_1b/2}{(m_2+0.5m_a)} \\ 0 & \frac{-(k_1+k_2)}{(m_2+0.5m_a)} & \frac{k_1}{(m_2+0.5m_a)} & 0 & \frac{-(c_1+c_2)}{(m_2+0.5m_a)} & \frac{c_1}{(m_2+0.5m_a)} & \frac{k_1b/2}{(m_2+0.5m_a)} & \frac{c_1b/2}{(m_2+0.5m_a)} \\ \frac{k_1}{m_H} & \frac{k_1}{m_H} & \frac{-2k_1}{m_H} & \frac{c_1}{m_H} & \frac{c_1}{m_H} & \frac{-2c_1}{m_H} & 0 & 0 \\ 0 & 0 & 0 & 0 & 0 & 0 & 0 & 1 \\ \frac{-k_1b}{2I_H} & \frac{-k_1b}{2I_H} & 0 & \frac{-c_1b}{2I_H} & \frac{-c_1b}{2I_H} & 0 & \frac{-k_1b^2}{2I_H} & \frac{-c_1b^2}{2I_H} \end{vmatrix}$$

(B-3)

The matrix B is:

$$B=\begin{vmatrix} \frac{c_2}{(m_2+0.5m_a)} & 0 \\ 0 & \frac{c_2}{(m_2+0.5m_a)} \\ 0 & 0 \\ \frac{-(c_1c_2+c_2^2-k_2m_2)}{(m_2+0.5m_a)} & 0 \\ 0 & \frac{-(c_1c_2+c_2^2-k_2m_2)}{(m_2+0.5m_a)} \\ \frac{c_1c_2}{m_H(m_2+0.5m_a)} & \frac{c_1c_2}{m_H(m_2+0.5m_a)} \\ 0 & 0 \\ \frac{c_1c_2b/2}{2I_H(m_2+0.5m_a)} & \frac{c_1c_2b/2}{2I_H(m_2+0.5m_a)} \end{vmatrix} \qquad \text{(B-4)}$$

APPENDIX C

PRELIMINARY STUDY RESULTS

Table C-1. Glendale Ave. Preliminary Study Results.

Run	Pattern	Speed	Cellphone	Mount	RQI
1	111	S1	C1	M1	2.49
2	121	S1	C2	M1	2.11
3	112	S1	C1	M2	2.32
4	213	S2	C1	NM	1.80
5	211	S2	C1	M1	2.08
6	212	S2	C1	M2	2.17
7	221	S2	C2	M1	2.15
8	111	S1	C1	M1	2.79
9	123	S1	C2	NM	1.87
10	222	S2	C2	M2	1.98
11	113	S1	C1	NM	1.95
12	212	S2	C1	M2	1.86
13	122	S1	C2	M2	2.25
14	223	S2	C2	NM	1.62
15	123	S1	C2	NM	1.82
16	222	S2	C2	M2	2.14
17	112	S1	C1	M2	1.79
18	221	S2	C2	M1	2.29
19	121	S1	C2	M1	2.06
20	211	S2	C1	M1	2.59
21	223	S2	C2	NM	1.52
22	122	S1	C2	M2	2.52
23	113	S1	C1	NM	1.88
24	213	S2	C1	NM	1.70
25	222	S2	C2	M2	1.94
26	211	S2	C1	M1	2.75
27	213	S2	C1	NM	1.79
28	212	S2	C1	M2	2.00
29	121	S1	C2	M1	3.00
30	122	S1	C2	M2	1.95
31	112	S1	C1	M2	2.03
32	113	S1	C1	NM	1.94
33	223	S2	C2	NM	1.84
34	123	S1	C2	NM	1.90
35	111	S1	C1	M1	1.87
36	221	S2	C2	M1	2.41

Table C-2. Van Buren St. Preliminary Study Results.

Run	Pattern	Speed	Cellphone	Mount	RQI
1	111	S1	C1	M1	4.42
2	121	S1	C2	M1	4.86
3	112	S1	C1	M2	3.42
4	213	S2	C1	NM	3.75
5	211	S2	C1	M1	4.58
6	212	S2	C1	M2	2.82
7	221	S2	C2	M1	3.82
8	111	S1	C1	M1	3.91
9	123	S1	C2	NM	3.28
10	222	S2	C2	M2	3.32
11	113	S1	C1	NM	3.47
12	212	S2	C1	M2	3.70
13	122	S1	C2	M2	3.15
14	223	S2	C2	NM	2.59
15	123	S1	C2	NM	2.70
16	222	S2	C2	M2	3.42
17	112	S1	C1	M2	3.60
18	221	S2	C2	M1	3.52
19	121	S1	C2	M1	3.52
20	211	S2	C1	M1	4.15
21	223	S2	C2	NM	3.21
22	122	S1	C2	M2	2.93
23	113	S1	C1	NM	3.60
24	213	S2	C1	NM	3.84
25	222	S2	C2	M2	3.19
26	211	S2	C1	M1	3.34
27	213	S2	C1	NM	3.43
28	212	S2	C1	M2	2.90
29	121	S1	C2	M1	3.64
30	122	S1	C2	M2	3.12
31	112	S1	C1	M2	4.09
32	113	S1	C1	NM	3.20
33	223	S2	C2	NM	2.83
34	123	S1	C2	NM	2.85
35	111	S1	C1	M1	5.16
36	221	S2	C2	M1	4.14

Table C-3. 44th St. Preliminary Study Results.

Run	Pattern	Speed	Cellphone	Mount	RQI
1	111	S1	C1	M1	2.53
2	121	S1	C2	M1	2.46
3	112	S1	C1	M2	1.21
4	213	S2	C1	NM	1.42
5	211	S2	C1	M1	2.80
6	212	S2	C1	M2	1.18
7	221	S2	C2	M1	2.19
8	111	S1	C1	M1	1.87
9	123	S1	C2	NM	1.27
10	222	S2	C2	M2	1.48
11	113	S1	C1	NM	1.78
12	212	S2	C1	M2	2.24
13	122	S1	C2	M2	1.73
14	223	S2	C2	NM	1.53
15	123	S1	C2	NM	1.34
16	222	S2	C2	M2	2.86
17	112	S1	C1	M2	2.01
18	221	S2	C2	M1	2.03
19	121	S1	C2	M1	1.92
20	211	S2	C1	M1	1.58
21	223	S2	C2	NM	1.31
22	122	S1	C2	M2	1.60
23	113	S1	C1	NM	1.64
24	213	S2	C1	NM	1.46
25	222	S2	C2	M2	1.80
26	211	S2	C1	M1	1.35
27	213	S2	C1	NM	1.41
28	212	S2	C1	M2	2.00
29	121	S1	C2	M1	2.10
30	122	S1	C2	M2	1.69
31	112	S1	C1	M2	2.13
32	113	S1	C1	NM	1.51
33	223	S2	C2	NM	1.20
34	123	S1	C2	NM	1.53
35	111	S1	C1	M1	1.78
36	221	S2	C2	M1	2.04

APPENDIX D

COMPREHENSIVE STUDY

Table D-1. Glendale Ave. Comprehensive Study-Sedan Results.

Run	Speed	Driver/Vehicle	Mount	Cell	RQI (m/km)
1	-1	D2	M1	L1	1.67
2	-1	D5	M1	L4	1.14
3	-1	D2	M2	L1	1.30
4	1	D2	M3	L3	1.84
5	1	D2	M4	L1	2.03
6	1	D2	M3	L2	
7	1	D3	M4	L2	2.94
8	1	D4	M4	L3	2.14
9	-1	D1	M2	L2	3.55
10	-1	D1	M4	L1	1.50
11	1	D1	M1	L4	3.15
12	-1	D2	M3	L4	1.49
13	-1	D3	M4	L3	2.92
14	-1	D1	M3	L2	2.30
15	1	D5	M2	L4	2.25
16	-1	D4	M1	L4	2.30
17	-1	D3	M2	L2	2.89
18	-1	D5	M3	L1	2.78
19	-1	D5	M2	L1	1.98
20	1	D5	M4	L4	2.12
21	1	D3	M1	L3	2.87
22	-1	D3	M3	L3	2.85
23	1	D5	M3	L2	2.83
24	1	D1	M3	L3	2.69
25	1	D2	M1	L4	1.27
26	-1	D3	M4	L4	2.80
27	1	D4	M2	L2	6.14
28	-1	D4	M3	L3	2.01
29	-1	D1	M3	L4	2.47
30	-1	D3	M3	L1	
31	1	D4	M4	L4	1.96
32	1	D1	M1	L4	2.59
33	-1	D4	M4	L2	4.78
34	1	D3	M3	L4	2.78
35	-1	D4	M1	L3	3.18
36	1	D2	M4	L4	2.68
37	1	D1	M3	L1	1.32
38	1	D3	M2	L1	

39	1	D4	M2	L3	3.01
40	1	D2	M2	L3	2.44
41	1	D4	M1	L1	4.12
42	-1	D4	M4	L1	3.59
43	1	D3	M2	L4	2.76
44	1	D4	M3	L2	3.69
45	-1	D4	M2	L4	3.63
46	1	D1	M4	L3	2.00
47	-1	D1	M1	L3	1.98
48	-1	D1	M2	L3	2.05
49	1	D5	M1	L2	
50	-1	D2	M4	L3	3.37
51	-1	D5	M4	L2	
52	1	D5	M4	L1	2.51
53	-1	D2	M1	L2	
54	-1	D3	M1	L1	2.74
55	1	D1	M4	L2	2.15
56	1	D1	M2	L1	1.41
57	-1	D1	M4	L4	2.55
58	-1	D5	M2	L3	2.23
59	-1	D3	M1	L2	
60	1	D5	M1	L3	1.91
61	1	D1	NM	L2	3.01
62	-1	D5	NM	L2	0.81
63	-1	D2	NM	L2	
64	-1	D3	NM	L1	
65	1	D4	NM	L2	2.79
66	1	D5	NM	L1	2.40
67	-1	D5	NM	L3	1.83
68	1	D3	NM	L2	
69	-1	D1	NM	L3	1.80
70	-1	D2	NM	L1	2.00
71	-1	D2	NM	L3	2.53
72	1	D4	NM	L1	1.56
73	1	D3	NM	L3	
74	1	D1	NM	L1	1.83
75	-1	D4	NM	L3	1.88

Table D-2. Glendale Ave. Comprehensive Study-Trucks Results.

Run	Speed	Driver/Vehicle	Mount	Cell	RQI m/km)
1	-1	D7	M1	L1	2.74
2	-1	D10	M1	L4	2.79
3	-1	D7	M2	L1	1.68
4	1	D7	M3	L3	2.85
5	1	D7	M4	L1	4.33
6	1	D7	M3	L2	4.16
7	1	D8	M4	L2	2.60
8	1	D9	M4	L3	2.25
9	-1	D6	M2	L2	3.95
10	-1	D6	M4	L1	2.43
11	1	D6	M1	L4	2.28
12	-1	D7	M3	L4	2.30
13	-1	D8	M4	L3	2.38
14	-1	D6	M3	L2	3.01
15	1	D10	M2	L4	2.78
16	-1	D9	M1	L4	1.43
17	-1	D8	M2	L2	2.78
18	-1	D10	M3	L1	2.77
19	-1	D10	M2	L1	2.76
20	1	D10	M4	L4	2.75
21	1	D8	M1	L3	2.26
22	-1	D8	M3	L3	2.30
23	1	D10	M3	L2	2.74
24	1	D6	M3	L3	1.98
25	1	D7	M1	L4	2.62
26	-1	D8	M4	L4	2.51
27	1	D9	M2	L2	3.40
28	-1	D9	M3	L3	2.10
29	-1	D6	M3	L4	2.19
30	-1	D8	M3	L1	1.71
31	1	D9	M4	L4	1.39
32	1	D6	M1	L4	3.01
33	-1	D9	M4	L2	3.82
34	1	D8	M3	L4	1.79
35	-1	D9	M1	L3	2.30
36	1	D7	M4	L4	4.45
37	1	D6	M3	L1	1.81
38	1	D8	M2	L1	1.69

39	1	D9	M2	L3	2.66
40	1	D7	M2	L3	2.61
41	1	D9	M1	L1	2.18
42	-1	D9	M4	L1	2.72
43	1	D8	M2	L4	2.52
44	1	D9	M3	L2	2.90
45	-1	D9	M2	L4	1.66
46	1	D6	M4	L3	2.81
47	-1	D6	M1	L3	2.42
48	-1	D6	M2	L3	2.40
49	1	D10	M1	L2	2.73
50	-1	D7	M4	L3	2.77
51	-1	D10	M4	L2	2.72
52	1	D10	M4	L1	2.71
53	-1	D7	M1	L2	3.83
54	-1	D8	M1	L1	1.88
55	1	D6	M4	L2	2.89
56	1	D6	M2	L1	1.74
57	-1	D6	M4	L4	2.28
58	-1	D10	M2	L3	2.70
59	-1	D8	M1	L2	3.82
60	1	D10	M1	L3	0.18
61	1	D6	NM	L2	2.88
62	-1	D10	NM	L2	
63	-1	D7	NM	L2	3.61
64	-1	D8	NM	L1	2.36
65	1	D9	NM	L2	1.86
66	1	D10	NM	L1	
67	-1	D10	NM	L3	
68	1	D8	NM	L2	3.07
69	-1	D6	NM	L3	1.92
70	-1	D7	NM	L1	2.06
71	-1	D7	NM	L3	1.56
72	1	D9	NM	L1	1.88
73	1	D8	NM	L3	1.90
74	1	D6	NM	L1	1.74
75	-1	D9	NM	L3	1.93

Table D-3. Glendale Ave. Comprehensive Study-SUV Results.

Run	Speed	Driver/Vehicle	Mount	Cell	RQI (m/km)
1	-1	D12	M1	L1	3.47
2	-1	D15	M1	L4	4.12
3	-1	D12	M2	L1	2.17
4	1	D12	M3	L3	2.83
5	1	D12	M4	L1	2.22
6	1	D12	M3	L2	4.65
7	1	D13	M4	L2	3.37
8	1	D14	M4	L3	1.76
9	-1	D11	M2	L2	4.28
10	-1	D11	M4	L1	2.58
11	1	D11	M1	L4	2.17
12	-1	D12	M3	L4	3.45
13	-1	D13	M4	L3	1.91
14	-1	D11	M3	L2	2.62
15	1	D15	M2	L4	1.62
16	-1	D14	M1	L4	2.53
17	-1	D13	M2	L2	5.55
18	-1	D15	M3	L1	4.26
19	-1	D15	M2	L1	1.53
20	1	D15	M4	L4	1.80
21	1	D13	M1	L3	2.57
22	-1	D13	M3	L3	2.43
23	1	D15	M3	L2	3.30
24	1	D11	M3	L3	1.99
25	1	D12	M1	L4	1.17
26	-1	D13	M4	L4	1.79
27	1	D14	M2	L2	3.40
28	-1	D14	M3	L3	2.23
29	-1	D11	M3	L4	1.76
30	-1	D13	M3	L1	3.48
31	1	D14	M4	L4	2.11
32	1	D11	M1	L4	3.05
33	-1	D14	M4	L2	2.44
34	1	D13	M3	L4	3.33
35	-1	D14	M1	L3	2.23
36	1	D12	M4	L4	1.61
37	1	D11	M3	L1	1.93
38	1	D13	M2	L1	2.01

39	1	D14	M2	L3	2.44
40	1	D12	M2	L3	3.02
41	1	D14	M1	L1	4.12
42	-1	D14	M4	L1	2.78
43	1	D13	M2	L4	1.71
44	1	D14	M3	L2	2.84
45	-1	D14	M2	L4	
46	1	D11	M4	L3	1.86
47	-1	D11	M1	L3	2.01
48	-1	D11	M2	L3	3.51
49	1	D15	M1	L2	3.10
50	-1	D12	M4	L3	1.99
51	-1	D15	M4	L2	2.88
52	1	D15	M4	L1	2.99
53	-1	D12	M1	L2	3.42
54	-1	D13	M1	L1	3.25
55	1	D11	M4	L2	3.02
56	1	D11	M2	L1	1.59
57	-1	D11	M4	L4	1.91
58	-1	D15	M2	L3	3.09
59	-1	D13	M1	L2	3.50
60	1	D15	M1	L3	2.32
61	1	D11	NM	L2	2.76
62	-1	D15	NM	L2	2.59
63	-1	D12	NM	L2	4.85
64	-1	D13	NM	L1	1.79
65	1	D14	NM	L2	2.11
66	1	D15	NM	L1	1.89
67	-1	D15	NM	L3	2.66
68	1	D13	NM	L2	2.70
69	-1	D11	NM	L3	1.45
70	-1	D12	NM	L1	4.90
71	-1	D12	NM	L3	2.31
72	1	D14	NM	L1	1.17
73	1	D13	NM	L3	1.98
74	1	D11	NM	L1	1.73
75	-1	D14	NM	L3	1.47

Table D-4. Van Buren St. Comprehensive Study-Sedan Results.

Run	Speed	Driver/Vehicle	Mount	Cell	RQI (m/km)
1	-1	D17	M1	L1	4.31
2	-1	D20	M1	L4	3.67
3	-1	D17	M2	L1	2.33
4	1	D17	M3	L3	3.79
5	1	D17	M4	L1	3.82
6	1	D17	M3	L2	3.94
7	1	D18	M4	L2	3.87
8	1	D19	M4	L3	2.65
9	-1	D16	M2	L2	9.31
10	-1	D16	M4	L1	3.78
11	1	D16	M1	L4	5.74
12	-1	D17	M3	L4	6.05
13	-1	D18	M4	L3	2.52
14	-1	D16	M3	L2	7.71
15	1	D20	M2	L4	2.64
16	-1	D19	M1	L4	2.76
17	-1	D18	M2	L2	4.66
18	-1	D20	M3	L1	3.56
19	-1	D20	M2	L1	2.00
20	1	D20	M4	L4	3.00
21	1	D18	M1	L3	3.28
22	-1	D18	M3	L3	2.88
23	1	D20	M3	L2	3.46
24	1	D16	M3	L3	3.35
25	1	D17	M1	L4	6.50
26	-1	D18	M4	L4	3.07
27	1	D19	M2	L2	
28	-1	D19	M3	L3	2.64
29	-1	D16	M3	L4	8.93
30	-1	D18	M3	L1	2.31
31	1	D19	M4	L4	2.42
32	1	D16	M1	L4	5.11
33	-1	D19	M4	L2	
34	1	D18	M3	L4	2.98
35	-1	D19	M1	L3	2.67
36	1	D17	M4	L4	5.05
37	1	D16	M3	L1	6.75
38	1	D18	M2	L1	2.24

39	1	D19	M2	L3	3.04
40	1	D17	M2	L3	3.50
41	1	D19	M1	L1	2.24
42	-1	D19	M4	L1	3.60
43	1	D18	M2	L4	2.62
44	1	D19	M3	L2	
45	-1	D19	M2	L4	5.78
46	1	D16	M4	L3	3.09
47	-1	D16	M1	L3	3.49
48	-1	D16	M2	L3	3.56
49	1	D20	M1	L2	3.46
50	-1	D17	M4	L3	3.24
51	-1	D20	M4	L2	3.96
52	1	D20	M4	L1	3.20
53	-1	D17	M1	L2	6.26
54	-1	D18	M1	L1	4.36
55	1	D16	M4	L2	8.79
56	1	D16	M2	L1	3.22
57	-1	D16	M4	L4	
58	-1	D20	M2	L3	2.72
59	-1	D18	M1	L2	3.62
60	1	D20	M1	L3	2.72
61	1	D16	NM	L2	5.56
62	-1	D20	NM	L2	3.62
63	-1	D17	NM	L2	
64	-1	D18	NM	L1	2.45
65	1	D19	NM	L2	
66	1	D20	NM	L1	3.05
67	-1	D20	NM	L3	2.49
68	1	D18	NM	L2	3.81
69	-1	D16	NM	L3	2.23
70	-1	D17	NM	L1	4.12
71	-1	D17	NM	L3	2.42
72	1	D19	NM	L1	3.02
73	1	D18	NM	L3	2.52
74	1	D16	NM	L1	3.80
75	-1	D19	NM	L3	2.38

Table D-5. Van Buren St. Comprehensive Study-Trucks Results.

Run	Speed	Driver/Vehicle	Mount	Cell	RQI (m/km)
1	-1	D22	M1	L1	2.95
2	-1	D25	M1	L4	4.46
3	-1	D22	M2	L1	5.11
4	1	D22	M3	L3	
5	1	D22	M4	L1	2.36
6	1	D22	M3	L2	
7	1	D23	M4	L2	4.67
8	1	D24	M4	L3	
9	-1	D21	M2	L2	6.75
10	-1	D21	M4	L1	4.26
11	1	D21	M1	L4	6.99
12	-1	D22	M3	L4	3.31
13	-1	D23	M4	L3	3.74
14	-1	D21	M3	L2	4.46
15	1	D25	M2	L4	3.04
16	-1	D24	M1	L4	3.94
17	-1	D23	M2	L2	
18	-1	D25	M3	L1	3.71
19	-1	D25	M2	L1	3.46
20	1	D25	M4	L4	2.57
21	1	D23	M1	L3	2.79
22	-1	D23	M3	L3	3.51
23	1	D25	M3	L2	3.01
24	1	D21	M3	L3	3.21
25	1	D22	M1	L4	3.91
26	-1	D23	M4	L4	4.51
27	1	D24	M2	L2	
28	-1	D24	M3	L3	3.33
29	-1	D21	M3	L4	6.28
30	-1	D23	M3	L1	6.13
31	1	D24	M4	L4	6.48
32	1	D21	M1	L4	6.64
33	-1	D24	M4	L2	
34	1	D23	M3	L4	5.66
35	-1	D24	M1	L3	4.28
36	1	D22	M4	L4	2.61
37	1	D21	M3	L1	4.56
38	1	D23	M2	L1	2.20

39	1	D24	M2	L3	4.75
40	1	D22	M2	L3	
41	1	D24	M1	L1	2.50
42	-1	D24	M4	L1	7.39
43	1	D23	M2	L4	3.46
44	1	D24	M3	L2	
45	-1	D24	M2	L4	3.94
46	1	D21	M4	L3	2.55
47	-1	D21	M1	L3	3.94
48	-1	D21	M2	L3	3.49
49	1	D25	M1	L2	4.66
50	-1	D22	M4	L3	
51	-1	D25	M4	L2	2.21
52	1	D25	M4	L1	
53	-1	D22	M1	L2	
54	-1	D23	M1	L1	2.07
55	1	D21	M4	L2	4.89
56	1	D21	M2	L1	2.63
57	-1	D21	M4	L4	4.65
58	-1	D25	M2	L3	3.74
59	-1	D23	M1	L2	3.91
60	1	D25	M1	L3	3.01
61	1	D21	NM	L2	4.89
62	-1	D25	NM	L2	4.59
63	-1	D22	NM	L2	
64	-1	D23	NM	L1	2.83
65	1	D24	NM	L2	
66	1	D25	NM	L1	5.91
67	-1	D25	NM	L3	2.64
68	1	D23	NM	L2	
69	-1	D21	NM	L3	2.21
70	-1	D22	NM	L1	3.06
71	-1	D22	NM	L3	3.18
72	1	D24	NM	L1	2.57
73	1	D23	NM	L3	
74	1	D21	NM	L1	3.23
75	-1	D24	NM	L3	3.03

Table D-6. Van Buren St. Comprehensive Study-SUV Results.

Run	Speed	Driver/Vehicle	Mount	Cell	RQI (m/km)
1	-1	D27	M1	L1	3.04
2	-1	D30	M1	L4	7.53
3	-1	D27	M2	L1	4.70
4	1	D27	M3	L3	2.86
5	1	D27	M4	L1	2.78
6	1	D27	M3	L2	3.41
7	1	D28	M4	L2	4.44
8	1	D29	M4	L3	3.11
9	-1	D26	M2	L2	4.45
10	-1	D26	M4	L1	2.56
11	1	D26	M1	L4	3.87
12	-1	D27	M3	L4	3.20
13	-1	D28	M4	L3	2.50
14	-1	D26	M3	L2	3.48
15	1	D30	M2	L4	8.46
16	-1	D29	M1	L4	4.64
17	-1	D28	M2	L2	6.54
18	-1	D30	M3	L1	3.18
19	-1	D30	M2	L1	2.36
20	1	D30	M4	L4	4.15
21	1	D28	M1	L3	3.49
22	-1	D28	M3	L3	2.29
23	1	D30	M3	L2	4.47
24	1	D26	M3	L3	2.75
25	1	D27	M1	L4	
26	-1	D28	M4	L4	2.98
27	1	D29	M2	L2	6.66
28	-1	D29	M3	L3	3.23
29	-1	D26	M3	L4	3.77
30	-1	D28	M3	L1	2.69
31	1	D29	M4	L4	4.63
32	1	D26	M1	L4	3.98
33	-1	D29	M4	L2	4.88
34	1	D28	M3	L4	3.17
35	-1	D29	M1	L3	2.91
36	1	D27	M4	L4	2.21
37	1	D26	M3	L1	4.21
38	1	D28	M2	L1	2.59

39	1	D29	M2	L3	5.51
40	1	D27	M2	L3	3.83
41	1	D29	M1	L1	4.11
42	-1	D29	M4	L1	3.32
43	1	D28	M2	L4	5.64
44	1	D29	M3	L2	6.52
45	-1	D29	M2	L4	9.50
46	1	D26	M4	L3	2.60
47	-1	D26	M1	L3	2.72
48	-1	D26	M2	L3	2.91
49	1	D30	M1	L2	4.17
50	-1	D27	M4	L3	2.68
51	-1	D30	M4	L2	4.05
52	1	D30	M4	L1	3.14
53	-1	D27	M1	L2	3.19
54	-1	D28	M1	L1	4.68
55	1	D26	M4	L2	3.49
56	1	D26	M2	L1	2.63
57	-1	D26	M4	L4	3.73
58	-1	D30	M2	L3	3.18
59	-1	D28	M1	L2	3.36
60	1	D30	M1	L3	3.09
61	1	D26	NM	L2	4.16
62	-1	D30	NM	L2	4.93
63	-1	D27	NM	L2	3.86
64	-1	D28	NM	L1	2.96
65	1	D29	NM	L2	3.77
66	1	D30	NM	L1	4.92
67	-1	D30	NM	L3	2.59
68	1	D28	NM	L2	3.54
69	-1	D26	NM	L3	2.32
70	-1	D27	NM	L1	2.18
71	-1	D27	NM	L3	2.23
72	1	D29	NM	L1	2.42
73	1	D28	NM	L3	2.46
74	1	D26	NM	L1	2.69
75	-1	D29	NM	L3	2.91

Table D-7. 44th St. Comprehensive Study-Sedan Results.

Run	Speed	Driver/Vehicle	Mount	Cell	RQI (m/km)
1	-1	D32	M1	L1	2.70
2	-1	D35	M1	L4	2.84
3	-1	D32	M2	L1	1.28
4	1	D32	M3	L3	1.50
5	1	D32	M4	L1	3.95
6	1	D32	M3	L2	
7	1	D33	M4	L2	2.51
8	1	D34	M4	L3	1.66
9	-1	D31	M2	L2	4.26
10	-1	D31	M4	L1	1.76
11	1	D31	M1	L4	2.72
12	-1	D32	M3	L4	2.34
13	-1	D33	M4	L3	1.65
14	-1	D31	M3	L2	2.21
15	1	D35	M2	L4	4.21
16	-1	D34	M1	L4	
17	-1	D33	M2	L2	3.99
18	-1	D35	M3	L1	2.20
19	-1	D35	M2	L1	1.43
20	1	D35	M4	L4	2.20
21	1	D33	M1	L3	2.11
22	-1	D33	M3	L3	2.03
23	1	D35	M3	L2	2.43
24	1	D31	M3	L3	1.75
25	1	D32	M1	L4	4.93
26	-1	D33	M4	L4	1.00
27	1	D34	M2	L2	3.32
28	-1	D34	M3	L3	1.72
29	-1	D31	M3	L4	3.70
30	-1	D33	M3	L1	3.52
31	1	D34	M4	L4	
32	1	D31	M1	L4	2.40
33	-1	D34	M4	L2	3.10
34	1	D33	M3	L4	1.39
35	-1	D34	M1	L3	1.53
36	1	D32	M4	L4	1.60
37	1	D31	M3	L1	2.50
38	1	D33	M2	L1	2.20

39	1	D34	M2	L3	1.92
40	1	D32	M2	L3	1.16
41	1	D34	M1	L1	2.69
42	-1	D34	M4	L1	3.29
43	1	D33	M2	L4	2.30
44	1	D34	M3	L2	2.75
45	-1	D34	M2	L4	
46	1	D31	M4	L3	1.34
47	-1	D31	M1	L3	2.37
48	-1	D31	M2	L3	2.50
49	1	D35	M1	L2	2.92
50	-1	D32	M4	L3	1.04
51	-1	D35	M4	L2	3.13
52	1	D35	M4	L1	2.33
53	-1	D32	M1	L2	
54	-1	D33	M1	L1	2.26
55	1	D31	M4	L2	1.57
56	1	D31	M2	L1	1.63
57	-1	D31	M4	L4	2.74
58	-1	D35	M2	L3	2.04
59	-1	D33	M1	L2	3.59
60	1	D35	M1	L3	1.93
61	1	D31	NM	L2	2.17
62	-1	D35	NM	L2	1.91
63	-1	D32	NM	L2	
64	-1	D33	NM	L1	2.17
65	1	D34	NM	L2	
66	1	D35	NM	L1	0.93
67	-1	D35	NM	L3	1.26
68	1	D33	NM	L2	2.12
69	-1	D31	NM	L3	1.39
70	-1	D32	NM	L1	
71	-1	D32	NM	L3	
72	1	D34	NM	L1	
73	1	D33	NM	L3	1.32
74	1	D31	NM	L1	1.38
75	-1	D34	NM	L3	

Table D-8. 44th St. Comprehensive Study-Trucks Results.

Run	Speed	Driver/Vehicle	Mount	Cell	RQI (m/km)
1	-1	D37	M1	L1	2.05
2	-1	D40	M1	L4	
3	-1	D37	M2	L1	1.07
4	1	D37	M3	L3	1.75
5	1	D37	M4	L1	2.21
6	1	D37	M3	L2	2.27
7	1	D38	M4	L2	2.92
8	1	D39	M4	L3	1.61
9	-1	D36	M2	L2	2.42
10	-1	D36	M4	L1	0.98
11	1	D36	M1	L4	
12	-1	D37	M3	L4	3.37
13	-1	D38	M4	L3	1.51
14	-1	D36	M3	L2	1.67
15	1	D40	M2	L4	
16	-1	D39	M1	L4	2.38
17	-1	D38	M2	L2	3.23
18	-1	D40	M3	L1	2.16
19	-1	D40	M2	L1	1.07
20	1	D40	M4	L4	
21	1	D38	M1	L3	1.78
22	-1	D38	M3	L3	1.55
23	1	D40	M3	L2	2.34
24	1	D36	M3	L3	1.66
25	1	D37	M1	L4	2.32
26	-1	D38	M4	L4	3.39
27	1	D39	M2	L2	2.19
28	-1	D39	M3	L3	1.75
29	-1	D36	M3	L4	
30	-1	D38	M3	L1	1.50
31	1	D39	M4	L4	1.43
32	1	D36	M1	L4	2.11
33	-1	D39	M4	L2	4.07
34	1	D38	M3	L4	3.26
35	-1	D39	M1	L3	2.07
36	1	D37	M4	L4	2.00
37	1	D36	M3	L1	1.74
38	1	D38	M2	L1	1.13

39	1	D39	M2	L3	2.33
40	1	D37	M2	L3	2.15
41	1	D39	M1	L1	3.99
42	-1	D39	M4	L1	1.83
43	1	D38	M2	L4	4.29
44	1	D39	M3	L2	2.59
45	-1	D39	M2	L4	3.63
46	1	D36	M4	L3	1.87
47	-1	D36	M1	L3	1.81
48	-1	D36	M2	L3	2.08
49	1	D40	M1	L2	2.69
50	-1	D37	M4	L3	1.94
51	-1	D40	M4	L2	2.32
52	1	D40	M4	L1	1.24
53	-1	D37	M1	L2	2.66
54	-1	D38	M1	L1	2.90
55	1	D36	M4	L2	2.48
56	1	D36	M2	L1	2.24
57	-1	D36	M4	L4	3.64
58	-1	D40	M2	L3	2.02
59	-1	D38	M1	L2	2.11
60	1	D40	M1	L3	
61	1	D36	NM	L2	3.26
62	-1	D40	NM	L2	
63	-1	D37	NM	L2	3.17
64	-1	D38	NM	L1	1.63
65	1	D39	NM	L2	2.64
66	1	D40	NM	L1	
67	-1	D40	NM	L3	
68	1	D38	NM	L2	2.45
69	-1	D36	NM	L3	2.31
70	-1	D37	NM	L1	1.75
71	-1	D37	NM	L3	1.75
72	1	D39	NM	L1	1.32
73	1	D38	NM	L3	1.64
74	1	D36	NM	L1	2.02
75	-1	D39	NM	L3	1.36

Table D-9. 44th St. Comprehensive Study-SUV Results.

Run	Speed	Driver/Vehicle	Mount	Cell	RQI (m/km)
1	-1	D42	M1	L1	3.58
2	-1	D45	M1	L4	1.81
3	-1	D42	M2	L1	1.33
4	1	D42	M3	L3	2.02
5	1	D42	M4	L1	1.89
6	1	D42	M3	L2	2.62
7	1	D43	M4	L2	2.07
8	1	D44	M4	L3	2.07
9	-1	D41	M2	L2	5.50
10	-1	D41	M4	L1	1.49
11	1	D41	M1	L4	
12	-1	D42	M3	L4	1.98
13	-1	D43	M4	L3	1.74
14	-1	D41	M3	L2	2.91
15	1	D45	M2	L4	1.51
16	-1	D44	M1	L4	3.75
17	-1	D43	M2	L2	3.36
18	-1	D45	M3	L1	1.71
19	-1	D45	M2	L1	1.71
20	1	D45	M4	L4	1.22
21	1	D43	M1	L3	1.84
22	-1	D43	M3	L3	1.47
23	1	D45	M3	L2	2.87
24	1	D41	M3	L3	2.08
25	1	D42	M1	L4	2.76
26	-1	D43	M4	L4	1.45
27	1	D44	M2	L2	3.70
28	-1	D44	M3	L3	1.79
29	-1	D41	M3	L4	
30	-1	D43	M3	L1	1.75
31	1	D44	M4	L4	2.67
32	1	D41	M1	L4	3.54
33	-1	D44	M4	L2	2.78
34	1	D43	M3	L4	1.39
35	-1	D44	M1	L3	2.16
36	1	D42	M4	L4	3.29
37	1	D41	M3	L1	1.53
38	1	D43	M2	L1	1.53

39	1	D44	M2	L3	1.67
40	1	D42	M2	L3	1.70
41	1	D44	M1	L1	2.85
42	-1	D44	M4	L1	2.90
43	1	D43	M2	L4	1.56
44	1	D44	M3	L2	2.30
45	-1	D44	M2	L4	2.26
46	1	D41	M4	L3	1.71
47	-1	D41	M1	L3	2.52
48	-1	D41	M2	L3	1.82
49	1	D45	M1	L2	4.37
50	-1	D42	M4	L3	1.56
51	-1	D45	M4	L2	3.96
52	1	D45	M4	L1	1.70
53	-1	D42	M1	L2	3.41
54	-1	D43	M1	L1	2.71
55	1	D41	M4	L2	3.24
56	1	D41	M2	L1	3.74
57	-1	D41	M4	L4	
58	-1	D45	M2	L3	1.88
59	-1	D43	M1	L2	2.39
60	1	D45	M1	L3	1.59
61	1	D41	NM	L2	3.78
62	-1	D45	NM	L2	3.81
63	-1	D42	NM	L2	3.50
64	-1	D43	NM	L1	2.17
65	1	D44	NM	L2	2.15
66	1	D45	NM	L1	1.99
67	-1	D45	NM	L3	1.68
68	1	D43	NM	L2	3.27
69	-1	D41	NM	L3	2.09
70	-1	D42	NM	L1	1.91
71	-1	D42	NM	L3	1.43
72	1	D44	NM	L1	1.71
73	1	D43	NM	L3	1.61
74	1	D41	NM	L1	1.66
75	-1	D44	NM	L3	1.48

APPENDIX E

HISTOGRAMS AND BOX PLOTS FOR ALL ASSUMED DISTRIBUTIONS AND PAVEMENT LOCATIONS

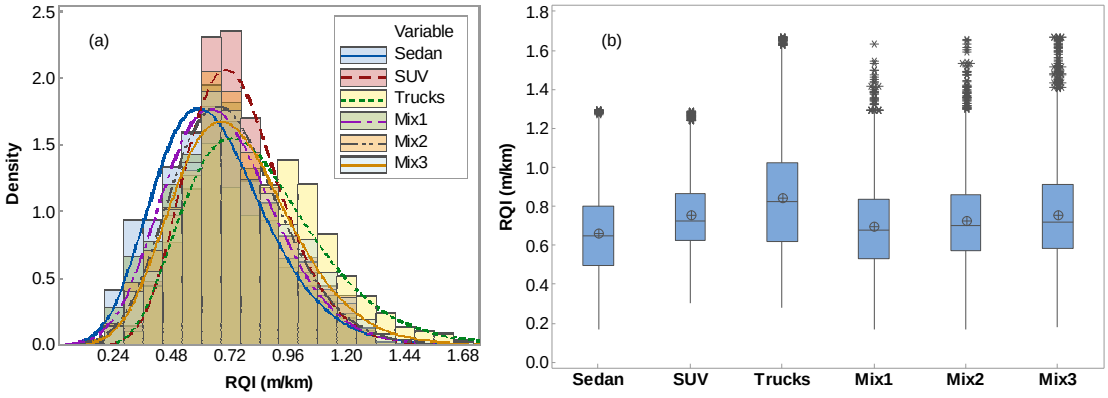

Figure E-1. Arizona-Skewed Distribution Assumption.

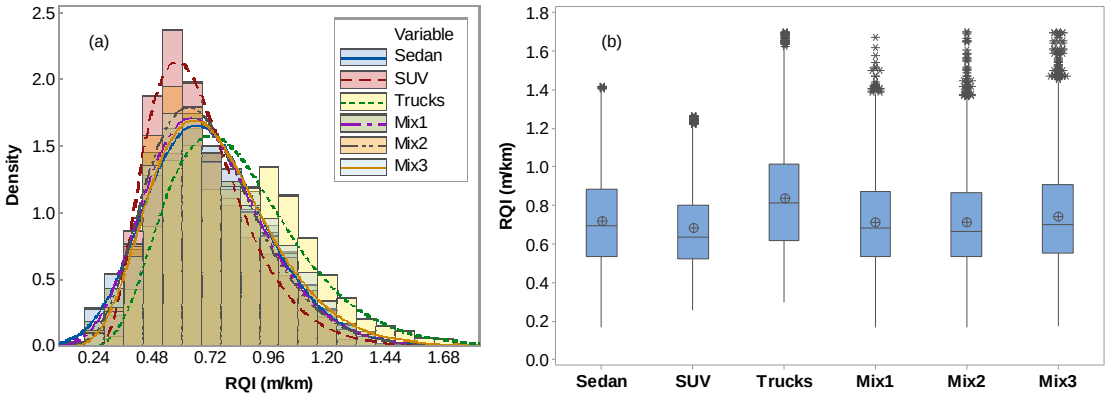

Figure E-2. Arizona-Uniform Distribution Assumption.

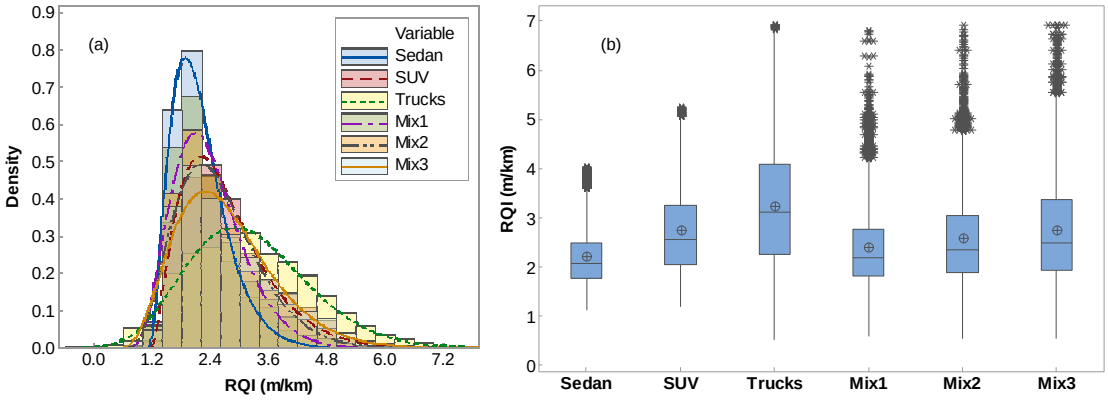

Figure E-3. Colorado-Skewed Distribution Assumption.

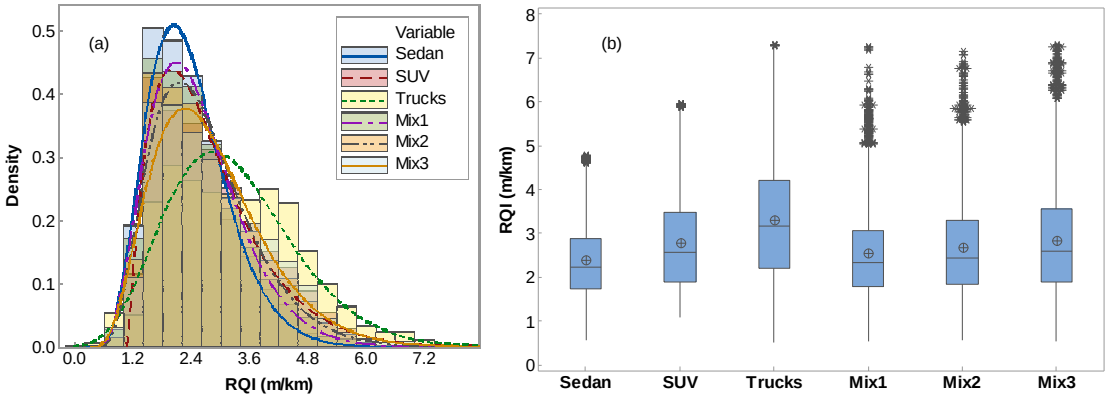

Figure E-4. California-Uniform Distribution Assumption.

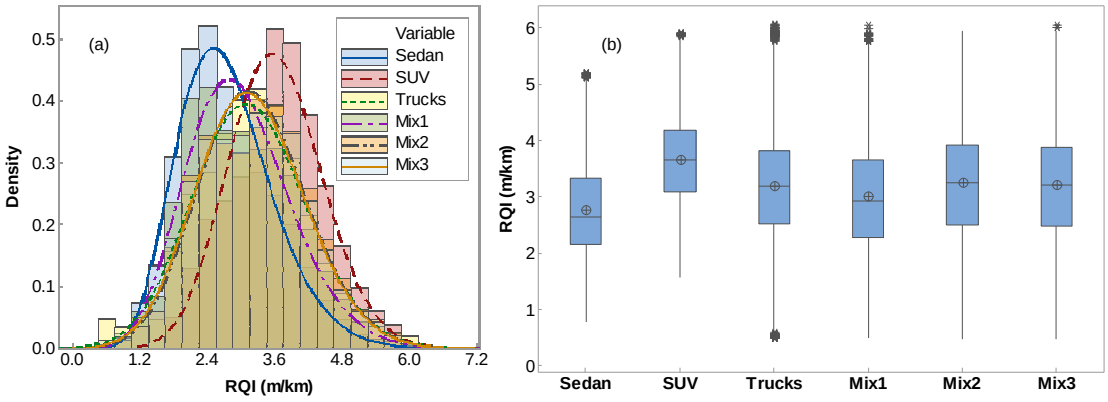

Figure E-5. California-Skewed Distribution Assumption.

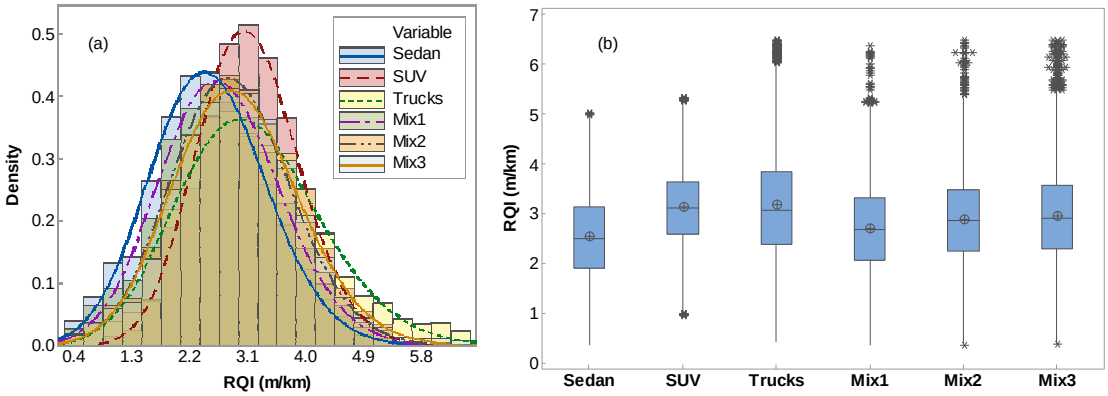

Figure E-6. California-Uniform Distribution Assumption.

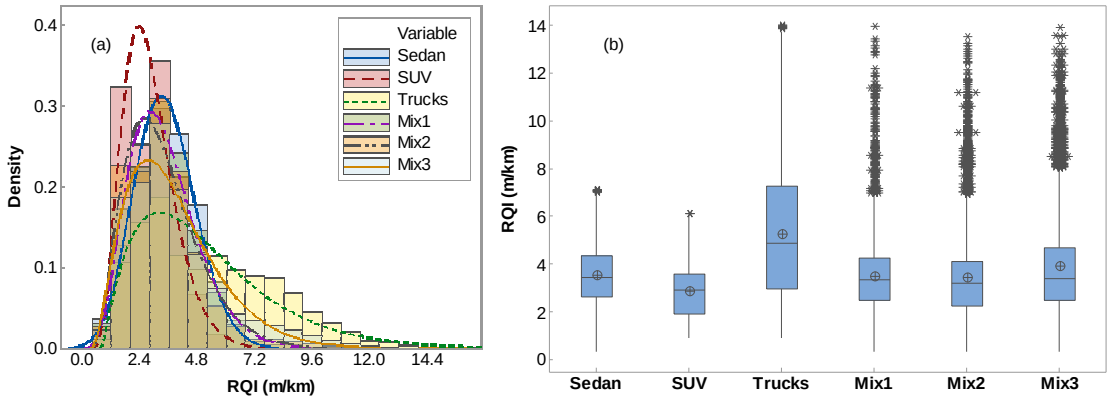

Figure E-7. Minnesota-Skewed Distribution Assumption.

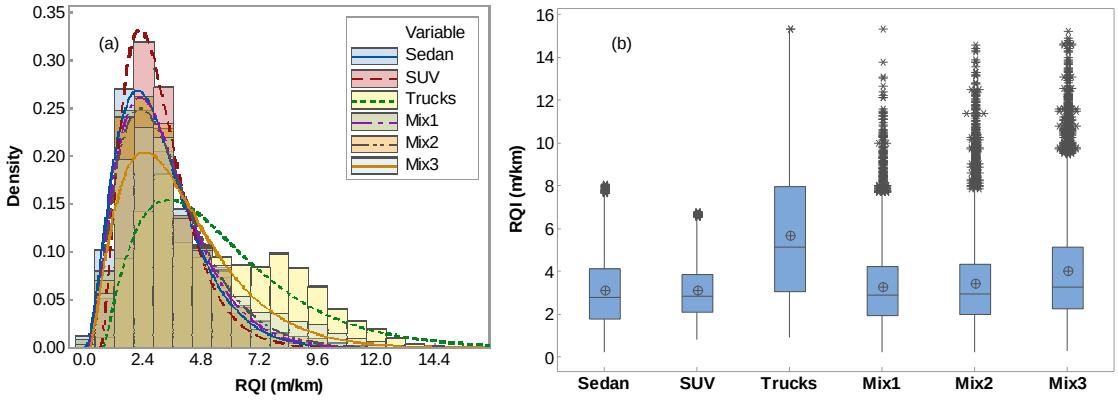

Figure E-8. Minnesota-Uniform Distribution Assumption.

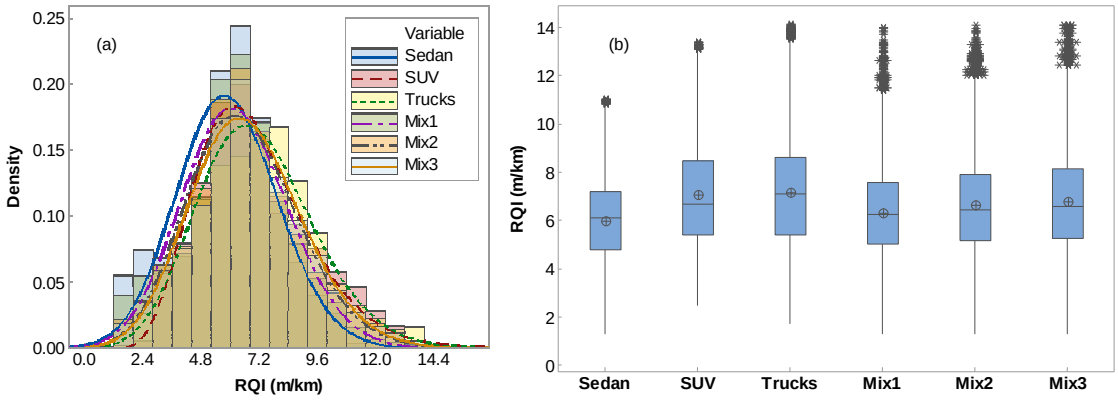

Figure E-9. New Jersey-Skewed Distribution Assumption.

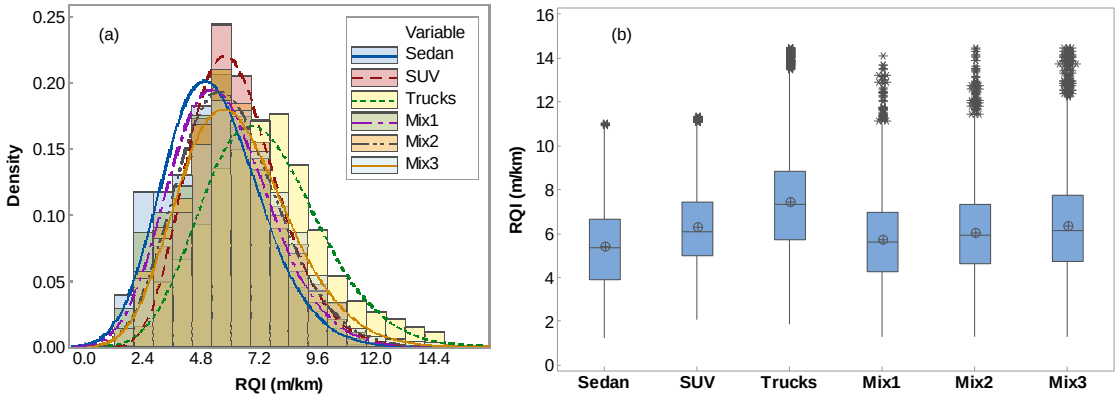

Figure E-10. New Jersey-Uniform Distribution Assumption.

APPENDIX F

SAMPLE SIZE AND RQI CALCULATIONS FOR A SINGLE LANE – NO WANDER

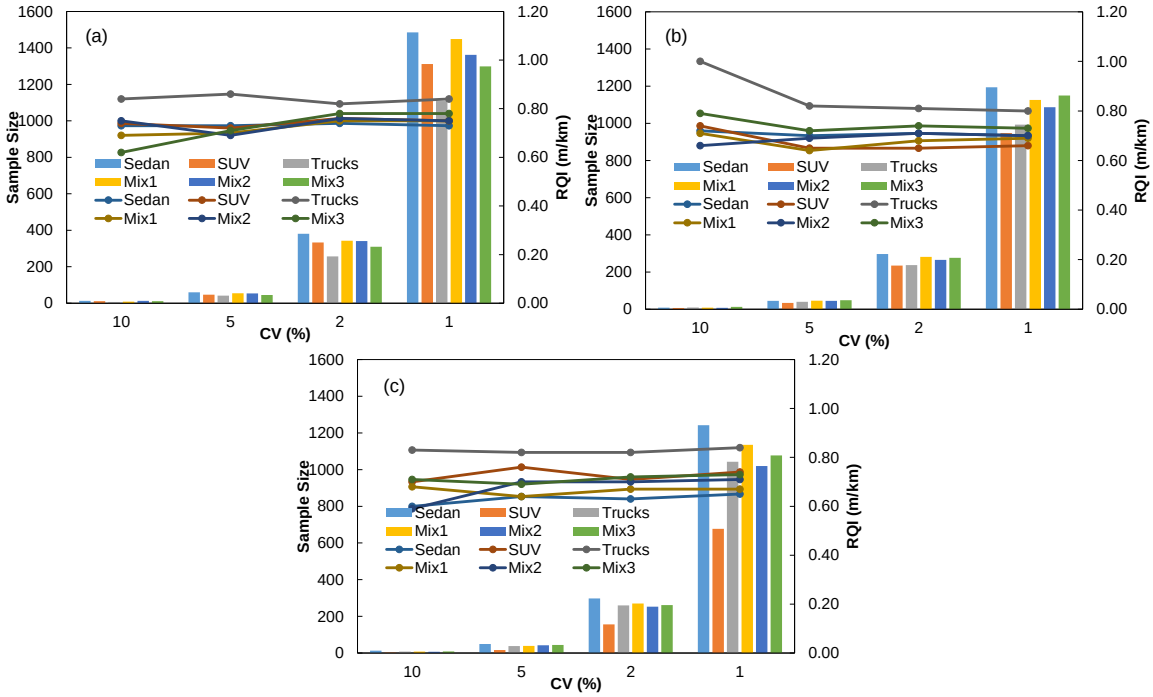

Figure F-1. Arizona (a) Normal, (b) Uniform, (c) Skewed.

Table F-1. Arizona RQI and Sample Size Estimation.

Normal			Uniform			Skewed		
Sedan			**Sedan**			**Sedan**		
Sample Size	CV (%)	RQI (m/km)	Sample Size	CV (%)	RQI (m/km)	Sample Size	CV (%)	RQI (m/km)
13	10	0.73	8	10	0.72	13	10	0.60
60	5	0.73	45	5	0.70	49	5	0.64
381	2	0.74	297	2	0.71	298	2	0.63
1485	1	0.73	1194	1	0.70	1242	1	0.65
SUV			**SUV**			**SUV**		
Sample Size	CV (%)	RQI (m/km)	Sample Size	CV (%)	RQI (m/km)	Sample Size	CV (%)	RQI (m/km)
11	10	0.74	6	10	0.74	3	10	0.70
47	5	0.72	34	5	0.65	16	5	0.76
333	2	0.76	235	2	0.65	156	2	0.71
1312	1	0.75	948	1	0.66	677	1	0.74
Trucks			**Trucks**			**Trucks**		
Sample Size	CV (%)	RQI (m/km)	Sample Size	CV (%)	RQI (m/km)	Sample Size	CV (%)	RQI (m/km)
7	10	0.84	9	10	1.00	8	10	0.83
42	5	0.86	40	5	0.82	38	5	0.82
257	2	0.82	237	2	0.81	260	2	0.82
1109	1	0.84	993	1	0.80	1043	1	0.84
Mix1			**Mix1**			**Mix1**		
Sample Size	CV (%)	RQI (m/km)	Sample Size	CV (%)	RQI (m/km)	Sample Size	CV (%)	RQI (m/km)
9	10	0.69	8	10	0.71	8	10	0.68
55	5	0.70	46	5	0.64	39	5	0.64
343	2	0.75	281	2	0.68	270	2	0.67
1449	1	0.75	1126	1	0.69	1135	1	0.67
Mix2			**Mix2**			**Mix2**		
Sample Size	CV (%)	RQI (m/km)	Sample Size	CV (%)	RQI (m/km)	Sample Size	CV (%)	RQI (m/km)
13	10	0.75	7	10	0.66	7	10	0.59
54	5	0.69	45	5	0.69	42	5	0.70
341	2	0.76	265	2	0.71	253	2	0.70
1362	1	0.75	1087	1	0.70	1020	1	0.71
Mix3			**Mix3**			**Mix3**		
Sample Size	CV (%)	RQI (m/km)	Sample Size	CV (%)	RQI (m/km)	Sample Size	CV (%)	RQI (m/km)
11	10	0.62	12	10	0.79	9	10	0.71
45	5	0.71	48	5	0.72	44	5	0.69
310	2	0.78	276	2	0.74	261	2	0.72
1299	1	0.78	1150	1	0.73	1077	1	0.73

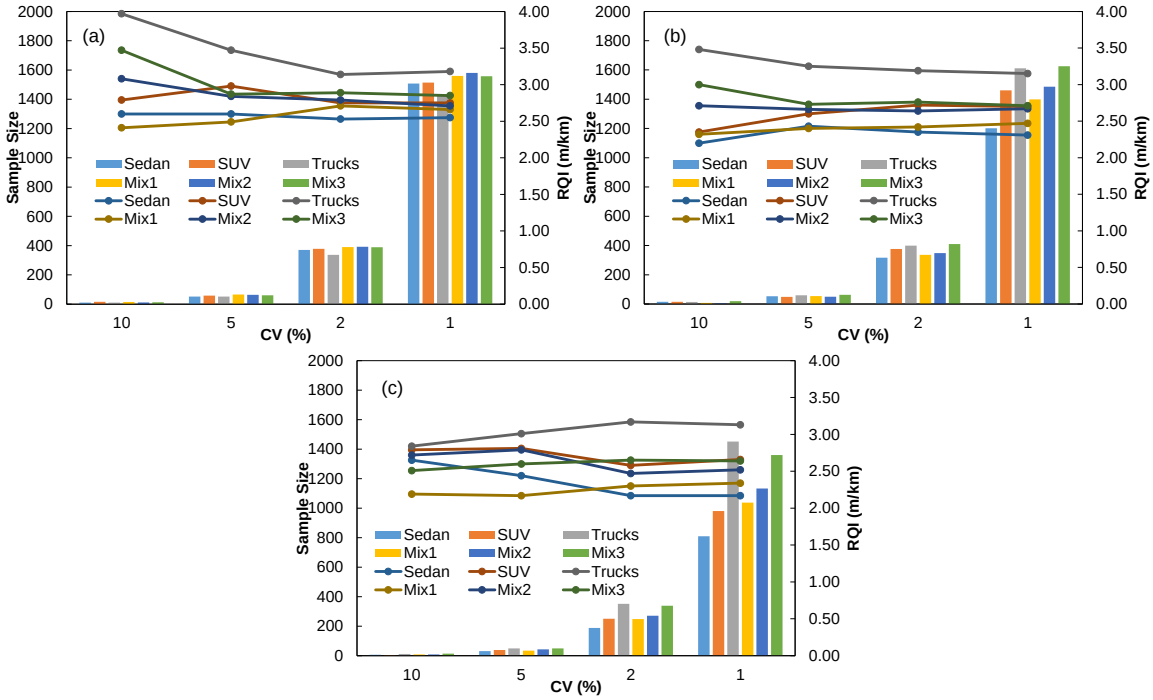

Figure F-2. Colorado (a) Normal, (b) Uniform, (c) Skewed.

Table F-2. Colorado RQI and Sample Size Estimation.

Normal			Uniform			Skewed		
Sedan			**Sedan**			**Sedan**		
Sample Size	CV (%)	RQI (m/km)	Sample Size	CV (%)	RQI (m/km)	Sample Size	CV (%)	RQI (m/km)
10	10	2.60	15	10	2.20	6	10	2.65
51	5	2.60	53	5	2.43	31	5	2.44
370	2	2.53	317	2	2.35	188	2	2.17
1508	1	2.55	1201	1	2.31	809	1	2.17
SUV			**SUV**			**SUV**		
Sample Size	CV (%)	RQI (m/km)	Sample Size	CV (%)	RQI (m/km)	Sample Size	CV (%)	RQI (m/km)
16	10	2.79	15	10	2.35	4	10	2.79
58	5	2.98	49	5	2.60	39	5	2.81
378	2	2.75	376	2	2.72	250	2	2.58
1514	1	2.75	1461	1	2.70	980	1	2.66
Trucks			**Trucks**			**Trucks**		
Sample Size	CV (%)	RQI (m/km)	Sample Size	CV (%)	RQI (m/km)	Sample Size	CV (%)	RQI (m/km)
10	10	3.97	14	10	3.48	12	10	2.84
52	5	3.47	60	5	3.25	49	5	3.01
337	2	3.14	399	2	3.19	351	2	3.17
1423	1	3.18	1611	1	3.15	1451	1	3.13
Mix1			**Mix1**			**Mix1**		
Sample Size	CV (%)	RQI (m/km)	Sample Size	CV (%)	RQI (m/km)	Sample Size	CV (%)	RQI (m/km)
15	10	2.41	8	10	2.32	8	10	2.19
66	5	2.49	54	5	2.40	34	5	2.17
390	2	2.71	336	2	2.42	248	2	2.30
1560	1	2.66	1399	1	2.47	1037	1	2.34
Mix2			**Mix2**			**Mix2**		
Sample Size	CV (%)	RQI (m/km)	Sample Size	CV (%)	RQI (m/km)	Sample Size	CV (%)	RQI (m/km)
11	10	3.08	4	10	2.71	8	10	2.72
63	5	2.84	50	5	2.66	43	5	2.79
392	2	2.79	348	2	2.64	271	2	2.47
1580	1	2.71	1485	1	2.67	1133	1	2.52
Mix3			**Mix3**			**Mix3**		
Sample Size	CV (%)	RQI (m/km)	Sample Size	CV (%)	RQI (m/km)	Sample Size	CV (%)	RQI (m/km)
12	10	3.47	19	10	3	14	10	2.51
60	5	2.87	63	5	2.73	49	5	2.6
389	2	2.89	410	2	2.76	338	2	2.65
1558	1	2.85	1625	1	2.71	1360	1	2.64

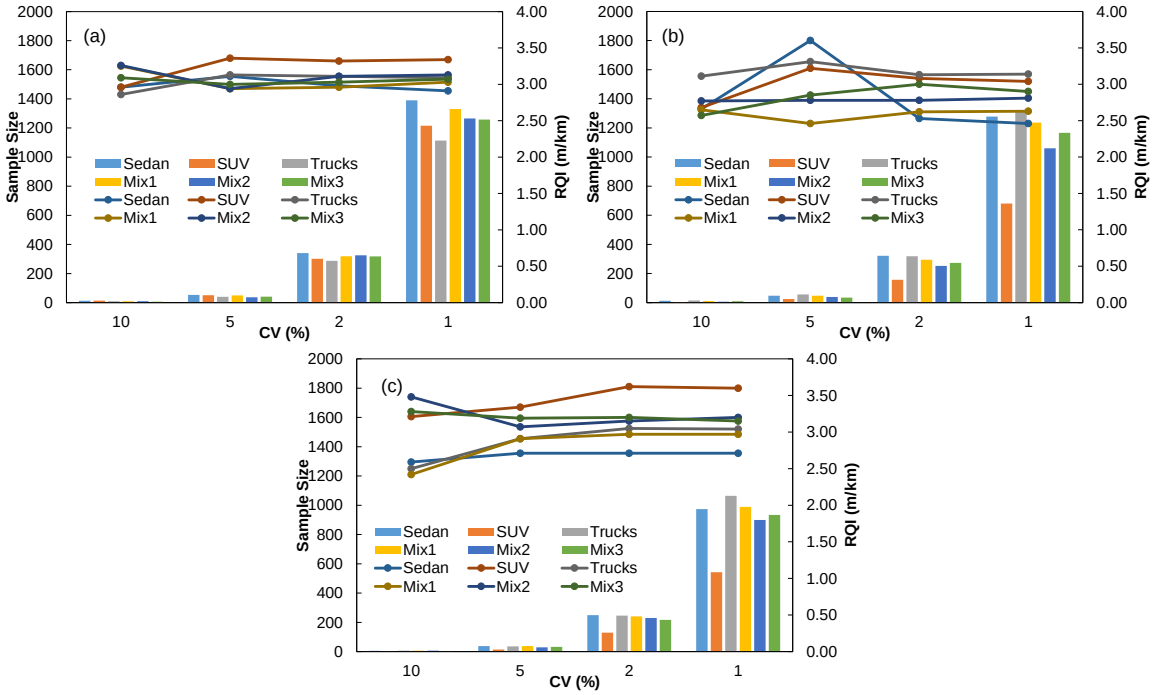

Figure F-3. California (a) Normal, (b) Uniform, (c) Skewed.

Table F-3. California RQI and Sample Size Estimation.

Normal			Uniform			Skewed		
Sedan			**Sedan**			**Sedan**		
Sample Size	CV (%)	RQI (m/km)	Sample Size	CV (%)	RQI (m/km)	Sample Size	CV (%)	RQI (m/km)
13	10	2.96	13	10	2.66	5	10	2.59
53	5	3.11	47	5	3.60	38	5	2.71
341	2	2.98	322	2	2.53	249	2	2.71
1390	1	2.91	1278	1	2.46	974	1	2.71
SUV			**SUV**			**SUV**		
Sample Size	CV (%)	RQI (m/km)	Sample Size	CV (%)	RQI (m/km)	Sample Size	CV (%)	RQI (m/km)
14	10	2.96	4	10	2.68	3	10	3.21
51	5	3.36	24	5	3.22	14	5	3.34
301	2	3.32	157	2	3.08	129	2	3.62
1215	1	3.34	680	1	3.04	542	1	3.60
Trucks			**Trucks**			**Trucks**		
Sample Size	CV (%)	RQI (m/km)	Sample Size	CV (%)	RQI (m/km)	Sample Size	CV (%)	RQI (m/km)
10	10	2.86	15	10	3.11	7	10	2.5
40	5	3.13	56	5	3.31	36	5	2.91
287	2	3.11	318	2	3.13	246	2	3.05
1114	1	3.09	1315	1	3.14	1064	1	3.04
Mix1			**Mix1**			**Mix1**		
Sample Size	CV (%)	RQI (m/km)	Sample Size	CV (%)	RQI (m/km)	Sample Size	CV (%)	RQI (m/km)
10	10	3.25	10	10	2.65	7	10	2.42
50	5	2.94	47	5	2.46	38	5	2.91
319	2	2.96	294	2	2.62	240	2	2.97
1330	1	3.03	1237	1	2.63	989	1	2.97
Mix2			**Mix2**			**Mix2**		
Sample Size	CV (%)	RQI (m/km)	Sample Size	CV (%)	RQI (m/km)	Sample Size	CV (%)	RQI (m/km)
10	10	3.26	6	10	2.77	6	10	3.48
37	5	2.94	38	5	2.78	29	5	3.07
325	2	3.11	252	2	2.78	230	2	3.15
1265	1	3.13	1060	1	2.81	899	1	3.20
Mix3			**Mix3**			**Mix3**		
Sample Size	CV (%)	RQI (m/km)	Sample Size	CV (%)	RQI (m/km)	Sample Size	CV (%)	RQI (m/km)
7	10	3.09	9	10	2.57	4	10	3.28
41	5	3.00	34	5	2.85	32	5	3.19
318	2	3.03	273	2	3.00	217	2	3.20
1258	1	3.07	1166	1	2.90	934	1	3.15

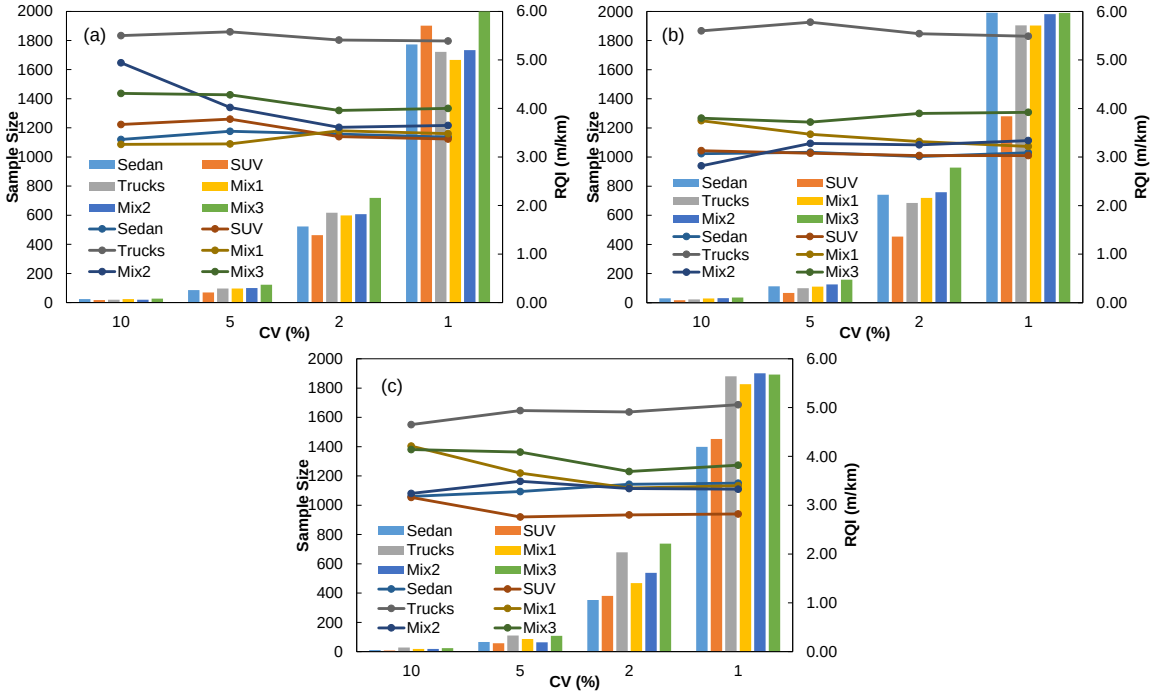

Figure F-4. Minnesota (a) Normal, (b) Uniform, (c) Skewed.

Table F-4. Minnesota RQI and Sample Size Estimation.

Normal			Uniform			Skewed		
Sedan			**Sedan**			**Sedan**		
Sample Size	CV (%)	RQI (m/km)	Sample Size	CV (%)	RQI (m/km)	Sample Size	CV (%)	RQI (m/km)
24	10	3.36	30	10	3.07	11	10	3.18
86	5	3.53	112	5	3.10	66	5	3.28
523	2	3.47	741	2	3.01	353	2	3.43
1773	1	3.41	1991	1	3.09	1399	1	3.45
SUV			**SUV**			**SUV**		
Sample Size	CV (%)	RQI (m/km)	Sample Size	CV (%)	RQI (m/km)	Sample Size	CV (%)	RQI (m/km)
17	10	3.67	17	10	3.13	8	10	3.16
69	5	3.78	67	5	3.08	57	5	2.76
463	2	3.42	454	2	3.03	381	2	2.80
1902	1	3.37	1280	1	3.03	1452	1	2.82
Trucks			**Trucks**			**Trucks**		
Sample Size	CV (%)	RQI (m/km)	Sample Size	CV (%)	RQI (m/km)	Sample Size	CV (%)	RQI (m/km)
19	10	5.50	22	10	5.60	28	10	4.65
97	5	5.58	99	5	5.78	110	5	4.94
617	2	5.41	685	2	5.54	678	2	4.91
1722	1	5.39	1905	1	5.49	1880	1	5.06
Mix1			**Mix1**			**Mix1**		
Sample Size	CV (%)	RQI (m/km)	Sample Size	CV (%)	RQI (m/km)	Sample Size	CV (%)	RQI (m/km)
24	10	3.26	29	10	3.75	18	10	4.21
97	5	3.27	110	5	3.47	86	5	3.66
599	2	3.54	720	2	3.32	468	2	3.35
1667	1	3.48	1904	1	3.22	1826	1	3.40
Mix2			**Mix2**			**Mix2**		
Sample Size	CV (%)	RQI (m/km)	Sample Size	CV (%)	RQI (m/km)	Sample Size	CV (%)	RQI (m/km)
19	10	4.94	31	10	2.82	18	10	3.24
100	5	4.02	125	5	3.28	64	5	3.49
607	2	3.61	758	2	3.25	538	2	3.34
1734	1	3.65	1982	1	3.34	1901	1	3.33
Mix3			**Mix3**			**Mix3**		
Sample Size	CV (%)	RQI (m/km)	Sample Size	CV (%)	RQI (m/km)	Sample Size	CV (%)	RQI (m/km)
27	10	4.31	35	10	3.80	24	10	4.14
123	5	4.28	158	5	3.72	108	5	4.09
719	2	3.96	928	2	3.90	738	2	3.69
1999	1	4.00	1990	1	3.92	1892	1	3.82

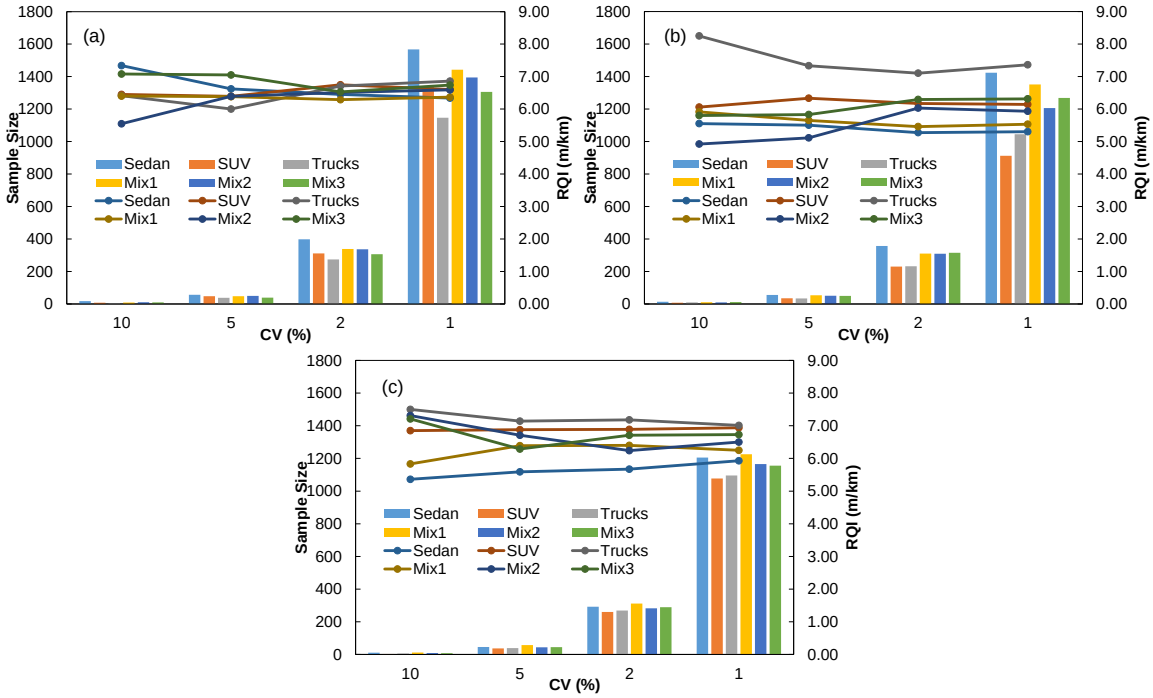

Figure F-5. New Jersey (a) Normal, (b) Uniform, (c) Skewed.

Table F-5. New Jersey RQI and Sample Size Estimation.

Normal			Uniform			Skewed		
Sedan			**Sedan**			**Sedan**		
Sample Size	CV (%)	RQI (m/km)	Sample Size	CV (%)	RQI (m/km)	Sample Size	CV (%)	RQI (m/km)
18	10	7.34	13	10	5.55	11	10	5.36
57	5	6.62	55	5	5.50	46	5	5.59
398	2	6.45	357	2	5.27	292	2	5.67
1567	1	6.34	1423	1	5.30	1205	1	5.93
SUV			**SUV**			**SUV**		
Sample Size	CV (%)	RQI (m/km)	Sample Size	CV (%)	RQI (m/km)	Sample Size	CV (%)	RQI (m/km)
8	10	6.45	7	10	6.06	3	10	6.85
48	5	6.39	35	5	6.33	37	5	6.88
311	2	6.75	230	2	6.17	260	2	6.89
1337	1	6.6	912	1	6.14	1077	1	6.94
Trucks			**Trucks**			**Trucks**		
Sample Size	CV (%)	RQI (m/km)	Sample Size	CV (%)	RQI (m/km)	Sample Size	CV (%)	RQI (m/km)
5	10	6.41	9	10	8.25	6	10	7.5
38	5	6.00	34	5	7.33	39	5	7.14
274	2	6.71	232	2	7.1	269	2	7.18
1147	1	6.86	1045	1	7.36	1096	1	7.01
Mix1			**Mix1**			**Mix1**		
Sample Size	CV (%)	RQI (m/km)	Sample Size	CV (%)	RQI (m/km)	Sample Size	CV (%)	RQI (m/km)
9	10	6.4	10	10	5.91	12	10	5.83
48	5	6.38	53	5	5.65	57	5	6.39
339	2	6.29	310	2	5.46	312	2	6.40
1442	1	6.37	1351	1	5.53	1226	1	6.25
Mix2			**Mix2**			**Mix2**		
Sample Size	CV (%)	RQI (m/km)	Sample Size	CV (%)	RQI (m/km)	Sample Size	CV (%)	RQI (m/km)
11	10	5.55	9	10	4.92	9	10	7.31
50	5	6.39	50	5	5.11	44	5	6.71
337	2	6.51	309	2	6.03	282	2	6.24
1395	1	6.59	1206	1	5.93	1165	1	6.50
Mix3			**Mix3**			**Mix3**		
Sample Size	CV (%)	RQI (m/km)	Sample Size	CV (%)	RQI (m/km)	Sample Size	CV (%)	RQI (m/km)
10	10	7.08	11	10	5.8	8	10	7.21
39	5	7.05	49	5	5.83	45	5	6.29
306	2	6.53	315	2	6.29	289	2	6.71
1306	1	6.74	1268	1	6.31	1156	1	6.73

APPENDIX G

SAMPLE SIZE AND RQI CALCULATIONS FOR A SINGLE LANE –WANDER

Arizona

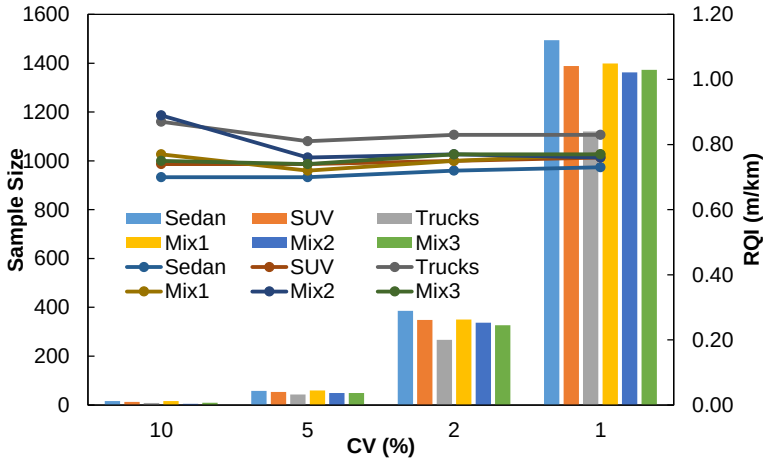

Figure G-1. Arizona Single Lane – Wander RQI and Sample Size.

Table G-1. Arizona RQI and Sample Size Tabular Form.

Sedan			**SUV**			**Trucks**		
Sample Size	CV (%)	RQI (m/km)	Sample Size	CV (%)	RQI (m/km)	Sample Size	CV (%)	RQI (m/km)
16	10	0.70	13	10	0.74	8	10	0.87
58	5	0.70	53	5	0.74	43	5	0.81
386	2	0.72	348	2	0.75	267	2	0.83
1494	1	0.73	1388	1	0.76	1120	1	0.83
Mix1			**Mix2**			**Mix3**		
Sample Size	CV (%)	RQI (m/km)	Sample Size	CV (%)	RQI (m/km)	Sample Size	CV (%)	RQI (m/km)
16	10	0.77	5	10	0.89	9	10	0.75
59	5	0.72	49	5	0.76	49	5	0.74
350	2	0.75	337	2	0.77	327	2	0.77
1399	1	0.77	1362	1	0.76	1373	1	0.77

Colorado

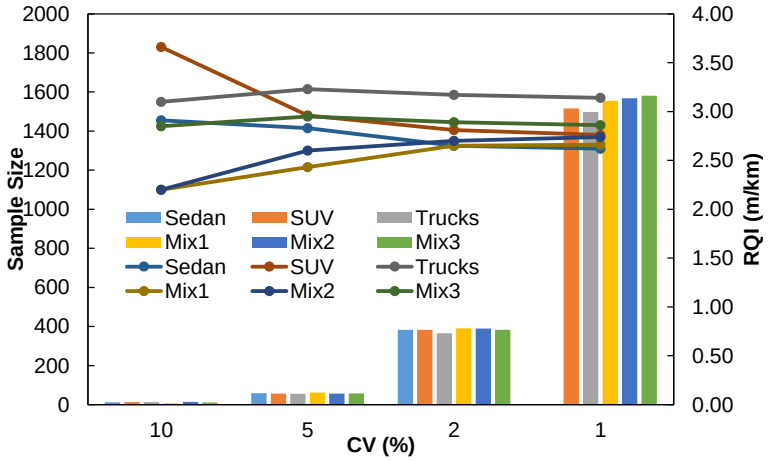

Figure G-2. Colorado Single Lane – Wander RQI and Sample Size.

Table G-2. Colorado RQI and Sample Size Tabular Form.

Sedan			**SUV**			**Trucks**		
Sample Size	CV (%)	RQI (m/km)	Sample Size	CV (%)	RQI (m/km)	Sample Size	CV (%)	RQI (m/km)
12	10	2.91	13	10	3.66	13	10	3.10
59	5	2.83	56	5	2.96	55	5	3.23
383	2	2.65	383	2	2.81	365	2	3.17
1	1	2.62	1516	1	2.76	1497	1	3.14
Mix1			**Mix2**			**Mix3**		
Sample Size	CV (%)	RQI (m/km)	Sample Size	CV (%)	RQI (m/km)	Sample Size	CV (%)	RQI (m/km)
6	10	2.20	14	10	2.20	11	10	2.85
62	5	2.43	56	5	2.60	58	5	2.95
390	2	2.65	389	2	2.70	383	2	2.89
1555	1	2.7	1568	1	2.7	1581	1	2.86

California

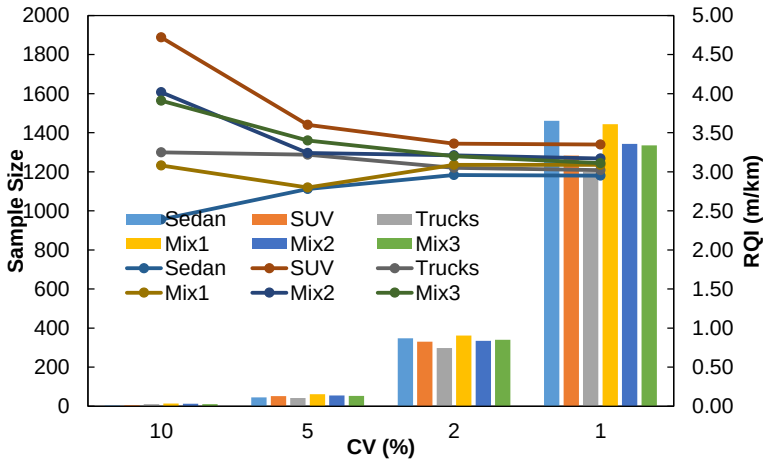

Figure G-3. California Single Lane – Wander RQI and Sample Size.

Table G-3. California RQI and Sample Size Tabular Form.

Sedan			**SUV**			**Trucks**		
Sample Size	CV (%)	RQI (m/km)	Sample Size	CV (%)	RQI (m/km)	Sample Size	CV (%)	RQI (m/km)
4	10	2.39	5	10	4.72	10	10	3.25
45	5	2.78	52	5	3.6	42	5	3.22
348	2	2.96	330	2	3.36	298	2	3.05
1461	1	2.95	1283	1	3.35	1200	1	3.02
Mix1			**Mix2**			**Mix3**		
Sample Size	CV (%)	RQI (m/km)	Sample Size	CV (%)	RQI (m/km)	Sample Size	CV (%)	RQI (m/km)
14	10	3.08	13	10	4.02	10	10	3.91
61	5	2.80	55	5	3.24	53	5	3.40
362	2	3.09	334	2	3.21	340	2	3.20
1444	1	3.09	1343	1	3.17	1335	1	3.11

Minnesota

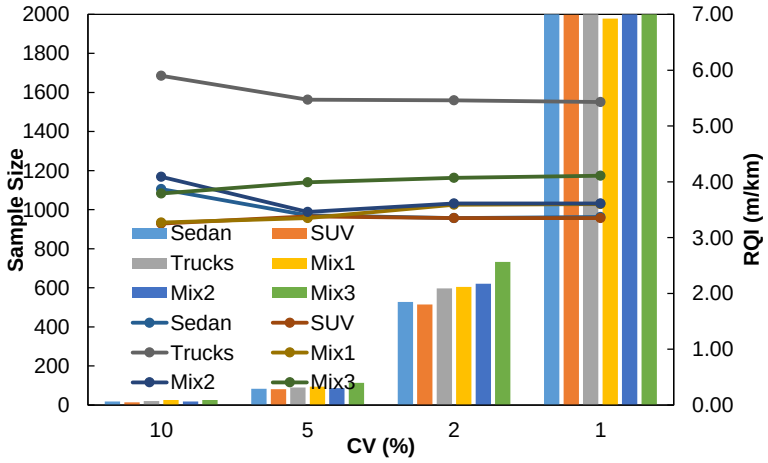

Figure G-4. Minnesota Single Lane – Wander RQI and Sample Size.

Table G-4. Minnesota RQI and Sample Size Tabular Form.

Sedan			**SUV**			**Trucks**		
Sample Size	CV (%)	RQI (m/km)	Sample Size	CV (%)	RQI (m/km)	Sample Size	CV (%)	RQI (m/km)
18	10	3.87	14	10	3.25	20	10	5.90
83	5	3.40	81	5	3.38	90	5	5.47
527	2	3.35	514	2	3.35	597	2	5.46
2000	1	3.37	1998	1	3.35	2000	1	5.43
Mix1			**Mix2**			**Mix3**		
Sample Size	CV (%)	RQI (m/km)	Sample Size	CV (%)	RQI (m/km)	Sample Size	CV (%)	RQI (m/km)
25	10	3.27	18	10	4.09	25	10	3.79
94	5	3.35	86	5	3.46	113	5	3.99
604	2	3.59	621	2	3.61	732	2	4.07
1978	1	3.60	2000	1	3.61	2000	1	4.11

New Jersey

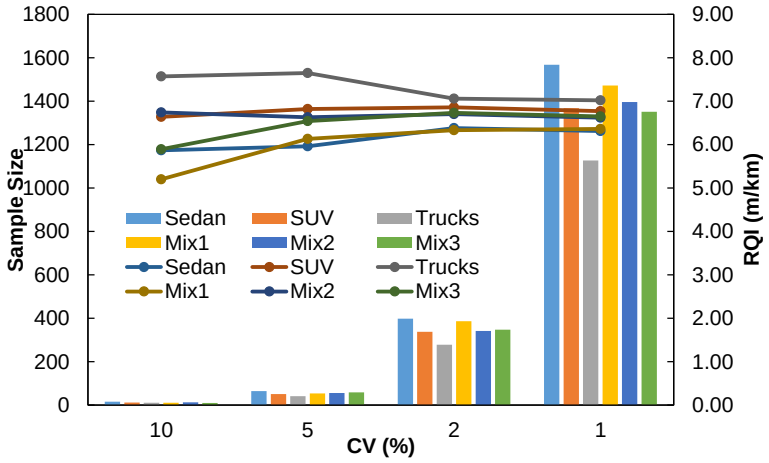

Figure G-5. New Jersey Single Lane – Wander RQI and Sample Size.

Table G-5. New Jersey RQI and Sample Size Tabular Form.

Sedan			**SUV**			**Trucks**		
Sample Size	CV (%)	RQI (m/km)	Sample Size	CV (%)	RQI (m/km)	Sample Size	CV (%)	RQI (m/km)
15	10	5.87	11	10	6.64	10	10	7.57
64	5	5.96	50	5	6.82	41	5	7.65
398	2	6.38	337	2	6.86	278	2	7.06
1568	1	6.31	1368	1	6.77	1127	1	7.02
Mix1			**Mix2**			**Mix3**		
Sample Size	CV (%)	RQI (m/km)	Sample Size	CV (%)	RQI (m/km)	Sample Size	CV (%)	RQI (m/km)
10	10	5.20	12	10	6.74	9	10	5.89
53	5	6.13	55	5	6.63	58	5	6.54
386	2	6.33	341	2	6.70	347	2	6.73
1472	1	6.36	1396	1	6.62	1351	1	6.65

APPENDIX H

SAMPLE SIZE AND RQI CALCULATIONS FOR A TWO LANES –WANDER

Table H-1. Arizona RQI and Sample Size Calculations.

	Sedan				SUV		
	S-NW	S-W	D-W	CV	S-NW	S-W	D-W
RQI (m/km)	0.73	0.70	0.62	5	0.72	0.74	0.71
Sample Size	60	58	79		47	53	66
RQI (m/km)	0.74	0.72	0.68	2	0.76	0.75	0.69
Sample Size	381	386	457		333	348	428

	HD Trucks				Mix1		
	S-NW	S-W	D-W	CV	S-NW	S-W	D-W
RQI (m/km)	0.86	0.81	0.78	5	0.70	0.72	0.72
Sample Size	42	43	51		55	59	63
RQI (m/km)	0.82	0.83	0.75	2	0.75	0.75	0.69
Sample Size	257	267	384		343	350	433

	Mix2				Mix3		
	S-NW	S-W	D-W	CV	S-NW	S-W	D-W
RQI (m/km)	0.69	0.76	0.68	5	0.71	0.74	0.69
Sample Size	54	49	65		45	49	58
RQI (m/km)	0.76	0.77	0.71	2	0.78	0.77	0.72
Sample Size	341	337	424		310	327	425

Table H-2. New Jersey RQI and Sample Size Calculations.

	Sedan				SUV		
	S-NW	S-W	D-W	CV	S-NW	S-W	D-W
RQI (m/km)	6.62	5.96	5.19	5	6.39	6.82	6.53
Sample Size	57	64	68		48	50	73
RQI (m/km)	6.45	6.38	5.77	2	6.75	6.86	6.49
Sample Size	398	398	477		311	337	440

	HD Trucks				Mix1		
	S-NW	S-W	D-W	CV	S-NW	S-W	D-W
RQI (m/km)	6.00	7.65	6.50	5	6.38	6.13	6.21
Sample Size	38	41	68		48	53	67
RQI (m/km)	6.71	7.06	6.5	2	6.29	6.33	6.08
Sample Size	274	278	399		339	386	460

	Mix2				Mix3		
	S-NW	S-W	D-W	CV	S-NW	S-W	D-W
RQI (m/km)	6.39	6.63	5.78	5	7.05	6.54	6.14
Sample Size	50	55	70		39	58	63
RQI (m/km)	6.51	6.7	6.22	2	6.53	6.73	6.16
Sample Size	337	341	460		306	347	434